

Division of Pharmaceutical Chemistry
Faculty of Pharmacy
University of Helsinki
Finland

Synthesis of Six-Membered Rings and Inhibitors of Protein Kinases

Alexandros Kiriazis

ACADEMIC DISSERTATION

To be presented, with the permission of the Faculty of Pharmacy of the University of Helsinki, for public examination in lecture room 1041, Viikki Biocenter 2 (Viikinkari 5), on 14 September 2012, at 12 noon.

Helsinki 2012

Supervised by

Professor Jari Yli-Kauhaluoma, PhD
Division of Pharmaceutical Chemistry
Faculty of Pharmacy
University of Helsinki
Helsinki, Finland

Reviewed by

Professor Tarek Ghaddar, PhD
Department of Chemistry
American University of Beirut
Beirut, Lebanon

Professor Angel Messeguer, PhD
Department of Chemical and Biomolecular Nanotechnology
The Institute for Advanced Chemistry of Catalonia
Consejo Superior de Investigaciones Científicas (CSIC)
Barcelona, Spain

Opponent

Professor Peter Goekjian, PhD
Lab. Chimie Organique 2-Glycosciences
Université de Lyon, France

© Alexandros Kiriazis 2012

ISBN 978-952-10-8192-7 (paperback)

ISBN 978-952-10-8193-4 (PDF)

ISSN 1799-7372

<http://ethesis.helsinki.fi>

Helsinki University Print
Helsinki 2012

Abstract

The six-membered rings have a privileged presence in both natural products and synthetic compounds such as drug molecules. Multiple methods to prepare them in the laboratory have been developed. The Diels-Alder reaction provides several pathways toward the construction of substituted six-membered rings with a high degree of regio-, diastereo- and enantioselectivity. It can be considered to be the most important and powerful carbon-carbon bond-forming reaction of all, in synthetic organic chemistry.

A practical synthetic method for the preparation of hexahydrocinnolines was developed here, as part of continuing research on polymer-supported pericyclic reactions in preparation of biologically interesting compounds. Some cinnoline derivatives from the literature were reported to show interesting biological properties, such as antimicrobial activity and inhibition of cancer cell lines. Hexahydro-1,2,4-triazolocinnoline-1,3-diones and related compounds were synthesized *via* aza Diels-Alder reaction on solid-phase.

Protein kinases are key regulators of cell function that constitute one of the largest and most functionally diverse gene families. By adding phosphate groups to substrate proteins, kinase driven phosphorylation plays a significant role in a wide range of cellular processes. More than 500 protein kinase genes are present in the the human genome, constituting about 2% of all human genes. They regulate many cellular processes such as growth, differentiation, and proliferation. Protein kinases are seen as potential therapeutic targets since their mutation and dysregulation is causal in multiple human diseases, including metabolic, immunological disorders, and cancer. The consistent structure of the catalytic site among protein kinases sets limits for the development of protein kinase inhibitors. Some protein kinases, however, have regulatory domains as part of their structure, such as protein kinase C (PKC), whose regulatory (C1) domain is unique and is found only in a small number of kinases. This offers a selectivity advantage, thus making the C1-domain an attractive drug target. In fact, the utilization of the the X-ray crystal structure of the PKC δ C1b domain, with molecular modeling, led to the discovery, in this work, of novel C1 domain ligands, the tricyclic γ -amino alcohols. Synthesis of these compounds was achieved by the utilization of the Diels-Alder reactions.

In the process of modifying a naturally occurring deep-blue colored hydrocarbon guaiazulene, a novel aminoguaiazulene derivative was synthesized. This novel derivative undergoes ring annulation reactions with 1,2-dicarbonyl reagents to yield tricyclic δ -lactams, types of benzo[*cd*]azulenes. Benzo[*cd*]azulenes derived from guaiazulene, are colorful synthetic carbocyclics with interesting chemical and biological properties. Some of the benzo[*cd*]azulenes synthesized in this study were recently characterized as selective Pim kinase inhibitors. Pim kinases have become intriguing targets for cancer therapy that possess unique structural features, among protein kinases, that offer a great potential in the design of selective Pim-inhibitors. Based on the promising Pim-kinase inhibition results from multiple cell-based assays, a further modification of the benzo[*cd*]azulenes was conducted, where some interesting findings in their chemical behavior were observed; new phenolic benzo[*cd*]azulene compounds were formed, with potent Pim-inhibitory activities. The benzo[*cd*]azulenes developed in this study were found to be useful research compounds, potential Pim-selective kinase inhibitors, and putative anti-cancer drug candidates. The new synthetic methods detailed in this study will be valuable tools in the further development of additional benzo[*cd*]azulenes and related systems in the future.

Acknowledgements

This study was carried out at the University of Helsinki, in the Drug Discovery Technology Center (DDTC) and in the Division of Pharmaceutical Chemistry, Faculty of Pharmacy, during the years 2005–2012. Funding was provided by The Graduate School in Pharmaceutical Research (GSPR), the European Commission (Contract No LSHB-CT-2004-503467), The National Technology Agency (Tekes), Hormos Medical Corp., Juvantia Pharma Ltd., Orion Pharma, Finnish Pharmaceutical Society and Alfred Kordelin Foundation (Gustav Komppa).

I am most grateful to my supervisor, Professor Jari Yli-Kauhaluoma, for the opportunity to work under his supervision at the Division of Pharmaceutical Chemistry. His never-ending enthusiasm in research and Science, his guidance, patience and friendship that made all possible to accomplish this study.

I want to thank all co-authors at the Division of Pharmaceutical Chemistry and the Division of Pharmacology and Toxicology for their collaboration and contributions. I am grateful to Dr. Ingo Aumüller for introducing me into the world of azulenes, and for all his guidance and enormous knowledge in the synthesis laboratory. I want to thank our collaborator Adjunct Professor Päivi Koskinen and her great research group at the University of Turku for all the biological results dealing with Pim-inhibition. Special thanks to Olli Aitio for NMR guidance and for original modeling of the PKC C1 domain ligands for this study.

I want to thank Professor Tarek Ghaddar (American University of Beirut, Lebanon) and Professor Angel Messeguer (Consejo Superior de Investigaciones Científicas, Spain) for reviewing thesis and Jennifer Rowland for the work in improving the English language. Special thanks to all my past and present colleagues in the JYK-group Kirsi, Mikko, Antti, Gusse, Leena, Raisa, Nenad, Timo, Irene, Paula, Rali, Mohan, Martina, Erik, Kristian, Ingo B and Sami. In addition, warm thanks for all fellows at the Division of Pharmaceutical Chemistry.

I am grateful to my family and friends for their generous support and understanding, and for my parents for their overwhelming financial help especially during the writing time of this thesis.

Helsinki, August 2012
Alexandros Kiriazis

“Chemical synthesis always has some element of planning in it. But, the planning should never been too rigid. Because in fact, the specific objective the synthetic chemist uses as the excuse for his activity is often not of special importance in the general sense, rather, the important things are those that he finds out in the course of attempting his objective.”

R. B. Woodward
Nobel Prize laureate in chemistry (1965)

Contents

Abstract	3
Acknowledgements	4
List of original publications	7
Abbreviations	8
1 Introduction	9
2 Review of the literature	12
2.1 Synthesis of six-membered ring of benzo[<i>cd</i>]azulenes	12
2.1.2 Synthesis of six-membered rings by the Diels-Alder reaction	17
2.1.2.1 Diels-Alder reactions on solution-phase	18
2.1.2.2 Diels-Alder reactions on solid-phase	22
2.2 Protein kinases	24
2.2.1 Protein kinase inhibitors	25
2.2.2 Protein kinase C	28
2.2.3 Pim kinases	34
3 Aims of the study	46
4 Experimental	47
5 Results and discussion	51
5.1 Synthesis of hexahydrocinnolines by aza Diels-Alder reaction	51
5.2 Synthesis of a tricyclic model compound targeting PKC C1b	53
5.3 Synthesis of new guaiazulene derivatives	56
5.3.1 Synthesis of 4-aminoguaiazulene and its δ -lactam derivatives	56
5.3.2 Synthesis of tricyclic benzo[<i>cd</i>]azulenes as potential Pim-1 inhibitors	59
6 Summary and conclusions	70
References	73

List of original publications

This thesis is based on the following publications:

- I** Kiriazis, A., Rüffer, T., Jäntti, S., Lang, H., and Yli-Kauhaluoma, J. Stereoselective Aza Diels-Alder Reaction on Solid-Phase: A Facile Synthesis of Hexahydrocinnoline Derivatives. *J. Comb. Chem.* **2007**, *9*, 263–266.
- II** Kiriazis, A. Aumüller, I. and Yli-Kauhaluoma, J. Synthesis of 4-amino-guaiazulene and its δ -lactam derivatives. *Tetrahedron Lett.* **2011**, *52*, 1151–1153.
- III** Alexandros Kiriazis, Gustav Boije af Gennäs, Virpi Talman, Elina Ekokoski, Timo Ruotsalainen, Irene Kylänlahti, Tobias Rüffer, Gloria Wissel, Henri Xhaard, Heinrich Lang, Raimo K. Tuominen and Jari Yli-Kauhaluoma. Stereoselective synthesis of (3-aminodecahydro-1,4-methanonaphthalen-2-yl)methanols targeted to the C1 domain of protein kinase C. *Tetrahedron* **2011**, *67*, 8665–8670.
- IV** Alexandros Kiriazis[‡], Riitta L. Vahakoski[‡], Sini Eerola, Niina M. Santio, Ralica Arnaudova, Eeva-Marja Rainio, Ingo B. Aumüller, Jari Yli-Kauhaluoma and Päivi J. Koskinen. Tricyclic benzo[*cd*]azulenes selectively inhibit activities of Pim kinases and restrict growth of Epstein-Barr virus-transformed cells. (Submitted) [‡]These authors contributed equally to this work.

The publications are referred to in the text by their roman numerals. The supporting information of original publications **I**, **II** and **IV** are not included in this thesis. This material is available from the author or via the Internet at <http://pubs.acs.org> for original publication **I** (56 pages) and at <http://www.sciencedirect.com/> and for original publication **II** (9 pages). The original publications **I**, **II** and **III** are reproduced with the permission of the copyright holders. In addition, one submitted manuscript (**IV**) is included.

Abbreviations

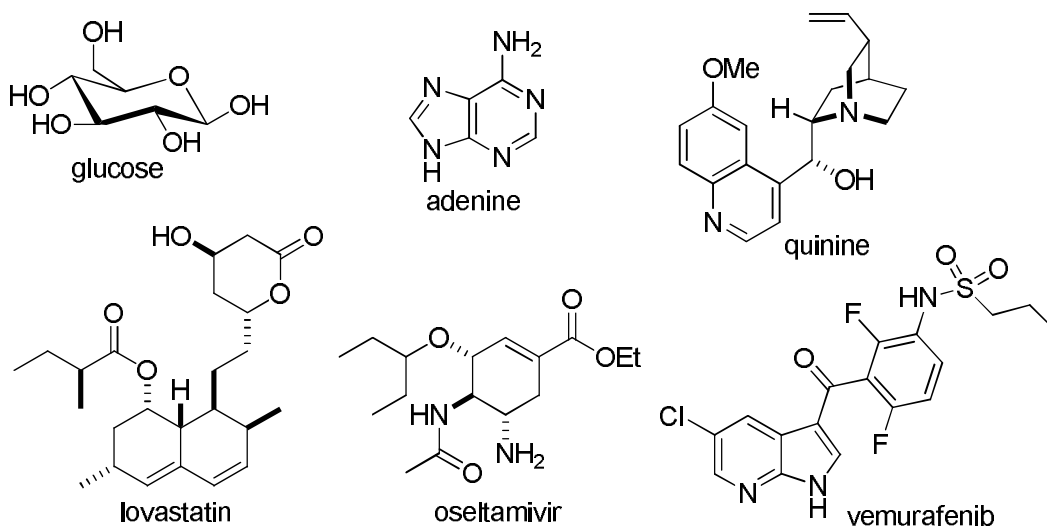
Ac	acetyl
AML	acute myeloid leukemia
ATP	adenosine-5'-triphosphate
BAD	Bcl-2-associated death promoter
Bn	benzyl
Bz	benzoyl
Cbz	carboxybenzyl
Chx	cyclohexyl
GSK-3	glycogen synthase kinase 3
D-A	Diels-Alder
DAG	1,2-diacylglycerol
DDQ	2,3-dichloro-5,6-dicyano-1,4-benzoquinone
DMF	<i>N,N</i> -dimethylformamide
DMSO	dimethyl sulfoxide
DPPA	diphenyl phosphoryl azide
EGFR	epidermal growth factor receptor
FT-IR	Fourier transform infrared spectroscopy
GC	gas chromatography
HMBC	heteronuclear multiple bond correlation
HRMS	high-resolution mass spectroscopy
HSQC	heteronuclear single quantum correlation
HTS	high-throughput screening
IBD	iodobenzene diacetate
IEDDA	inverse electron demand Diels-Alder
LC	liquid chromatography
LDA	lithium diisopropylamide
LUMO	lowest unoccupied molecular orbital
<i>m</i> CPBA	<i>meta</i> -chloroperoxybenzoic acid
MOM	methoxymethyl ether
MS	mass spectrometry
MW	microwave
MYC	v-myc myelocytomatosis viral oncogene homolog (avian)
NMR	nuclear magnetic resonance
Pim	provirus integration site for Moloney murine leukemia virus
PKA	protein kinase A
PKC	protein kinase C
PPA	polyphosphoric acid
rt	room temperature
TAD	1,2,4-triazole-3,5-dione
TEA	triethylamine
TFA	trifluoroacetic acid
THF	tetrahydrofuran
TLC	thin-layer chromatography
TBDMS	<i>tert</i> -butyldimethylsilyl

1 Introduction

The fact that natural compounds are mostly composed of cyclic structures has made the cyclization reactions perhaps the most important pathways in organic chemistry. The challenge to mimic living organisms in their ability to build complex molecular structures in near quantitative conversions, and with complete stereocontrol, forms an ultimate driving force and inspiration to the scientists working in the field of synthetic organic chemistry.

As a generalization, alicyclic (aliphatic and cyclic) compounds hardly differ in their chemical properties from their open-chain analogs. As stated by Nobel Prize laureate Leopold Ružička in 1945, “Many investigations have shown however, that in spite of this close chemical similarity, the alicyclic analogs can exhibit entirely different physiological properties.”¹ August Kekulé, the principal founder of the theory of chemical structure, first introduced the carbon six-membered ring into structural chemistry in his formula for benzene in 1865.² Since then the six-membered ring maintained its unique position in the classification of organic chemistry.

The privileged presence of six-membered ring structures in biologically interesting molecules is obvious. Natural products, such as carbohydrates (glucose), DNA bases (adenine), alkaloids (quinine), and cholesterol-reducing lovastatin carry the six-membered ring(s) as a pivotal element in their structure. Similarly, synthetic compounds, such as drugs, also carry six-membered rings, as exemplified in antiviral oseltamivir and B-raf kinase inhibitor vemurafenib. With the continued discovery of increasingly complex polycyclic natural compounds, the need to understand how and why six-membered rings form becomes ever more important.



Multiple synthetic methods for the preparation of six-membered rings exist. Some selected examples from the literature are listed with examples of the particular six-member ring forming reactions utilized in the natural product synthesis in Table 1. The Diels-Alder reaction is covered in detail in the literature review, since it represents a major contribution to this thesis and is not listed in Table 1.

Table 1. Selected methods for preparation of six-membered rings in natural product synthesis.

Method	Example	References
Robinson annulations	<p>Michael-addition base</p> <p>Aldol cond. -H₂O</p> <p>Wieland-Miescher ketone</p> <p>Taxol + > 50 other natural products</p>	Robinson, ³ Wieland ⁴
Intramolecular Michael reaction	<p>EtAlCl₂</p> <p>(rac)-nootkatone</p> <p>bis-Michael BOMO TBAF</p> <p>(MeO)₂HC Me OH</p> <p>MeO₂C Me salvinorin A</p> <p>BOM = benzyloxymethyl</p>	Majetich, ⁵ Evans ⁶
Intramolecular ene reaction	<p>Δ or ZnBr₂</p> <p>citronellal</p> <p>(-)-hispiduleg (major isomer)</p> <p>Δ or AlCl₃</p> <p>lanosterol</p>	Oppolzer and Snieckus ⁷ (review)
Polyene (cation-olefin) cyclization	<p>squalene epoxide</p> <p>lanosterol</p>	Johnson ⁸ (review), Abe ⁹ (review)
Free radical cyclization	<p>Bu₃SnH</p> <p>seyschellene</p>	Jaspere ¹⁰ (review)
Electrocyclic reactions	<p>endiandric acid D</p>	Nicolaou ¹¹
Dieckmann condensation	<p>Dieckmann cond.</p> <p>1,7-diester</p> <p>medicinal chemistry building blocks and natural products</p>	Powers ¹²
Ring closing metathesis	<p>Et Ru-catalyst</p> <p>(+)-amburidin</p>	Fürstner ¹³ (review), Deiters ¹⁴ (review),
Beckmann rearrangement	<p>Beckmann rearrangement</p> <p>dr 11:1</p> <p>(+)-codeine</p>	White ¹⁵

The literature review that follows in Chapter 2 is divided into two sections. The first part concentrates on the methods for construction of the six-membered rings of benzo[*cd*]azulenes; colourful synthetic carbocyclic compounds with interesting chemical and biological properties. A general review of the Diels-Alder reaction covering historical and basic principles is provided, since it constitutes a major contribution to ring synthesis in this thesis work. Both solution and solid-phase methods are included. The second part concentrates on the biology and inhibition of two protein kinases, namely protein kinase C and Pim kinases (Pim-1, Pim-2 and Pim-3), both phosphoryl transferring enzymes that are central to this study. The results of the work from the reported publications I–IV are

detailed in Chapter 5, which describes the development of a practical synthetic method for the preparation of biologically interesting six-membered ring compounds by Diels-Alder reactions on solid-phase. By selecting carbonylazo compounds as highly reactive N=N azadienophiles with polymer-bound diene, solid-phase synthesis of hexahydrocinnolines was introduced.

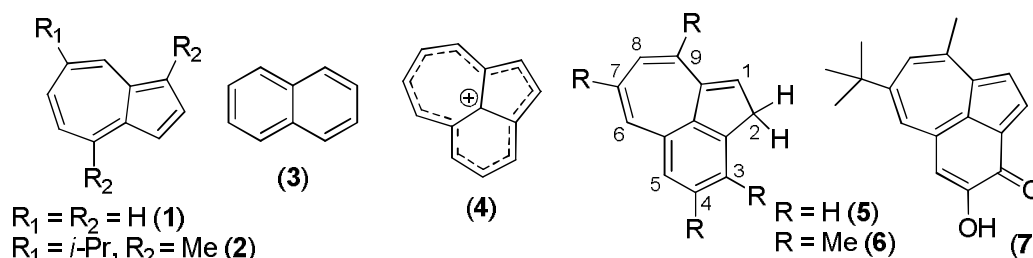
Utilization of the the X-ray crystal structure of the PKC δ C1b domain combined with molecular modeling, (3-aminodecahydro-1,4-methanonaphthalen-2-yl)methanol was discovered as a novel C1-domain ligand. This led to the synthesis of two tricyclic γ -amino alcohols, where the construction of their decahydronaphthalene core with six continuous stereocenters was achieved by extensive utilization of the Diels-Alder reaction.

During the modification studies of guaiazulene, a naturally occurring deep-blue coloured bicyclic sesquiterpenoid hydrocarbon, a method for nitrogen insertion into the seven-member ring, was developed. Guaiazulene 4-carboxylic acid was converted to the novel 7-isopropyl-1-methylazulen-4-amine in two reaction steps. Further elaboration with 1,2-dicarbonyl electrophiles led to the synthesis of δ -lactams with a six-membered heterocyclic ring fused to azulenes aromatic core.

Some of the benzo[*cd*]azulenes synthesized in our laboratory were recently characterized as selective Pim kinase inhibitors. Based on the promising results for Pim kinase inhibition in multiple cell-based assays, a further modification of the benzo[*cd*]azulenes was conducted with an aim to develop more potent Pim inhibitors. In addition, during the course of modification of benzo[*cd*]azulen-3-ones, some interesting findings in their chemical behavior were observed. This led to the synthesis of new phenolic benzo[*cd*]azulene compounds with potent Pim-inhibitory activities. Some of the studied benzo[*cd*]azulenes were able to inhibit intracellular activities of Pim kinases with promising low-micromolar EC₅₀ values. Furthermore, treatment with benzo[*cd*]azulenes significantly slows down migration of adherent cancer cells derived from either prostate- cancer or squamocellular carcinomas. Development of additional benzo[*cd*]azulenes derivatives is expected to further improve their efficacy as Pim-selective kinase inhibitors and possible anti-tumor drug candidates.

2 Review of the literature

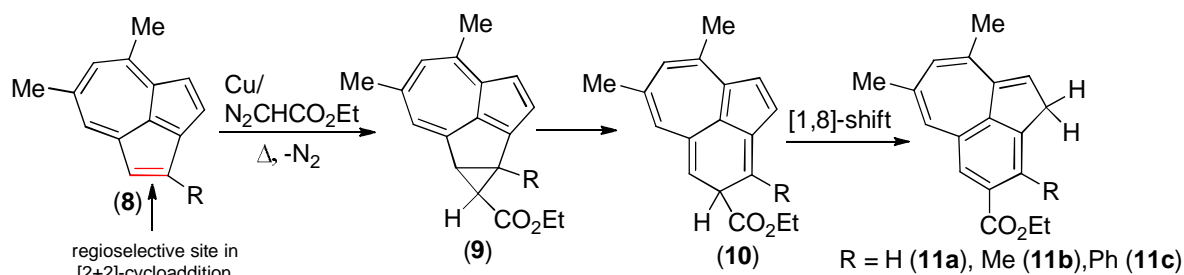
2.1 Synthesis of six-membered ring of benzo[*cd*]azulenes



Azulene (1) and guaiazulene (2) are hydrocarbons consisting of a five- and a seven-membered rings fused to form an unsaturated bicyclic system. The azulene (1) can be considered an isomer of naphthalene (3). Whereas naphthalene is colorless, azulenes are intensely blue. The history of azulenes dates back to the 15th century when it was recognized as the azure-blue chromophore obtained by steam distillation of German chamomile (*Matricaria chamomilla* L.). The chromophore was discovered in 1863 by Septimus Piesse,¹⁶ who applied the descriptive name azulene to azure-blue distillates discovered in yarrow and wormwood. Its structure was first reported by Lavoslav Ružička, followed by its synthesis in 1937 by Plattner and Pfau,¹⁷ who named the parent compound of the family as bicyclo[5.3.0]decapentaene. These compounds are now collectively referred to as the azulenes.

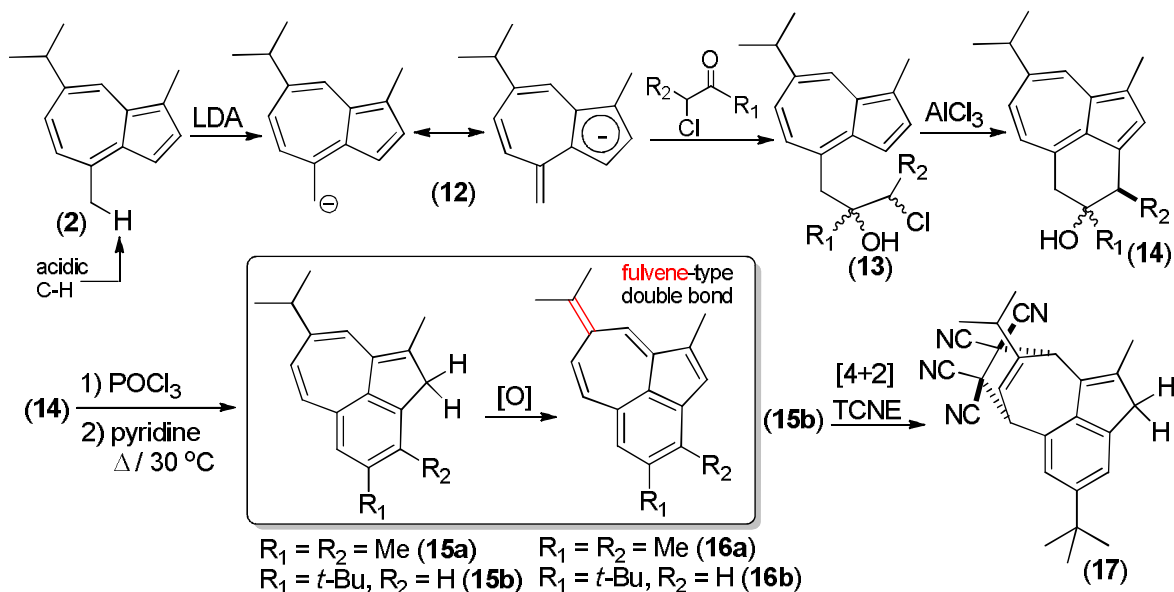
The benzo[*cd*]azulene system (4) has attracted interest due to its unique theoretical property as an odd nonalternant analog of phenalene.¹⁸ Boekelheide and Smith were among the first to report the synthesis of 2*H*-benzo[*cd*]azulenes.¹⁹ The parent compound (5) was prepared by means of a difficult multistep route based on the carbene-mediated ring expansion of the acenaphthene framework. 2*H*-benzo[*cd*]azulene (5), was however only obtained in small quantities and is very susceptible to polymerization, thus can only be handled at low temperatures in dilute solution.¹⁹ Previously, Hafner and Schaum had reported the synthesis of 3,4,7,9-tetramethyl-2*H*-benzo[*cd*]azulene (6)²⁰ by base-catalyzed cyclization. This crystalline product is however susceptible to decomposition. The six-membered ring of 7-(*tert*-butyl)-4-hydroxy-9-methyl-3*H*-benzo[*cd*]azulene-3-one can be synthesized in similar manner.²¹ Syntheses of (6) and (7), however, were reported without yields or adequate experimental procedures.

Hafner and Rieper reported the synthesis of 2*H*-benzo[*cd*]azulenes by [2+2]-cycloaddition of cyclopenta[*cd*]azulene (8) with *in situ* generated ethoxycarbonylcarbene followed by its ring expansion (Scheme 1).²² The copper-catalyzed thermolysis of ethyl diazoacetate at 90–110 °C in the presence of (8) leads directly to the 2*H*-benzo[*cd*]azulene framework. In a one-pot procedure a regioselective cycloaddition of (8) giving (9) is probably followed by valence isomerization of the latter to compound (10), which undergoes a [1,8]-hydrogen shift to stable 7,9-dimethyl-2*H*-benzo[*cd*]azulene-4-carboxylate (11a) in 60% yield. When R is methyl or phenyl, the cycloaddition occurs in similar fashion to the same site of cyclopenta[*cd*]azulene to yield the 3-methyl (11b) and 3-phenyl (11c) analogs in 64% and 59% yields, respectively.



Scheme 1. Carbene-mediated ring-expansion strategy to 2H-benzo[cd]azulenes.

McGlinchey *et al.*²³ synthesized benzo[cd]azulenes by extending the guaiazulene (**2**) carbon framework through nucleophilic addition of the resonance-stabilized anion (**12**) to α -chloroketones (Scheme 2). The diastereomeric alcohols (**13**) were used for the subsequent reaction, whereby the formation of the six-member rings in (*cis/trans*-**14**) was accomplished through AlCl_3 -promoted Friedel-Crafts alkylation. Finally, the subsequent treatment of alcohols (**14**) with POCl_3 , followed by refluxing in pyridine for 8 hours enabled the [1,5] sigmatropic rearrangements leading to the desired 2H-benzo[cd]azulene (**15a**) and to the oxidized heptafulvene (**16a**) in 59% and 9% yields, respectively (Scheme 2). For the alcohol (**15b**) the conversion to its 4-*tert*-butylbenzo[cd]azulene (**15b**) and its oxidized analog (**16b**) was accomplished in less drastic conditions (30 °C, 3 h) and in slightly better yields (61% and 23%, respectively).



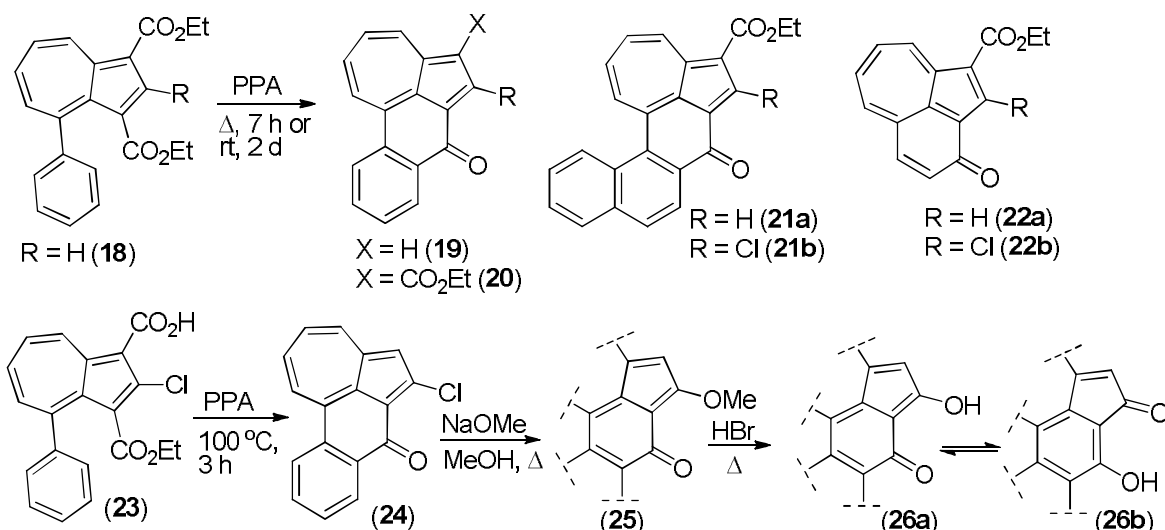
Scheme 2. McGlinchey's approach to benzo[cd]azulenes and heptafulvenes.

The same authors reported an interesting reaction of TCNE (tetracyanoethylene) with benzo[cd]azulene (**15b**) at room temperature to produce the tetracyclic Diels-Alder adduct (**17**) (Scheme 2) in 96% yield.²³ On the other hand, the oxidized heptafulvene (**16b**) participates not in [4+2], yet in a regioselective [2+2] cycloaddition across the C6–C7 double bond. The cycloaddition chemistry of heptafulvenes and related systems has been comprehensively reviewed.²⁴

Abe *et al.*^{25,26} communicated the synthesis of 7H-naphtho[cd]azulen-7-ones, which are structurally related to the benzo[cd]azulenyl system. Intramolecular Friedel-Crafts cyclization of diethyl 4-phenylazulene-1,3-dicarboxylate (**18**) with polyphosphoric acid (PPA) at 100 °C for 7 h gives a mixture of two tetracyclic products, (**19**) in 10% yield, and

(**20**) in 60% yield (Scheme 3). The same reaction performed at room temperature for 2 days, gives the ethyl ester (**20**) as a single product (67%). Alkaline ester hydrolysis of (**20**) and the following decarboxylation upon heating in hot PPA for 3 h yields (**19**) in 61% yield. 2-Substituted analogs of (**18**) (R = Me, Ph, Cl) gave similarly derivatives (**19** and **20**).²⁵

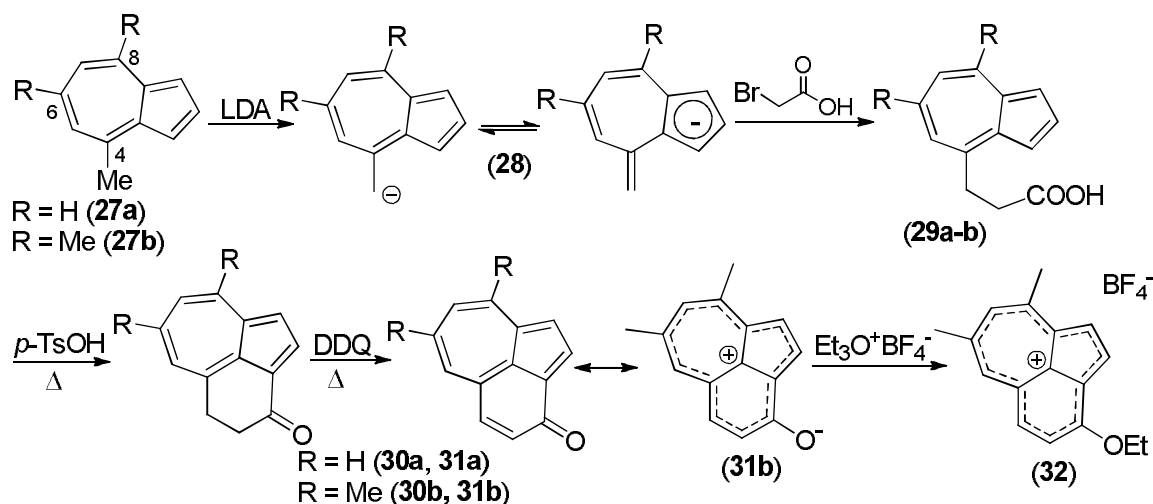
The Friedel-Crafts cyclization is not only restricted to the 4-phenyl derivatives. While the cyclization of 4-(α -naphthyl)azulene-1,3-dicarboxylates with polyphosphoric acid yields pentacyclic 7*H*-azuleno[1,8-*bc*]phenanthren-7-ones (**21a–b**) as main products,²⁵ the 4-vinyl derivatives under similar conditions (PPA, rt, 1 d) give tricyclic benzo[*cd*]azulones (**22a–b**) (Scheme 3).²⁷



Scheme 3. Friedel-Crafts cyclizations to fused tri-, tetra- and pentacyclic azulones.

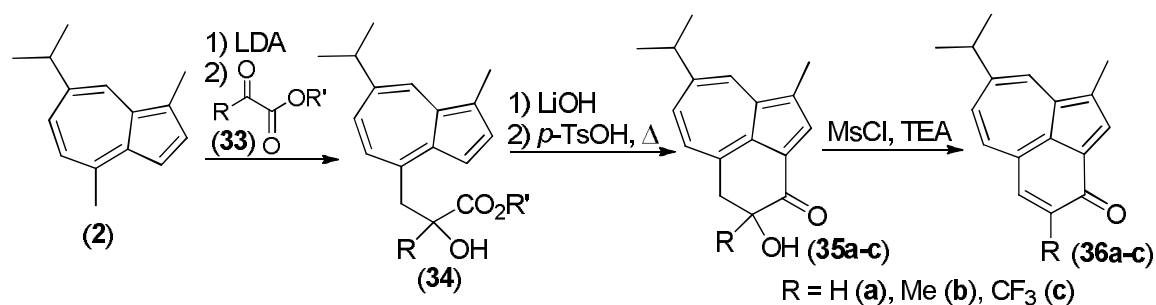
When the monocarboxylic acid (**23**) is heated in PPA at 100 °C for 3 hours, tetracyclic product (**24**) is obtained in 90% yield (Scheme 3).²⁸ The chloro substituent is replaceable with nucleophilic reagents to give the corresponding substitution products. Thus, the treatment of (**24**) in methanol with sodium methoxide (reflux, 1 h) gives 6-methoxy-substituted naphtho[*cd*]azulene-7-one (**25**) in a quantitative yield. When heated in 48% hydrobromic acid (90 °C, 40 min), (**25**) is easily hydrolyzed to give a quantitative yield of an acidic compound (**26**).²⁸ The ring carbonyl in (**26**) is found to be highly polarized²⁸ and can exist as a tautomeric mixture. The authors showed spectroscopically (IR) that (**26**) exists as a mixture of (**26a**) and (**26b**), in which (**26a**) predominates.²⁸

Neidlein *et al.*^{29,30} have reported the synthesis of 3*H*-benzo[*cd*]azulene-3-ones (Scheme 4) starting from 4,6,8-trimethylazulene (**27a**) and 4-methylazulene (**27b**). Regioselective metalation of (**X**) with LDA, followed by treating the anion (**28**) with bromoacetic acid, gave azulene 4-propionic acids (**29a–29b**). These groups undergo cyclization upon heating to 4,5-dihydro-3*H*-benzo[*cd*]azulene-3-ones (**30a**, 57%, **30b**, 73%) in the presence of *p*-toluenesulfonic acid. Finally, oxidation of (**30a–30b**) with DDQ (2,3-dichloro-5,6-dicyanobenzoquinone) at 110 °C yields the fully conjugated benzo[*cd*]azulene-3-ones (**31a**, **31b**). The enol tautomer of (**31b**) can be trapped by *O*-alkylation to give ethoxy[*cd*]benzazulenium tetrafluoroborate (**32**) (Scheme 4).



Scheme 4. Synthesis of 3H-benzo[cd]azulen-3-ones.

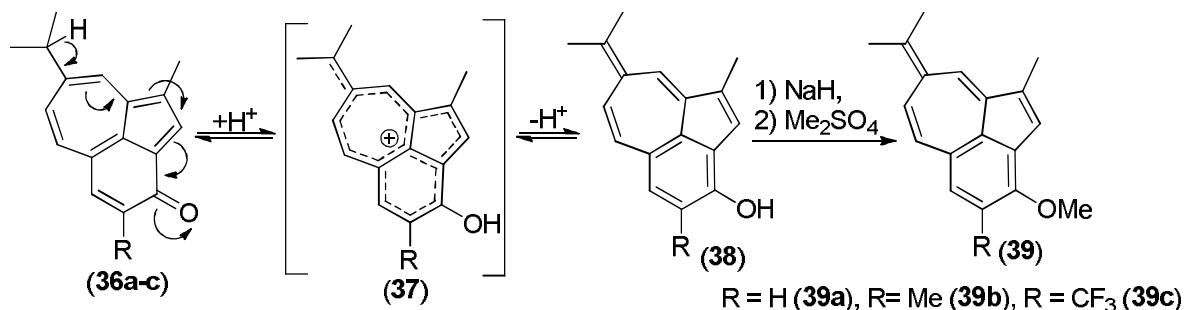
Very recently, Aumüller *et al.* published a communication where they describe a facile four-step synthesis of tricyclic benzo[cd]azulen-3-ones from commercially available guaiiazulene (**2**) (Scheme 5).³¹ The nucleophilic attack of the guaiiazulene-derived carbanion proceeds predominantly at the ketone carbonyl instead of the ester carbonyl of the carboxylic acid esters (**33**). The utilization of (**33**) offers an advantage over the use of bromoacetic acid, as different substituents (R) can be introduced in the 4-position of the resulting benzo[cd]azulene skeleton. After the successful hydrolysis of esters (**34**) with lithium hydroxide, the corresponding carboxylic acids take part in the acid-catalyzed intramolecular electrophilic acylations, as reported previously by Neidlein *et al.*^{29,30} for a related system. When R is a trifluoromethyl or methyl, the 4,5-dihydrobenzo[cd]azulen-3-ones (**35a–b**) are isolable in high yields (92%, 80%, respectively) but only with a modest yield with a hydrogen (**35c**, 32%). The α -hydroxy ketones (**35a–c**) were converted to fully conjugated benzo[cd]azulen-3-ones (**36a–c**) by the one-pot mesylation/ base-assisted elimination sequence.



Scheme 5. Syntheses of 4-substituted benzo[cd]azulen-3-ones

The same authors reported a successful application of an interesting acid-catalyzed tautomerization reaction that proceeds *via* isomerization of π -bonds across the azulene moieties of tricyclic benzo[cd]azulen-3-ones (Scheme 6). Concentrated hydrochloric acid was found to be a suitable catalyst for the initial protonation of the carbonyl oxygens of (**36a–c**) leading to the formation of cationic benzo[cd]azulenium species (**37**) being detectable by intensive and rapid color change from green to bright orange/red. Subsequently, the positive charge in (**37**) is stabilized by the release of a proton from the alkyl substituent in the eight-position to form the phenols (**38**) with a fulvene-type exocyclic

double bond on the seven-membered ring, resembling McGlinchey's tricyclic heptafulvenes.²³ The primary tautomerized products could not be isolated as phenols (**38**) due to the reverse nature of the reaction. However, *in situ* derivatization by deprotonation with a strong base (sodium hydride), followed by methylation (dimethyl sulphate), allows the isolation of heptafulvenic reaction products as orange phenol ethers (**39a–c**).³¹

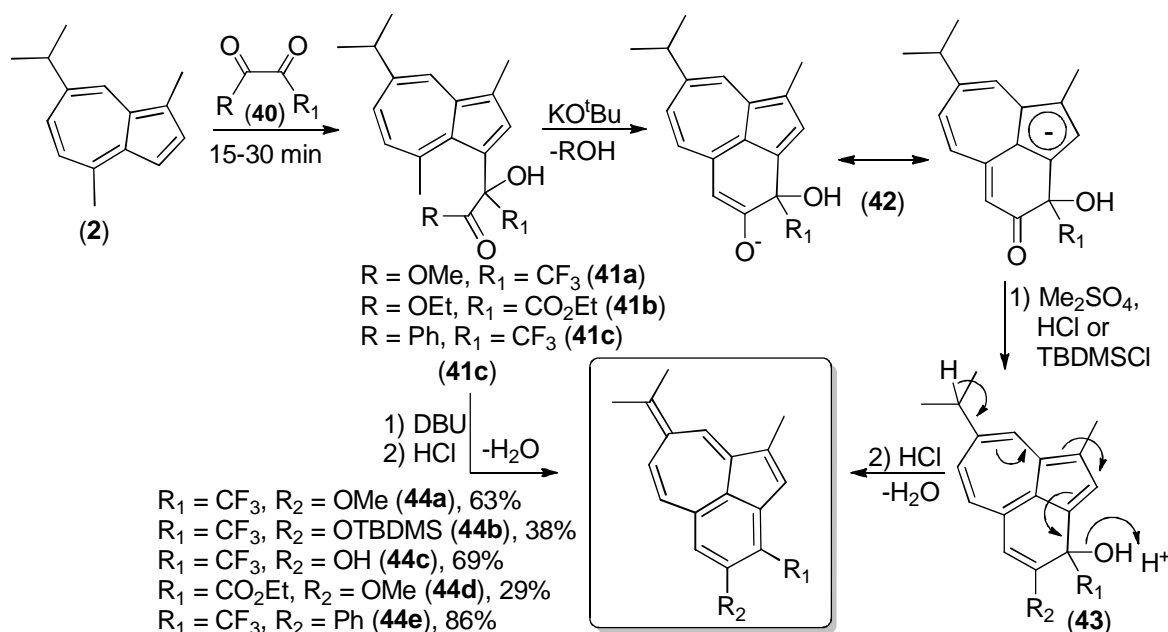


Scheme 6. Acid-mediated tautomerization of benzo[cd]azulen-3-ones to heptafulvenes.

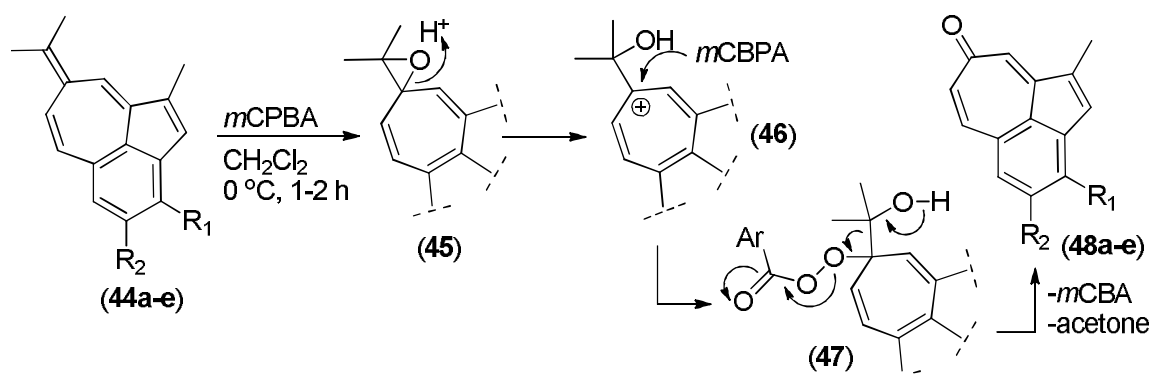
Aumüller *et al.*³² communicated also a facile two-step synthesis of heptafulvenes from guaiazulene (**2**). Electrophilic aromatic substitution reactions between dicarbonyl electrophiles (**40**) and C3 of guaiazulene (**2**) proceed without an added catalyst in high yields (Scheme 7). The intermediate methylene carbanions generated *in situ* from 3-hydroxyacyl azulenes (**41a–b**) instantly attack the neighboring carbonyl group to form the six-membered ring of the benzo[cd]azulene skeleton (Scheme 7). The subsequent one-pot elimination of the corresponding alcohol gives the enolates (**42**), which are stabilized by an aromatic cyclopentadienyl anion. Alkylation, silylation, or protonation of enolates (**42**) leads to intermediates (**43**). The addition of HCl readily initiates an interesting type of acid-catalyzed elimination reaction, where the release of a proton from the alkyl substituents at the 8-position leads to the formation of semicyclic C=C double bonds, which characterize the tricyclic products as heptafulvenes (**44a–d**) with variable substituents on 3- and 4-positions of the six-membered ring.

The phenylketone in (**41c**) accounts for a different route, since the cyclized intermediate is an alkoxide that cannot be converted into an enolate. After deprotonation with DBU (1,8-diazabicyclo[5.4.0]undec-7-ene) followed by the double elimination of water, however, 4-phenyl-substituted heptafulvene (**44e**) is isolated in excellent yield (86%) (Scheme 7); this represents the highest yield of the entire series.

The same authors expanded the scope of the method by examining the oxidations of the heptafulvenes (**44a–e**) (Scheme 8). Syntheses of tropones *via* heptafulvenes are not well documented in the literature and the cleavage of C=C double bonds is unusual for *m*CPBA (*m*-chloroperoxybenzoic acid). The hypothetical reaction mechanism suggests the epoxide is formed first (**45**) by 1 equiv of *m*CPBA. Presumably, the epoxide is prone to ring-opening reactions, due to the effective stabilization of the positive charge by the conjugated π -system (the seven-membered ring) in the resulting cations (**46**). Subsequently, the acyl peroxides (**47**) are formed by nucleophilic attack of another equivalent of *m*CPBA. Finally, the exit of the leaving group *m*CBA initiates the fragmentation of (**47**), yielding tropones (**48a–e**) with moderate to high yields (48–82%) and acetone as a byproduct.³² Evidence that supports the described reaction mechanism was recently obtained by rapid analysis of reaction intermediates by electrospray ionization-mass spectrometry.³³ The *m*CPBA oxidation of phenolic heptafulvene (**44c**) led to the identification of an ion at m/z 515 ($[M+Na]^+$), which supports the presence of acyl peroxide intermediate of (**47**) (Scheme 8.)



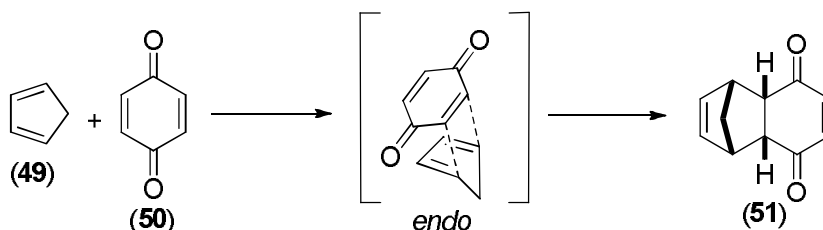
Scheme 7. Syntheses of heptafulvenes by Aumüller et al.



Scheme 8. Proposed reaction mechanism of *m*CPBA oxidation of heptafulvenes to tropones. For R_1 and R_2 , see Scheme 7.

2.1.2 Synthesis of six-membered rings by the Diels-Alder reaction

The Diels-Alder (D-A) reaction belongs to a larger class of thermal pericyclic reactions. It is a concerted 6π -electron process where conjugated diene and dienophile react in $[4\pi + 2\pi]$ manner, providing several pathways toward the construction of substituted six-membered rings with a high degree of regio-, diastereo- and enantioselectivity. Since its discovery in 1928 (Scheme 9), the Diels-Alder reaction is one of the most important and powerful carbon-carbon bond-forming reactions in synthetic organic chemistry.³⁴ The authors Otto Diels and Kurt Alder soon anticipated the importance of this discovery, particularly as it was applied to natural product synthesis: “Thus it appears to us that the possibility of synthesis of complex compounds related to, or identical with, natural products such as terpenes, sesquiterpenes, perhaps even alkaloids, has been moved to the near prospect.” Diels and Alder were awarded the Nobel Prize in Chemistry in 1950 for their work on the reaction.



Scheme 9. The original Diels-Alder reaction reported by Otto Diels and Kurt Alder in 1928.

2.1.2.1 Diels-Alder reactions on solution-phase

Dienes

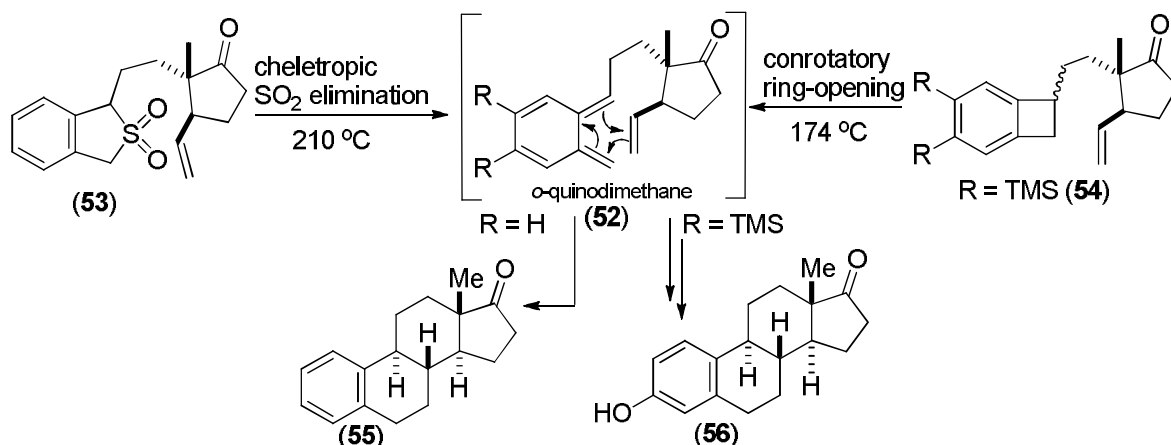
The diene component in the Diels-Alder reaction can be open-chain or cyclic with a large variety of different substituents. Heteroatom(s) can be incorporated into the diene moiety so that the scope of the reaction can be widened for the construction of six-membered heterocyclic compounds.³⁵ The diene must be able to exist in the *s-cis* conformation. Butadiene for example normally prefers the *s-trans* conformation due to its energy minimization. In case of substituents larger than hydrogen, steric hindrance may influence the relative stabilities of the conformations. For simple cases, the barrier to rotation around the central bond is small, and rotation to the less favorable but reactive *s-cis* conformation is rapid.

Cyclic dienes that are permanently in the *s-cis* conformation are more reactive in the Diels-Alder reactions due to rigid *cisoid* conformation. Among the cyclic dienes, cyclopentadiene (49) is the most reactive and undergoes self dimerization at room temperature. In a [4+2] cycloaddition with *p*-benzoquinone (50) it gives bridged tricyclic adduct (51), as reported by Diels and Alder in 1928 (Scheme 9).³⁴ Cyclic dienes being permanently in the *s-trans* conformation cannot adopt the *cisoid* conformation and therefore will not participate in the D-A reaction at all.^{36,37}

Unstable dienes, such as *ortho*-quinodimethanes, are reactive and versatile intermediates, which have been utilized as four-carbon units^{38,39} in the [4+2] cycloaddition for the construction of natural compounds. Early examples of this strategy were reported by Nicolaou⁴⁰ and Vollhardt⁴¹ in an intramolecular context, where *o*-quinodimethanes (52) generated *in situ* from sulfolene precursor (53), by cheletropic elimination of SO₂ or by conrotatory thermal ring-opening of benzocyclobutane (54), gave œstratrienone (55) and estrone (56) as single diastereomers and in high yields (Scheme 10).

The use of such an unstable diene is advantageous in that the products will contain newly formed aromatic six-membered rings. Polycyclic aromatic hydrocarbons can similarly participate in the D-A reaction. For example, anthracene (57) and its derivatives behave as a diene at sites C9 and C10 (Scheme 12), where the lowest (computational) benzenoid character is resided.³⁵

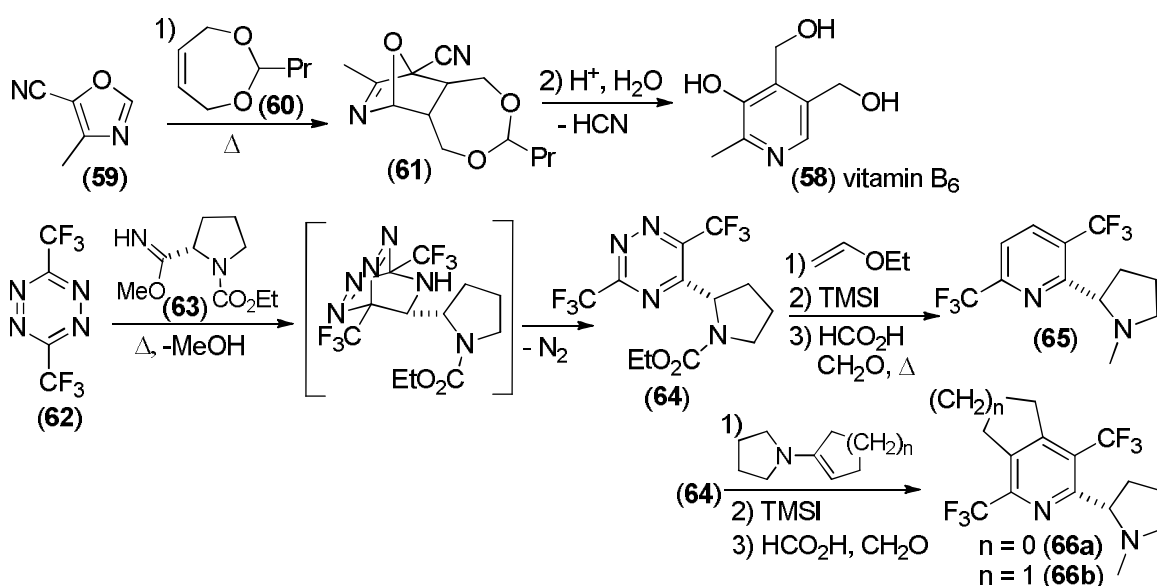
Among the heterodienes 1- and 2-aza-1,3-butadienes are the most widely studied and are useful for the construction of tetrahydropyridine derivatives. Pyrones and pyridines,⁴² with some aromatic character, are suitable dienes in the D-A reaction yielding aromatic products after extrusion of the heteroatom bridge (*retro* D-A reaction).



Scheme 10. Examples of *in situ* generated *o*-quinodimethanes in the synthesis of steroidal skeleton: α estratrienone (55)⁴⁰ and estrone (56).⁴¹

Inverse electron demand D-A reactions

Many nitrogen containing heteroaromatic compounds are electron deficient and participate in the *inverse electron demand Diels-Alder* (IEDDA)^{43,44} reactions with electron rich dienophiles (e.g. acetals, enol ethers, enamines). In a commercial synthesis of pyridoxine (vitamin B₆, 58) the IEDDA between oxazole diene (59) and acetal (60) provides tricyclic intermediate (61) (Scheme 11). The subsequent fragmentation, elimination (HCN), and acid-catalyzed deprotection finally gives the aromatic pyridoxine cycloadduct (58).⁴³



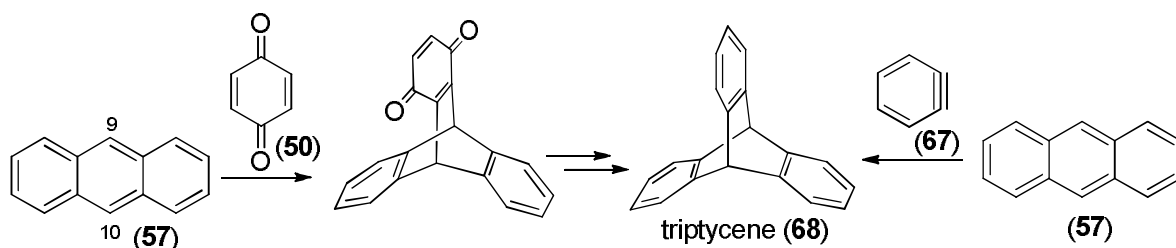
Scheme 11. Inverse electron demand D-A reactions in synthesis of functionalized pyridines.

Heteroaromatic azadienes with multiple nitrogen atoms, such as 1,3,5-triazines and 1,2,4,5-tetrazines are effective dienes in the IEDDA reaction and highly useful for the construction of diversely substituted six-membered nitrogen heterocycles, such as pyridines.^{43,44} An example of this strategy is utilized in the synthesis of new optically active analogs of (–)-nicotine,⁴⁵ where a tandem inverse electron demand Diels-Alder sequence with a trifluoromethyl-activated tetrazine (62) and proline-derived heterodienophilic imidate (63) produce 1,2,4-triazine cycloaddition product (64) after elimination of methanol and

dinitrogen (Scheme 11, (*S*)-enantiomers shown). The diazadiene system in (**64**) is electron deficient and efficiently undergoes the second IEDDA [4+2]-cycloaddition with electron rich dienophiles such as enol ethers and enamines. TMSI (trimethylsilyl iodide) mediated removal of the protecting group (CHCl_3 , Δ), and methylation of the subsequent nornicotines (HCO_2H , CH_2O , Δ) finally yields pyridine-modified nicotine analogs (**65**, **66a–b**) in high yields.

Dienophiles

The dienophile in the Diels-Alder reaction is generally an alkene or an alkyne bearing electron withdrawing functional groups. In the normal Diels-Alder reaction, the reactivity of the dienophile is increased by the presence of electron withdrawing substituents, such as formyl, ester, keto, nitro and nitrile groups conjugated to the alkene C=C double bond. Diels-Alder reactions can be promoted by different factors,⁴⁶ such as the use of high pressure, and most popularly the use of Lewis acids (e.g. AlCl_3), which coordinate to the dienophile's heteroatom bearing a lone pair of electrons such as carbonyl oxygen. Isolated triple bonds, such as those in acetylene, do not readily take part in the Diels-Alder reactions. However, cyclic alkynes⁴⁷ such as benzyne (**67**)⁴⁸ are extremely reactive species in the D-A reaction with a variety of dienes due to the strained triple bond. This is illustrated in the synthesis of triptycene (**68**)⁴⁹ (Scheme 12), which is incorporated in many organic compounds as a molecular scaffold, and has found application, for instance, in molecular motors.⁵⁰ Cyclopropenes⁵¹ are also excellent dienophiles due to the high reactivity caused by a large angle strain, and ability to donate a three-carbon unit to form the cycloadduct.



Scheme 12. Synthesis of triptycene (**68**) by the Diels-Alder reaction with *p*-benzoquinone (**50**) and benzyne (**67**) as dienophiles by Bartlett⁴⁹ and Wittig,⁵² respectively.

Heteroatom-containing dienophiles⁵³ are commonly used for the Diels–Alder reactions and are valuable tools for the synthesis of biologically important heterocyclic and natural compounds, such as various alkaloids and pyranoids. In fact, one of the first examples of a hetero Diels-Alder reaction was disclosed by Alder himself in 1943, when he discovered serendipitously that an imine tautomer could engage appropriate dienes in a productive [4+2] cycloaddition.⁵⁴ In a similar manner, carbonyl groups can be used as dienophiles in the oxo Diels-Alder reaction. Amidines and imidates are electron-rich C=N dienophiles participating in the IEDDA reaction as seen in the previous example (Scheme 11). 1,2,4-Triazole-3,5-diones, and other carbonylazo compounds, are known to be powerful dienophiles in [4+2] cycloaddition reactions.^{55,56} The lower LUMO energy of the N=N bond, in contrast to the corresponding C=C bond in alkenes⁵⁷ allows reactions to proceed more rapidly and often at ambient temperatures.

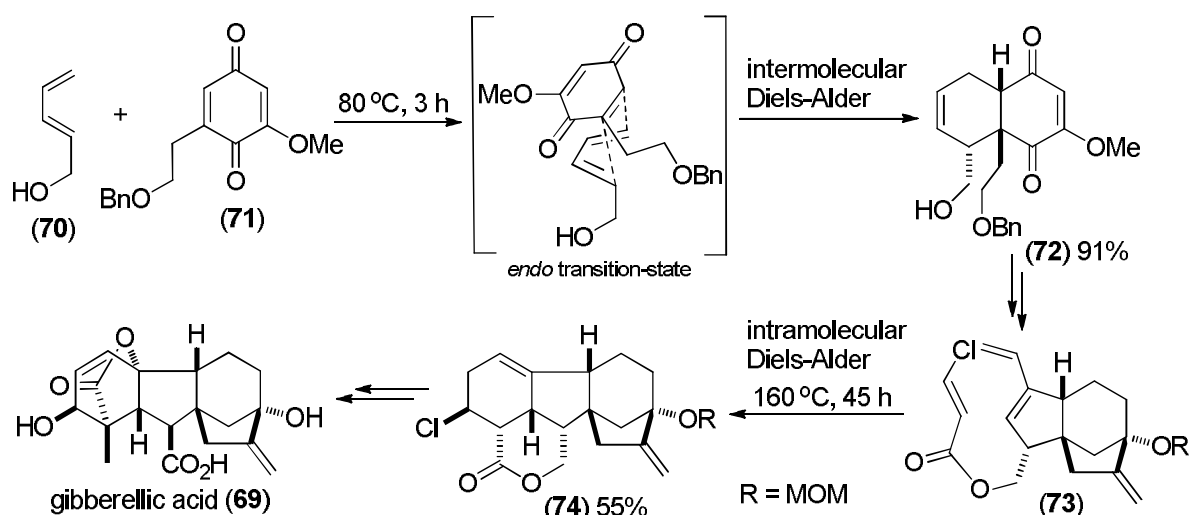
Cis principle

The relative stereochemical outcome of the Diels-Alder reaction can be predicted on the basis of the empirical rule formulated by Alder and Stein in 1937, known as the *cis* principle.⁵⁸ This means that if a *cis*-dienophile is reacted, both of the *cis*-substituents will end up on same side (face) of the product. When a *trans*-dienophile is used, both of the substituents will end up on different sides of the product. The same principle applies to dienes. *Trans, trans* 1,4-disubstituted dienes will end up on same side of the ring being *cis* relative to each other, whereas the *cis, trans* isomer of the dienes gives adducts where the 1,4-substituents will be oriented towards different faces of the ring.⁵⁹

Endo approach

The substituents of the dienophile can be either *endo* or *exo* in the product, depending upon the orientation of the diene and dienophile with each other in the transition state. The substituents on the dienophile can be down towards the diene (*endo* approach) or up away from the diene (*exo* approach). Based on the stereochemistry of a large number of Diels-Alder reactions, Alder formulated an empirical rule known as *endo* addition rule.^{58,60} According to this rule, the most stable transition state results, when a maximum accumulation of unsaturated centers of the diene and dienophile overlap. Such an overlap is known as a secondary orbital interaction and will lead to energetically more favorable *endo* transition state with a 3 kcal⁻¹ mol difference to the *exo* transition state, sufficient enough to tip the scale in favor of the *endo* product.⁶¹

An example of *endo* selective D-A reaction where the power of strategies to exert stereochemical control is reflected in the total synthesis of the plant hormone gibberellic acid (**69**) by Corey *et al.*⁶² The initial chemo- and regioselective Diels-Alder reaction between diene (**70**) and quinone (**71**) leads to *cis*-decalin (**72**) as a single diastereomer in excellent yield via *endo* transition-state (Scheme 13). The subsequent elaboration to (**73**) enabled a substrate-controlled intramolecular Diels-Alder reaction, which proceeded with selective formation of the expected product (**74**). Further modification of tetracyclic intermediate (**84**) produced gibberellic acid (**69**).



Scheme 13. Use of both inter- and intramolecular Diels-Alder reactions in the stereocontrolled synthesis of gibberellic acid (**69**) by Corey *et al.*⁶²

The outcome of the Diels-Alder reaction in these intramolecular instances is generally predictable based on the stereochemical requirements of the resident set of functionalities.

However, the use of high temperature and extended reaction time can lead to a formation of a thermodynamically more favorable *exo* product due to the reversible nature of Diels-Alder with elevated temperatures.⁶¹

Regioselectivity

When the Diels-Alder reaction takes place between an unsymmetrical diene and a unsymmetrical dienophile, a formation of mixtures of regioisomers is possible. Dienes with a substituent on the 1-position can give 1,2- (*ortho*) and 1,3- (*meta*) disubstituted adduct. When the substituent is on the 2-position, a mixture of 1,3- and 1,4- (*para*) adduct can be formed, however, the Diels-Alder reaction gives *ortho* and *para* adducts predominately over *meta* adducts (an example of 1,2-adduct for compound (**72**)). This observed high regioselectivity can be explained by frontier orbital theory, and by the coefficients of the frontier orbitals of the diene and dienophile.⁶³

2.1.2.2 Diels-Alder reactions on solid-phase

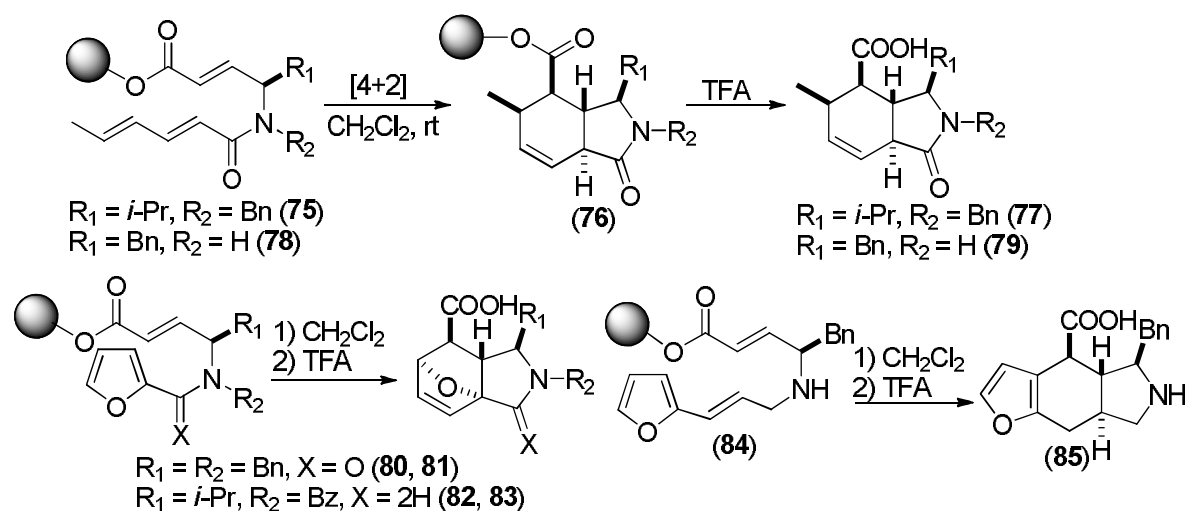
Originally developed for a peptide synthesis, Merrifield⁶⁴ introduced solid-phase synthesis of a tetrapeptide in 1963. He was later awarded the Nobel Prize in chemistry in 1984 for the significance and novelty of the method. Solid-phase methods were used first in peptide synthesis where the high efficiency of the method was demonstrated. Later in the 1970s, the method was applied to the synthesis of small organic compounds for the first time. During the 1990s, the development of solid-phase organic chemistry progressed rapidly and numerous novel solid-phase synthesis methods were utilized in combinatorial chemistry.^{65,66,67} In addition, the first total syntheses of complex natural products, such as epothilone⁶⁸ and sarcodictyin,⁶⁹ were performed on solid support.

The Diels-Alder reactions have been conducted with either the dienophile or the diene linked to the support. The reaction conditions and the regio- and stereoselectivities observed are similar to those in solution. Therefore, it is not surprising that several examples of solid-phase Diels-Alder reactions were reported in the literature, including classical intermolecular, inverse electron demand, hetero- and intramolecular Diels-Alder reactions performed on polymeric support.⁷⁰ Two selected examples of D-A reactions conducted on solid-phase are presented below.

Sun and Murray⁷¹ investigated several solid-phase Diels-Alder reactions of amino acid trienes in intramolecular context. These reactions gave highly functionalized hydroisoindole derivatives. The polymer-bound triene (**75**) participates in the intramolecular Diels-Alder reaction in CH₂Cl₂ at ambient temperature to give resin-bound cycloadduct (**76**) (Scheme 14). The product (**77**) was obtained as a carboxylic acid in 48% yield after trifluoroacetic acid-mediated ester cleavage from the resin. In similar fashion, the intramolecular [4+2] cycloaddition of the triene (**78**) in CH₂Cl₂ at room temperature gives the cycloadduct (**79**) as a single reaction product in 55% yield. According to the authors, the diastereoselectivity of the solid-phase cycloaddition reactions resembles that of the corresponding solution-phase reactions. The favored reaction pathway traverses through the *endo* transition-state, and the steric bulk of the γ -substituent (R₁ = Bn) affects the 1,3-allylic interaction of the dienophilic part of the triene.

The same authors studied the intramolecular solid-phase Diels-Alder reaction of trienes containing a furan ring moiety, which has been found to be a useful auxiliary in the

synthesis of functionalized heterocyclic compounds. The resin-bound furoic amide triene (**80**) underwent the intramolecular Diels-Alder reaction at room temperature to produce the epoxyhydroisoindoline (**81**) in 55% yield (Scheme 14). A furfuryl group was also tested for the intramolecular Diels-Alder reactions. The isopropyl-substituted triene (**82**), with an *N*-benzoyl tertiary amine, participated in the [4+2]-cyclization reaction that was carried out in CH₂Cl₂ for 60 h. The product (**83**) was isolated as a single isomer in 65% yield, being the highest of the entire series.

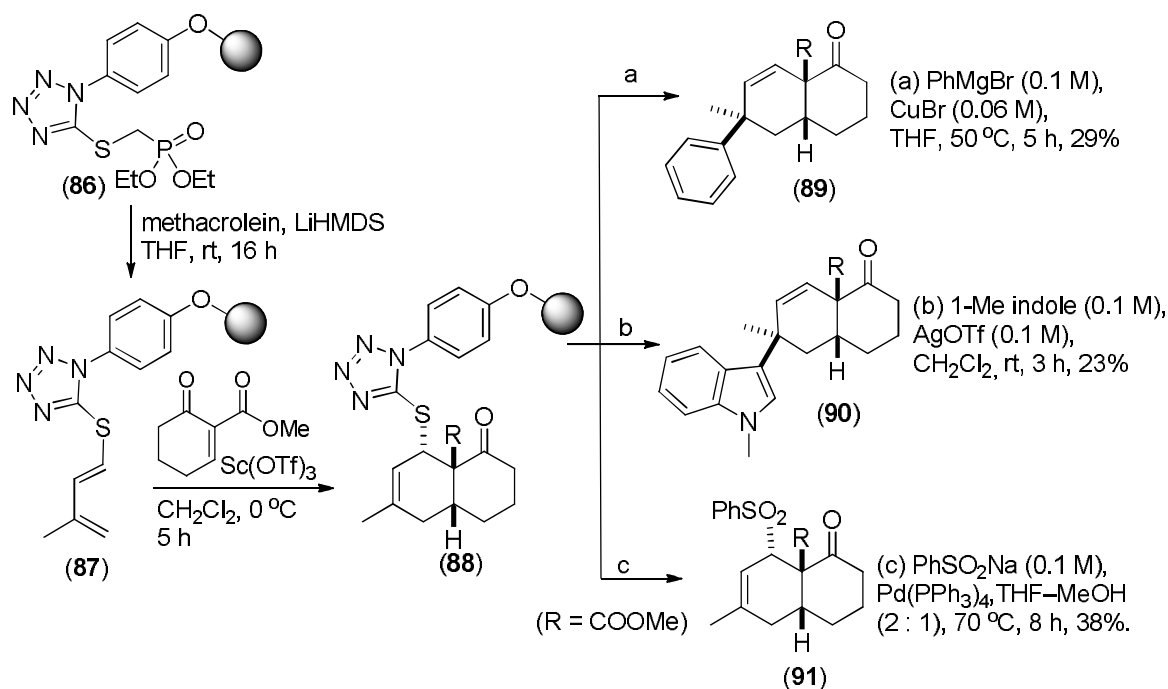


Scheme 14. A series of intramolecular Diels-Alder cycloadditions studied on solid-phase.

All of the intramolecular cycloaddition reactions of furan-substituted trienes studied followed the *endo* route.⁷¹ Finally, Sun and Murray investigated the solid-phase intramolecular Diels-Alder reaction of the vinylfuran derivative (**84**) (Scheme 14).⁷¹ The reaction of triene (**84**) went to completion in CH₂Cl₂ at room temperature for 2 days. The intramolecular Diels-Alder reaction was followed by a rearrangement process where the aromaticity of the furan ring was restored. The *trans*-fused tricyclic product (**85**) was obtained in 37% yield

Compound libraries based on the decalin-scaffold occurring in numerous natural products have yielded novel and potent inhibitors of several tyrosine kinases such as VEGFR-2 (vascular endothelial growth factor receptor 2), reported by the group of Waldmann.^{72,73} Recently, the authors reported a traceless synthesis of a functionalized decalin scaffold on solid support, including a diversity generating cleavage.⁷⁴ The 5-thiazole linker was immobilized on a polymeric support (Rink amide) and the polymer-bound diethyl phosphonate (**86**) was used in the Horner-Wadsworth-Emmons olefination with methacrolein and LiHMDS (lithium hexamethyldisilazide) as a base to give the polymer-bound diene (**87**) (Scheme 15). The subsequent Diels-Alder reaction, with 2-methoxycarbonyl cyclohexenone as a dienophile and Sc(OTf)₃ as a Lewis acid catalyst, gave the desired polymer-supported *cis*-1,2-dehydrodecalin derivative (**88**) with full conversion (by NMR) after TFA release from resin (Scheme 15).

The allylic position of the 5-thiotetrazole linker allowed an elegant diversity-generating cleavage by metal-assisted nucleophilic reactions. Employing Pd(0), Cu(I), and Ag(I) reagents significantly extended the scope of the linker system and the released functionalized *cis*-decalins (**89–91**) (Scheme 15).⁷⁴ Interestingly, the use of palladium led to the replacement with stereochemical net retention (double inversion) of the 5-thiotetrazole moiety, when phenylsulfinate was employed in compound (**91**).



Scheme 15. Synthesis of *cis*-decalin (**88**) on solid support and subsequent diversity generating cleavage by metal catalysis.

Since its discovery, the Diels-Alder reaction has been the most widely used synthetic tool in organic chemistry. Many modifications have been developed, such as inverse electron demand,^{43,44} hetero,^{43,53,75} intramolecular^{76,77,78} and asymmetric^{79,80,81,82,83,84,85} Diels-Alder reactions. Control of both diastereoselectivity and enantioselectivity is very important in the field of total synthesis, where the use of the D-A reaction has afforded numerous solutions and applications in the construction of natural products.⁸⁶ Nature's repertoire of biosynthetic transformations has been recognized to include the biosynthetic Diels-Alder cycloaddition reactions including five isolated and purified enzymes thus far, that are consistent in the catalysis of the Diels-Alder reaction.^{87,88,89,90,91}

2.2 Protein kinases

Protein kinases, known also as phosphotransferases, are key regulators of cell function that constitute one of the largest and most functionally diverse gene families. By adding phosphate groups to substrate proteins, protein phosphorylation plays a significant role in a wide range of cellular processes. The human genome contains 518 protein kinase genes and they constitute about 2% of all human genes.⁹² Up to 30% of all human proteins may be modified by kinase activity, and protein kinases are known to mediate most of the signal transduction in eukaryotic cells by modification of substrate activity. Protein kinases also control many other cellular processes, including metabolism, transcription, cell cycle progression, cytoskeletal rearrangement, cell movement, apoptosis, and differentiation. Since protein kinases have profound effects on a cell, their activity is highly regulated. Kinases are turned on or off by phosphorylation (sometimes by the kinase itself by autophosphorylation), by binding of activator proteins, inhibitor proteins, or small molecules, or by controlling their location in the cell relative to their substrates. Protein kinases are seen as potential therapeutic targets since mutations and dysregulation of protein

kinases play causal roles in multiple human diseases, affording the possibility of developing modulators (inhibitors) of these enzymes for use in disease therapy.^{93,94,95}

2.2.1 Protein kinase inhibitors

Background – the discovery of staurosporine

The importance of protein phosphorylation became known more than 30 years ago when the first connections between abnormal protein phosphorylation and disease also became evident.⁹⁶ In 1981, Nishizuka and his colleagues discovered that tumor-promoting phorbol esters (**92**) were potent activators of protein kinase C (PKC).⁹⁷ The first protein-kinase inhibitors were developed in the early 1980s based on the discovery of isoquinoline sulphonamides, which showed inhibition of cyclic nucleotide-dependent protein kinase and protein kinase C. One of the compounds, fasudil hydrochloride,⁹⁸ progressed to human clinical trials and was approved for the treatment of cerebral vasospasm, however being a non-specific inhibitor of several protein kinases.⁹⁹

In 1977 the discovery of staurosporine¹⁰⁰ (**93**, antibiotic AM-2282) (Figure 1), a natural product fungicide produced by the bacterium *Streptomyces staurosporeus*, was the first of over 50 alkaloids to be isolated with this type of bis(indole) chemical structure and showed nanomolar inhibition of PKC.¹⁰¹ Despite the structure determination in 1978, the first total chemical synthesis was achieved in 1996.¹⁰² The same bacterium also produces bis(indole) maleimide rebeccamycin¹⁰³ (**94**, Figure 1), with high structural similarity to staurosporine, but has surprisingly no affinity to protein kinases. Rebeccamycin does however carry significant antitumor properties *in vitro* by inhibiting topoisomerase I.^{104,105} Staurosporine (**93**) had enormous impact on the pharmaceutical industry, where it was used along with its derivatives in cell-based assays by hundreds of laboratories to invoke a myriad of roles for PKC. However, it and several other bisindolylmaleimides were later shown to lack specificity, since their inhibition of multiple other protein kinases *in vitro* as well.⁹⁹ Several staurosporine analogs have progressed to human clinical trials, despite the fact that it is unclear whether their efficacy overcomes the inhibition of PKC, another protein kinase, or the combined inhibition of several kinases. Naturally occurring 7-hydroxystaurosporine¹⁰⁶ (**95**) (Figure 1) blocks cell-cycle progression and might act by inhibiting the cell-cycle checkpoint-control kinase (CHK1). *N*-benzoylstaurosporine,¹⁰⁷ (**96**) also known as midostaurin, is a multi-target kinase inhibitor entered in phase III clinical trials for treatment of acute myeloid leukemia (AML).¹⁰⁸ Ruboxistaurin^{109,110} (**97**, LY333'531) belongs to a class of synthetic macrocyclic bisindolylmaleimides with a simplified structure, and was reported to inhibit PKC β isoform (IC₅₀ = 4.7 nM)¹¹⁰ more potently over other PKC isoforms. It has been shown to normalize the elevated levels of PKC activity in the retina and kidneys of diabetic rats¹¹¹ and is currently in phase III clinical trials for the treatment of diabetic microvascular disease and retinopathy.

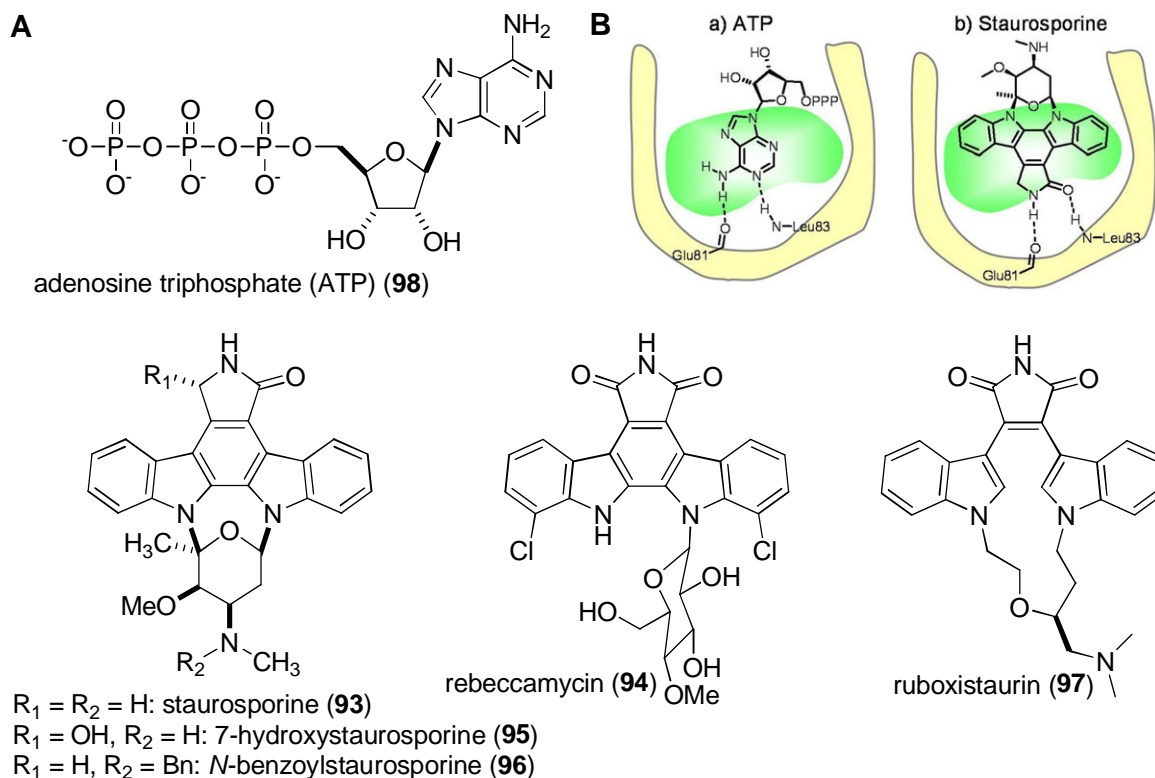


Figure 1. *A*) Chemical structures of ATP and some ATP-competitive natural, semisynthetic and synthetic bis(indole) alkaloids. *B*) A schematic example of ATP-binding pocket in cyclin dependent protein kinase 2 (CDK2) in complex with a) ATP and b) staurosporine. The green area indicates protein surface with high hydrophobicity.¹¹²

The first selective protein kinase inhibitors

The majority of the protein-kinase inhibitors that were developed by the end of the 1980s had bis(indole)alkaloid in their structures. Due to the ATP-competitive mode of action, it became obvious that such compounds were insufficient to compete with the high intracellular concentrations of ATP (**98**) (2–10 mM). In addition, the determination of the first 3D-structure of a protein kinase A (PKA)¹¹³ showed that the residues involved in ATP binding pocket possessed high similarity from kinase to kinase. Therefore, at that time it was strongly believed that it was ‘impossible’ to develop specific protein kinase inhibitors with the required high affinity. However, the identification of the cellular targets for cyclosporin A¹¹⁴ and FK506¹¹⁵ (tacrolimus) in 1991 changed that belief, since it was found that both of these agents were potent and specific inhibitors of calcineurin,¹¹⁶ a Ca^{2+} -calmodulin-dependent protein kinase.

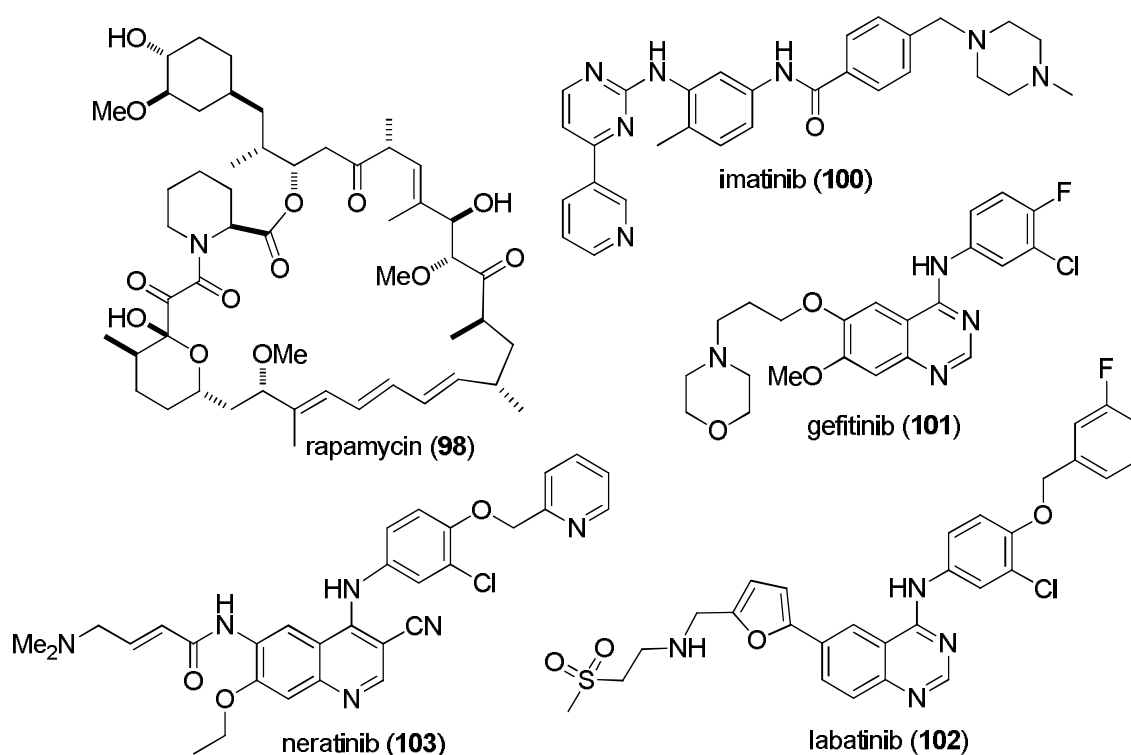
Maybe the most important finding was related to immunosuppressant drug rapamycin¹¹⁷ (**98**, sirolimus), which is produced by *Streptomyces hygroscopicus*, a soil bacterium that originates from Easter Island. Rapamycin was identified more than 30 years ago and was originally developed as an antifungal agent. The anticancer properties of rapamycin were noticed after its discovery but the mechanism of action remained unclear until the molecular target of rapamycin in yeast was identified to be a protein kinase, named “target of rapamycin” (Tor).¹¹⁸ The mammalian homolog mTOR was identified later. Rapamycin (**98**) was the first drug approved for clinical use that inhibited one protein kinase specifically.⁹⁹ Despite the fact that cyclosporine A, FK506, and rapamycin (**98**) are highly potent and useful compounds as immunosuppressants and anti-cancer agents, they lack one crucial

property – they are not orally bioavailable – therefore their medicinal use is hampered.

Imatinib – first selective and orally available small molecule kinase inhibitor

In the field of oncology, efforts to develop orally active drugs that target specific protein kinases have been extensively focused and a number of kinase inhibitors have already been developed and approved for cancer treatment. Some of the most promising drugs developed are inhibitors of protein tyrosine kinases, which have been seen as excellent targets for cancer chemotherapy. Imatinib¹¹⁹ (**100**) was the first member of this new class of agents by specifically inhibiting Abelson tyrosine kinase (ABL) and is used for treatment of chronic myelogenous leukemia (CML). Although imatinib is an ATP competitive inhibitor, the determination of the 3D structure of ABL in complex with it showed that the drug extends much further into the catalytic site¹²⁰ and binding of imatinib induces a structural transition, where the kinase adopts the inactive conformation.

Another important tyrosine kinase in the field of oncology is EGFR (epidermal growth factor receptor), which is overexpressed in many cancers of epithelial origin. Gefitinib (**101**),¹²¹ erlotinib¹²¹ and lapatinib (**102**)¹²² are selective inhibitors of EGFR with a common 4-anilinoquinazoline structure, used in clinics against a variety of cancers. The second generation inhibitors of tyrosine kinases such as neratinib (**103**),¹²³ are able to irreversibly inhibit Her2/neu (human epidermal growth factor receptor 2) and EGFR kinases, and are currently being used in human clinical trials.



While the protein kinase inhibitors have shown their efficiency in the treatment of various cancers, the long-term side effects are not known. Resistance can also be an issue since many patients who were treated with imatinib have become resistant, due to mutations in Abl. Therefore, kinase inhibitors might be most effective if administered in combination.⁹⁵

2.2.2 Protein kinase C

The protein kinase C (PKC) family of serine/threonine protein kinases includes at least ten mammalian isoforms¹²⁴ that are involved in intracellular signal transduction cascades and in cellular events such as proliferation, differentiation and apoptosis.^{125,126} The PKC family can be divided into three subgroups according to their structures and activation mechanisms.¹²⁴ Classical/conventional PKCs (cPKCs: α , β_I , β_{II} , and γ) require calcium and diacylglycerol (DAG, **104**) (Figure 2) for activation, whereas novel PKCs (nPKCs: δ , ϵ , η , and θ) need only endogenous DAG for activation. In contrast to cPKCs and nPKCs, atypical PKCs (aPKCs: ζ , ι/λ) require neither calcium nor DAG for activation. Only the regulatory C1 domains of cPKCs and nPKCs are capable of binding DAG and tumor-promoting phorbol esters (**92**) (Figure 2), leading to enzyme activation.⁹⁷ Aberrant signaling through PKC isoforms and other C1 domain containing proteins has been correlated to a number of human ailments, including neurological diseases;¹²⁷ especially Alzheimer's disease,^{128,129,130} immunological^{131,132} in addition to cardiovascular^{133,134,135} diseases and cancer.^{136,137,138} Therefore, PKC and other C1 domain-containing proteins have been subjects of intensive research and drug development.¹³⁹

Structure, function and regulation

The structure of all PKCs consists of a regulatory domain and a catalytic domain tethered by a proteolytically labile hinge region. The C-terminal catalytic domain is highly conserved among all the different isoforms, whereas the N-terminal regulatory domain is less consistent.¹²⁴ The amino terminus of the PKCs contain several shared subregions. Diacylglycerol (**104**) is a pivotal lipid second messenger and a natural agonist of the C1 domain which is present in all of the isoforms of PKC. The phorbol esters (**92**) (Figure 2) are shown to bind similarly as DAG to the C1 domain. However, in atypical PKCs, the C1 domain is incapable of binding neither DAG nor phorbol esters. The Ca^{2+} -binding C2 domain can be found in the regulatory part of conventional and novel isoforms, but is functional as a Ca^{2+} sensor only in the cPKCs. Extensive biochemical studies have established that protein kinase C is allosterically regulated by its pseudosubstrate.^{124,140} This small oligopeptide mimics the substrate and binds in the substrate-binding cavity in the catalytic domain, thus keeping the enzyme inactive.

The PKCs are non-receptor kinases, which in the inactive conformation can be found in the cytoplasm of cells.¹²⁵ When calcium and DAG are present in sufficient concentrations, they bind to the C2 and C1 domain, respectively, enabling PKC to localize into various membranes.^{141,142} Actually, the isoform-specific effects on cells are a result of the different subcellular localizations of the isoforms of PKC.^{143,144} The interaction with the membrane induces the conformational change of the enzyme causing the pseudosubstrate to move out from the ATP-binding site.¹²⁵ The conformational change of the enzyme reveals the hinge region which becomes proteolytically labile and if cleaved, reveals the essential kinase domain.¹²⁴

The catalytic domain of protein kinase C has approximately 40% amino acid identity with PKA.¹²⁴ Molecular modeling based on the solved structure of protein kinase A¹¹³ has been useful in identifying surface-exposed residues.¹⁴⁴ The residues involved in both catalysis and maintenance of the fold of the kinase domain, are conserved, with differences in residues found primarily on the surface of the protein. The conventional and novel PKCs have three phosphorylation sites; the activation loop, the turn motif, and the hydrophobic motif. The atypical PKCs are phosphorylated only on the activation loop and the turn motif.

These phosphorylation events are essential for the activity of the enzyme and for its correct intracellular localization.¹²⁴ 3-Phosphoinositide-dependent protein kinase-1 (PDK-1)^{124,145} is the upstream kinase for all protein kinase C isoforms and is responsible for initiating the process by transphosphorylation of the activation loop.¹⁴⁶

The C1 domain of PKC

In conventional and novel PKCs the regulatory part contains two DAG-/ phorbol-binding C1 domains, named C1a and C1b.^{124,147} Atypical protein kinase C's contain a single copy of the domain and are not able to bind phorbol esters. The crystal structure available for C1 domain was determined for PKC δ complexed with phorbol 13-*O*-acetate by Zhang *et al.* in 1995 (Figure 2b).¹⁴⁸ In addition, the crystal structure of the full-length β II isoform of protein kinase C was published in 2011.¹⁴⁹ Crystal and NMR¹⁵⁰ structures have revealed that C1 domain is Cys-rich region of approximately 50-residue long sequence containing two zinc finger structures, where the Zn²⁺ ions are coordinated by His and Cys residues at opposite ends of the primary sequence, helping to stabilize the domain. Elucidation of the structure of the C1b domain of PKC δ in the presence and absence of bound phorbol acetate unveiled the mechanism of how ligand binding recruits the C1 domain to be partly buried in the membrane.^{148,151} Binding of the ligand does not result in any significant conformational change in the domain. However, it dramatically alters the surface properties of the polar groove, where the ligand acts as a cap on the top part of the domain to produce a continuous hydrophobic surface and thus masking the polar groove for membrane interaction.¹⁴⁹ It should be mentioned that many proteins unrelated to protein kinase C contain typical or atypical C1 domains, capable of binding phorbol esters.¹⁵²

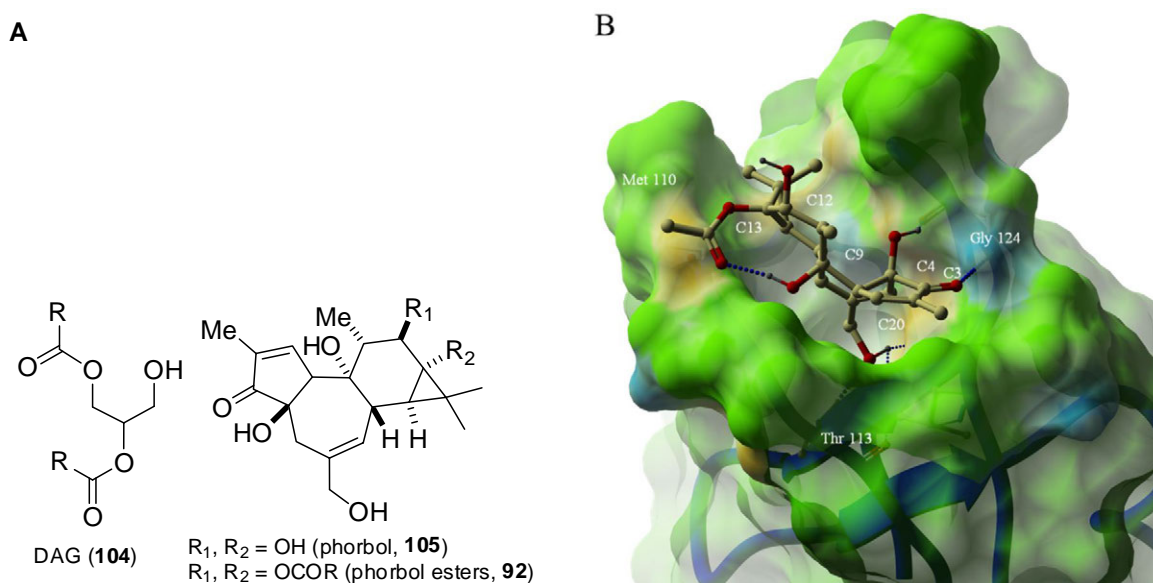


Figure 2. **A)** Structures of 1,2-diacylglycerol (DAG, 104), phorbol (105) and phorbol esters (92). **B)** The crystal structure of the PKC δ C1b domain complexed with phorbol 13-*O*-acetate (ball and stick representation) (2.2 Å resolution, PDB ID: 1PTR).¹⁴⁹ Top view of the binding pocket of the crystal structure. The surface is colored as: oxygen atoms (yellow), nitrogen atoms (blue), carbon atoms (green) and rest of the C1b surface is colored (green). The figure is created with ICM-Browser (version 3.7-2a, MolSoft L.L.C.).

The C1-domain as a target for natural and synthetic compounds

As discussed earlier, the high intracellular concentrations of ATP together with the consistent structure of the catalytic site among protein kinases sets limits for the development of protein kinase inhibitors for clinical use with a high risk of producing side effects.¹⁵³ Since many protein kinases such as PKA and PKC have regulatory domains as part of their structure, however, another strategy to modify protein kinase activity presents itself. The PKC regulatory domain, C1, is unique to PKC and found only in a small number of kinases, offering a selectivity advantage, making the C1-domain an attractive drug target.¹⁵⁴ Such kinase inhibitor would probably have specificity for PKCs over other kinases and it would enable the possibility to discover PKC isozyme selective inhibitors. In addition, unlike agents that binds to the ATP binding site thereby inhibiting kinase function, C1 domain binders could inhibit or activate kinase activity.¹⁵⁵ A number of natural compounds targeting the C1 domain of PKC have been discovered. Some of them will be presented as examples here together with some simplified synthetic analogs.

Bryostatins

The bryostatins are a group of 20 macrolide lactones first isolated from the marine bryozoan *Bugula neritina* in 1968 followed by the elucidation of the structure of bryostatin 1 (**106**) (Figure 3) in 1982.¹⁵⁶ It has been established that the true source of the bryostatins is not actually bryozoans but rather its bacterial symbiont.¹⁵⁷ Regardless of bryostatin 1 being (**106**) a well-known natural compound, its highly complex structure featured with three heavily substituted pyran rings (A, B and C) with numerous stereocenters, it was nearly 30 years before the first total synthesis of bryostatin 1 was published.¹⁵⁸ Bryostatins (Figure 3) are potent modulators (activators) of protein kinase C and bind in a similar fashion to phorbol esters and diacylglycerols in the cysteine-rich C1a and C1b domains of PKC.¹⁵⁹ However, while the phorbol esters (**92**) are tumor promoters, the bryostatins have antineoplastic activity. Bryostatin 1 (**106**) induces a rapid activation and autophosphorylation of PKC that results in the translocation of the PKC enzyme to the membrane. Interest in the bryostatins has been intense due to a wide range of potent bioactivities associated with them. The most well-studied bryostatin 1 (**106**) has nanomolar affinity (K_i 1.40 nM) for PKC α .¹⁶⁰ It has shown activity against a range of cancers *in vivo*¹⁶¹ and been used, therefore, in numerous clinical trials, despite its low natural abundance, difficult isolation,¹⁶² and structural complexity.

In addition to its anticancer properties, bryostatin 1 (**106**) has been shown to synergize the effects of other antineoplastic agents,^{163,164} and is active against conditions, such as stroke¹⁶⁵ and diabetes.¹⁶⁶ Unlike most antineoplastic agents, it also stimulates the immune system.¹⁶⁷ Bryostatin improves learning and extends memory in animal models,^{168,169} serving as a significant lead for treatment of cognitive dysfunctions, including Alzheimer's disease.¹⁷⁰ The development of new methods to produce bryostatin has received much focus, due to its low natural abundance. Mendola and his colleagues have developed an efficient in-sea aquaculture method for producing *Bugula neritina*, capable of providing 100–200 g of bryostatin 1 annually.¹⁷¹ The group of Haygood, in tandem, have discovered the *Bry* genes, and is attempting to transfect these genes into other bacteria.¹⁶¹

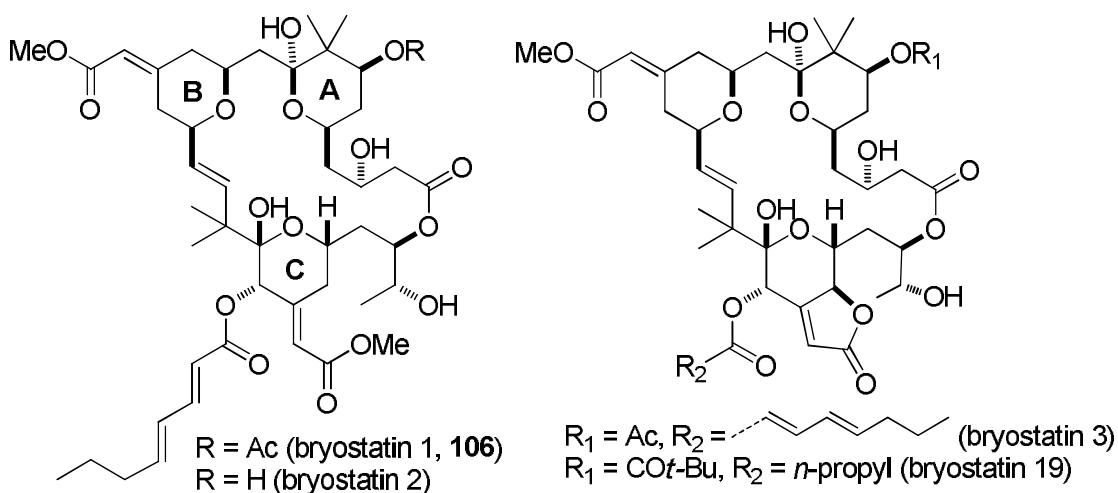


Figure 3. Some members of natural bryostatin macrolide lactones.

Bryostatin analogs

Since the total syntheses of bryostatins require generally over 40 linear steps,^{172,173} substantial interest in the synthesis of simplified analog structures has emerged.¹⁷² Wender *et al.* have developed synthetic routes to stripped derivatives of bryostatins for 25 years by reducing the number of synthetic steps.^{174,175,176} Among the first members of biologically active synthetic bryostatins, analog (**107a**)¹⁷⁴ (Figure 4), bearing B-ring cyclic acetal construction and several other structural simplifications (stripped A and B rings, lack of 7-OAc, 8-dimethyl and 9-OH groups, and absence of B-ring C13 olefin substituent), was reported to show *in vitro* activity comparable to that of bryostatin 1 (bryostatin 1: $K_i = 1.35$ nM; (**107a**): $K_i = 3.4$ nM).¹⁷⁴ The same authors proved that the secondary hydroxy at C3 of (**107a**) (Figure 4) is essential for the correct orientation of the macrocycle and thus for the high affinity.¹⁷⁴ When the methyl substituent at C26 of compound (**107a**) was replaced with a hydrogen atom, compound (**107b**, picolog)¹⁷⁶ was reported to be 100-fold more potent than bryostatin 1 at inhibiting the growth of numerous human cancer cell lines and showed promise in treating mice with leukemia.¹⁷⁶

Another group of important synthetic bryostatin derivatives introduced by the Keck group, are so-called Merles, which bear the same structural feature of A, B-ring bipyran construction, found in natural bryostatins (Figure 4).^{177,178} For example, the three reported that analogs with C7,13 *exo*-methylene substituents on both A- and B-rings (**108a–c**) have higher affinity for PKC α than bryostatin 1 (**106**). The same authors reported preparation of simplified analogs around both A- and B-rings. Despite high structural similarity to bryostatins, the derivatives with a simplified A-ring interestingly did not behave like bryostatins but rather like tumor-promoting phorbol esters (**92**).^{179,180} However, Keck's compound (**109**, Merle 28)¹⁸⁰ (Figure 4) bearing the critical residues of the C7–C9 region around the A-ring has antiproliferative properties that are similar to the natural bryostatin 1.

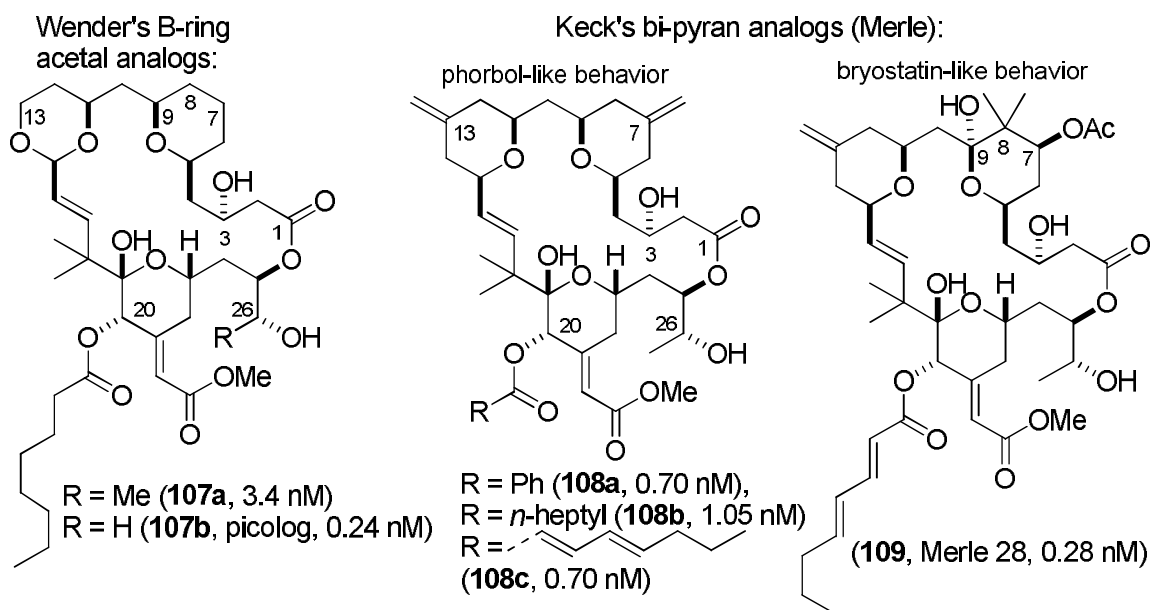
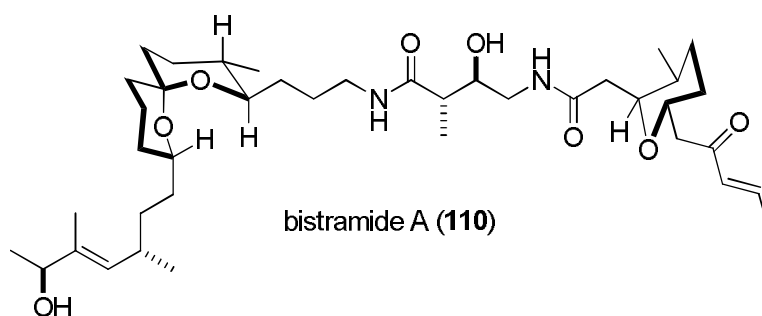


Figure 4. Synthetic derivatives of bryostatins. K_i values for PKC α in brackets.

Bistramides

The discovery of a novel marine metabolite from ascidian *Lissoclinum bistratum* in New Caledonia, named bistramide A (**110**) (bistratene A) was reported by Verbist *et al.* in 1988,¹⁸¹ followed by the isolation of four additional members (bistramide B–D, K) of the family four years later.¹⁸² In 2004, the Kozmin group reported the total synthesis of bistramide A (**110**), with complete assignment of the stereochemistry.¹⁸³ Bistramide A was initially found to possess potent cytotoxic¹⁸⁴ and neurotoxic^{185,186} properties and with profound impact on cell cycle regulation, leading to growth arrest, differentiation, and apoptosis in several cell lines.^{187,188} Subsequent studies revealed that bistramide A induced highly selective activation of a single PKC isotype δ .¹⁸⁹ However, bistramide A (**110**) shows only micromolar affinity against PKC δ ($K_i = 28 \mu\text{M}$), thus is not very potent. The primary cellular receptor for bistramide A was described to be actin, by Statsuk *et al.* in 2005.¹⁸⁸ In addition, it is reported that bistramide A (**110**) does not activate PKC δ *in vitro* and either does it compete with phorbol esters in the C1 domain.^{188,190,191} While bistramide A failed to translocate green fluorescent protein (GFP)-PKC δ in rat basophilic leukemia (RBL) cells,¹⁸⁸ the immunostaining and fractionation studies showed migration of PKC δ to the perinuclear region rather than nuclear or plasma membrane.¹⁸⁹ In addition, only specific substrates were shown to be phosphorylated in the presence of (**110**), and therefore it is discussed to be a result of a plausible atypical mode of activation.¹⁹²

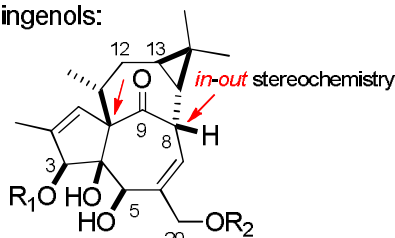


Ingenols

Isolated in 1968 by Hecker,¹⁹³ ingenol (**111**) (Figure 5) belongs to a group of naturally occurring ingenane diterpenes that possess the same bicyclo[4.4.1]undecane ring system with variation in peripheral functionalities.¹⁹⁴ Compared to structurally closely related phorbol (**105**), ingenol (**111**) is more lipophilic and shows micromolar affinity to PKC (K_i values 10 mM and 30 μ M, respectively). Ingenol esters, like ingenol 3-hexadecanoate (**112**)^{193,195} and ingenol 3-tetradecanoate (semisynthetic, **113**)¹⁹⁶ (Figure 5), are however highly potent tumor promoters and powerful activators of PKC.¹⁹⁷ Since the early 1980s, numerous attempts have been made to synthetically reproduce the combination of important biological function and challenging complex architecture,¹⁹⁸ leading finally to the total synthesis of ingenol (**111**), published by Winkler *et al.* in 2002.¹⁹⁹ The importance of the indispensable *trans* bridgehead or *in-out* stereochemistry of the ingenol core is clear since the thermodynamically less strained and more stable C8 epimeric (*out-out*) isoingenol analog (**114**, Figure 5),²⁰⁰ having the fully elaborated AB-ring, completely lacks the biological activity related to ingenol esters.

Ingenols can be extracted from the sap of *Euphorbia peplus* L., and used in traditional medicine to treat conditions such as skin tumors, migraines and parasites. In addition, the ingenanes display interesting biological profiles that range from tumor-promoting, to *anti-leukemic*, and *anti-HIV* activities.²⁰¹ Ingenol angelate, or PEP005 (**115**) (Figure 5), is a selective activator of the classical and novel PKC isoenzymes and has both *anti-cancer* and proinflammatory effects, and has shown promising results in the treatment of skin tumors.^{202,203} Naturally occurring C20-acetylingenol angelate (PEP008, **116**) (Figure 5), was recently reported to arrest the growth of solid tumors derived from breast cancer, colon cancer, and melanoma cell lines *in vitro*.²⁰⁴

natural ingenols:

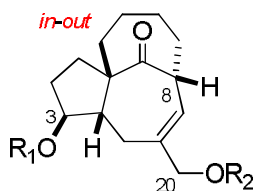
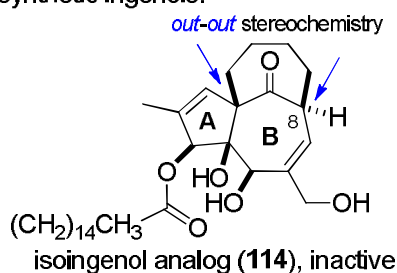


$R_1 = R_2 = H$ (ingenol, **111**)
 $R_1 = CO(CH_2)_{14}CH_3$, $R_2 = H$ (ingenol 3-hexadecanoate **112**)
 $R_1 = CO(CH_2)_{12}CH_3$, $R_2 = H$ (**113**, semisynthetic)
 $R_1 = R_2 = Bz$ (IDB, **117**)

$R_1 = \text{angelate}$, $R_2 = H$ (3-ingenol angelate, PEP005, **115**)

$R_1 = \text{acetyl}$, $R_2 = Ac$ (PEP008, **116**)

synthetic ingenols:



$R_1 = R_2 = Bz$ (**118a**)
 $R_1 = Bz$, $R_2 = H$ (**118b**)

Figure 5. Natural ingenol diterpenoids and examples of synthetic derivatives.

The polyhydroxylated southern region plays a key role in the biological activity of ingenoids.²⁰⁵ The apoptotic activity of ingenol (**111**), ingenol dibenzoate²⁰⁶ (IDB, **117**, Figure 5) and various C3, C5, and C20 analogs was investigated in the leukaemia Jurkat-cell line by Blanco-Molina *et al.*²⁰¹ The authors reported that esterification of the 20-hydroxy was required to induce apoptosis, while a free 5-hydroxy was critical for PKC

activation. The dibenzoate (**117**) induced apoptosis in a dose-dependent manner, however not *via* a PKC-mediated pathway, but *via* caspase-3 activation.²⁰³ In contrast, ingenol itself (**111**) did not induce significant apoptosis even at the higher doses.

Winkler *et al.*²⁰⁷ reported the synthesis of simplified ingenol analogs with the same *in-out* stereochemistry (Figure 5) as found in natural ingenols. While the C3,20-dibenzoyl compound (**118a**) was found to be inactive for PKC α , the 3-monobenzoate derivative (**118b**) showed micromolar affinity with a K_i of 0.17 μ M.²⁰⁷ The same authors hypothesized that loss of the C20 ester of ingenol might occur *in vivo*, giving the more active monoester.

Summary of the natural and synthetic compounds targeting the C1 domain

Though compounds binding to C1 domain can be obtained from natural sources, the isolated yields are usually very low with a need to be harvested from sensitive ecosystems, such as seas and oceans. In addition, the compounds often have highly complex structures and therefore the total syntheses of the compounds are laborious. However, studies with these compounds have yielded valuable pharmacophores, which have been used to develop simplified analogs of the natural compounds, such as those found in synthetic bryostatin (**107–109**), for example.

While the biological potential of synthetic ingenols has been somehow disappointing, the discovery of new naturally occurring ingenols is encouraging. Ingenol angelate (PEP005, **115**) has been shown to be a potential treatment of skin tumors and PEP008 (**116**), another naturally occurring ingenol derivative, has only recently been reported to arrest the growth of a variety of solid tumors *in vitro*. A comprehensive review on recent developments in the C1 domain targeting compounds has been published recently.¹³⁹

2.2.3 Pim kinases

The three Pim family members (Pim-1, Pim-2 and Pim-3) form an evolutionary distinct subgroup of serine/threonine-specific kinases belonging to the group of calcium/calmodulin-dependent (CAMK) protein kinases. The name Pim refers to the original identification of the pim-1 gene in 1984 as a frequent proviral insertion site in Moloney murine leukemia virus-induced T-cell lymphomas.²⁰⁸ Pim kinases are highly homologous to each other and have partially overlapping functions and expression patterns.²⁰⁹ Interestingly, unlike most other protein kinases, Pim kinases are unusual since they are kept in a constitutively active conformation,²¹⁰ thus the enzymatic activity in a cell is dependent on the absolute amount of protein present. In hematopoietic cells, expression of Pim kinases is stimulated by numerous growth factors and cytokines such as interleukins.²¹¹ When overexpressed, Pim kinases are oncogenic and have been implicated both in hematopoietic malignancies such as leukemias and lymphomas²¹² and in numerous solid tumors such as prostate, colon, oral, hepatic and pancreatic cancers.^{213,214,215} Pim-1, -2 and -3 deficient mice have been generated and, while viable and fertile, have shown reduced body size and impairment of proliferation of hematopoietic cells in response to growth factors.²⁰⁹

Pim kinases promote tumorigenesis by supporting cell survival²¹⁶ and by enhancing resistance of cancer cells against chemotherapy²¹⁷ and radiation therapy.²¹⁸ Pim-1 is able to interact and phosphorylate several targets that are involved in cell cycle progression or apoptosis. Pim-1 can inhibit apoptosis through interactions with the anti-apoptotic molecules, bcl-2 (B-cell lymphoma 2) and Gfi-1 (growth factor independent 1 transcription repressor).²¹¹ In addition, all Pim family members phosphorylate and thereby inactivate the

pro-apoptotic BAD protein reported by several groups.^{219,220,221} This may explain why Pim kinases so efficiently cooperate with MYC (v-myc myelocytomatosis viral oncogene homolog) family transcription factors in the development of lymphoid or solid tumors. Even though MYC-overexpressing cells proliferate faster, they are more prone to apoptosis, therefore, a growth advantage is given to cells that also co-overexpress Pim kinases, which regulate the balance between anti- and pro-apoptotic factors and boost activities of transcription factors, that are essential for the production of cytokines and other survival factors. These conclusions are supported by recent reports by Wang *et al.*,^{222,223} showing that Pim-1 synergizes with MYC, both to induce advanced prostate carcinoma and to maintain tumorigenicity of the cancer cells. Furthermore, it was recently demonstrated that Pim kinases increase the metastatic potential of adherent cancer cells.²²⁴ Mice lacking activities of all the three Pim kinases are fertile and show only minor phenotypic abnormalities,²⁰⁹ therefore compounds selectively inhibiting Pim activity are not expected to have adverse side effects. For all these reasons, Pim kinases have become intriguing targets for cancer therapy.²²⁵

The crystal structure of Pim-1 and development of Pim inhibitors

Recently, the development of small molecule inhibitors against different types of protein kinases has enormously progressed, including compounds targeting Pim kinases.^{226,227} The potential for the development of Pim-selective inhibitors is enhanced by the crystal structure of Pim-1 (Figure 6)²¹⁰, which was solved in 2005 by multiple groups.^{210,228,229}

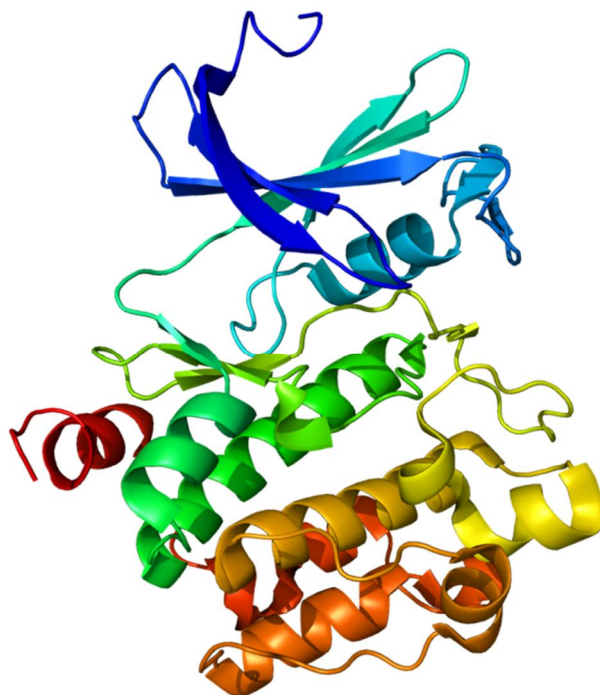


Figure 6. *Structural overview of the Pim-1 crystal structure at 2.1 Å resolution (PDB-code: 1XQZ).*²¹⁰

The hinge region that contains the ATP binding site of Pim-1 has a novel architecture, containing an additional amino acid residue not found in other protein kinases. This residue Pro123 lacks a key amide hydrogen bond donor and therefore does not allow the formation

of two hydrogen bonds to ATP present typically in protein kinase ATP complexes. This important and unique structural feature²³⁰ offers tremendous potential as a target for the design of Pim-inhibitors, which do not compete against more than 500 kinases that carry a conserved ATP-binding site to access high intracellular levels of ATP.

Staurosporine analogs

Several simplified staurosporine-like compounds have been investigated as Pim inhibitors, including macrocyclic bis(indolyl)maleimides such as PKC β inhibitor ruboxistaurin (**97**). The potency of (**97**) is much weaker against both Pim-1 (IC₅₀ = 200 nM,²³¹ 55 nM²²⁶) and Pim-2 (IC₅₀ = 20 μ M) than the stronger potency staurosporine (**93**), (Pim-1: IC₅₀ = 10 nM).²²⁸ However, (**97**) was found to effectively induce cell death and suppress growth of leukemia cells.²³¹ Another bis(indolyl)maleimide derivative (BIM-1, **119**) (Figure 7), with simplified structure, has been described along with the crystal structure of Pim-1 to show low nanomolar potency (Pim-1: IC₅₀ = 27 nM),²²⁸ thus inhibiting other kinases including PKC, MSK-1 (mitogen- and stress-activated protein kinase) and GSK-3 (glycogen synthase kinase 3).¹⁰⁰

The Meggers group has described staurosporine-mimicking, ruthenium-containing, organometallic complexes that show high potential as protein kinase inhibitors (Figure 7).^{232,233,234} In such metal complexes the coordinative bonds are kinetically inert and thus stable in biological environments: Thus they should behave as purely organic compounds, without displaying any metal-related cytotoxicities.²³⁵ Meggers *et al.* have previously reported potent, and Pim-1 selective, chiral ruthenium complexes, such as (*R*-**120a**) and (*S*-**120b**) substituted with a cyclopentadienyl ring and the CO group to the pseudotetrahedral ruthenium center.²³² The latter inhibits Pim-1 at concentrations more than two orders of magnitude lower compared to staurosporine (*S*-**120b**: IC₅₀ = 0.22 nM; staurosporine, **93**: IC₅₀ = 10 nM).²³² When the cyclopentadienyl ring is replaced with a tridentate 1,4,7-trithiacyclononane ligand, the racemic octahedral ruthenium complex (*rac*-**121a**)²³⁴ has nearly 20-fold potency for Pim-1 compared to staurosporine (**93**) (IC₅₀ = 0.45 nM) but unfortunately also displays affinity to GSK-3 α (IC₅₀ = 100 nM). In the very recent example, derivative (**121b**)²³⁶ (Figure 7), reported with two additional hydroxy groups on the pyridocarbazole scaffold, has subnanomolar affinity to the Pim-1 (IC₅₀ = 0.075 nM at 100 μ M ATP) and at the same time a selectivity over other kinases, such as PAK-1 (p21-activated kinase 1) and GSK-3 α , of 1093 times and 267 times, respectively.²³⁶

The crystal structure of Pim-2 has been recently elucidated in a complex with organoruthenium complex (*rac*-**120a**).²³⁷ The structure is highly similar to Pim-1, particularly in the ATP pocket, which is nearly completely conserved in comparison to the overall sequence identity of 55%. The main structural distinction between the two kinases is the absence of the C-terminal α J helix (colored in red, Figure 6) in Pim-2, which removes a significant stabilizing interaction close to the interface between the N and C-terminal lobes. The last 23 residues of Pim-2 share little sequence identity with Pim-1 and are disordered. The same authors reported SAR study for 14 organoruthenium complexes, where additional hydrogen bonding groups at the R₁ and R₂ positions dramatically increase the potency against Pim-1 and Pim-2 kinases.²³⁷ The majority of compounds were slightly more potent against Pim-1 than Pim-2. The most potent inhibitor for Pim-2 (*rac*-**120c**)²³⁷ (Figure 7) bearing an additional carboxyl group at the pyridine ring (R₂) gave almost complete inhibition at a concentration of 10 nM for Pim-2, and was marginally less effective against Pim-1.

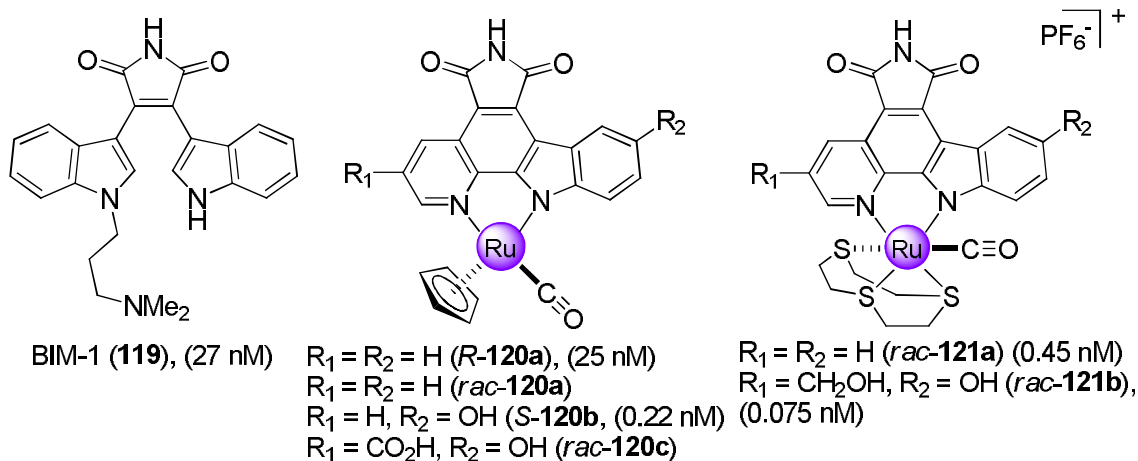


Figure 7. Structures of BIM-1 and staurosporine-mimicking ruthenium complexes as efficient kinase inhibitors. IC_{50} values for the inhibition of Pim-1 are given.

Imidazo-, pyrazolo- and triazolopyridazines

Bullock *et al.*^{228,238} were among the first to report Pim inhibitors with unusual binding mode. The high-resolution crystal structure of a Pim-1 inhibitor (**122a**) complex revealed that imidazo[1,2-*b*]pyridazines (class **I**, Figure 8A) binds to the opposite side of the ATP binding pocket and surprisingly interact with the amino terminal lobe helix αC rather than with the kinase hinge region, thus represent ATP competitive but not ATP mimetic compounds with nanomolar potency for Pim kinases (Figure 8A).^{228,238} One of the reported compounds (**122a**) was highly Pim-1 selective when screened against a panel of 50 kinase catalytic domains. In addition, (**122a**) has *in vitro* antileukemic activity in various cell line models and significantly suppresses *in vitro* growth of leukemic blasts from AML patients samples.²³⁸ In 2009, SuperGen (now Astex Pharmaceuticals) developed the *N*-methylpiperidine derivative (**122b**, SGI-1776)²³⁹ (Figure 8A) with a reported low nanomolar affinity for Pim-1 ($IC_{50} = 7.0$ nM). It has recently advanced to phase I clinical trials and therefore became the first clinical-stage investigational drug specifically targeting Pim kinases.^{239,225} Pyrazolo[1,5-*a*]pyrimidines (class **II**) such as (**123**) (Figure 8A), with no reported IC_{50} value, shows 10% residual Pim-1 activity at 1 μM concentration.²²⁸

Triazolo[4,3-*b*]pyridazines (class **III**, structurally related to **I** and **II**) were identified as highly selective inhibitors of Pim-1 by Vertex Pharmaceuticals;^{240,241} however, the binding mode is different from imidazo[1,2-*b*]pyridazines (class **I**). In the crystal structure of compound (**124a**) (Figure 8A), *m*-CF₃-phenyl ring makes contact with the hinge Glu121 by way of a bifurcated hydrogen bond between the aromatic protons on C5 and C6 and the backbone carbonyl of Glu121 (Figure 8B).²⁴⁰ The poor solubility and permeability of the potent Pim selective inhibitor (**124a**) ($K_i = 11$ nM) was enhanced by modification of the cyclohexyl ring. A 4-hydroxycyclohexylamino analog (**124b**) (Figure 8A) with an improved aqueous solubility is reported to inhibit Pim-1 below the limit of the detection assay ($K_i < 5$ nM) and to show a high level of selectivity when screened against a panel of 21 kinases.²⁴¹

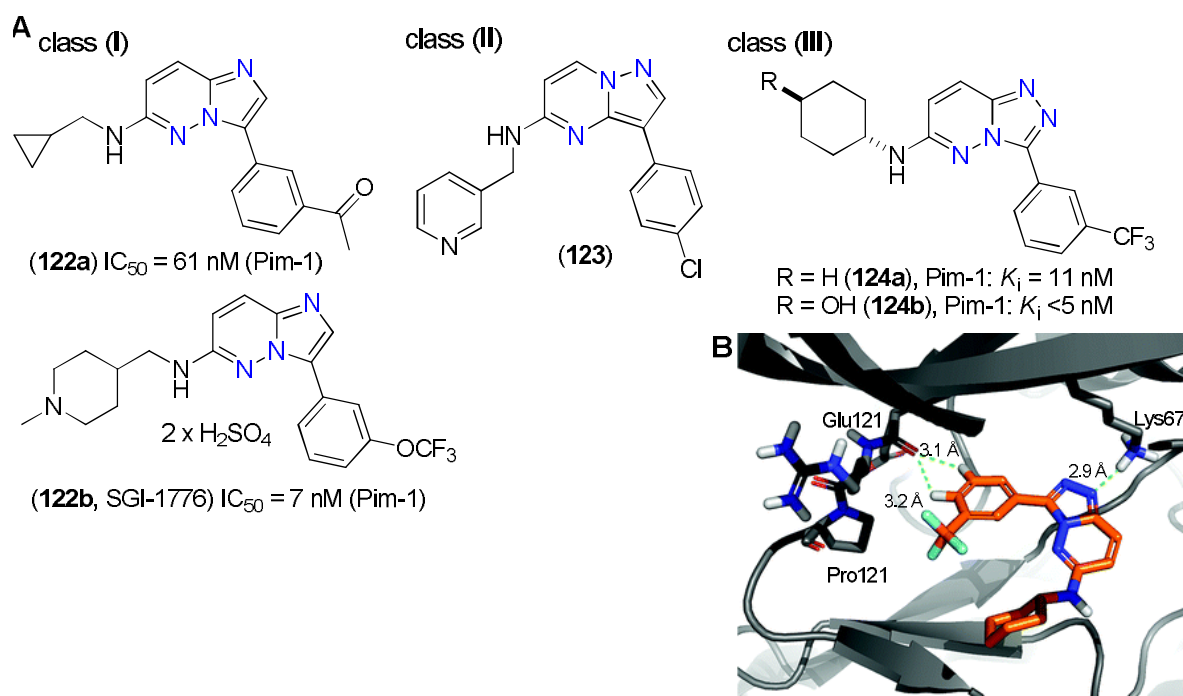


Figure 8. *A*) Heteroaromatic Pim inhibitors with *in vitro* and *in vivo* activity. *B*) The crystal structure of triazolo[4,3-*b*]pyridazine (**X**) bound to Pim-1. Key interactions with Glu121 and Lys67 are highlighted in green.²⁴⁰

3,5-Disubstituted indoles

In 2011, Nishiguchi *et al.*²⁴² described a potent pan-Pim inhibitor identified by high-throughput screening with a novel heteroaromatic 1*H*-pyrazolo[3,4-*b*]pyridine scaffold (**125a**, X, Y = N) (Figure 9). Despite the fact that (**125a**) had attractive potency against all three Pim isoforms (IC_{50} : Pim-1, Pim-2, Pim-3: 9 nM, 39 nM 12 nM, respectively) it showed low nanomolar activity against several other kinases as well, and contained a possible metabolically labile phenolic group. The X-ray crystal structure studies revealed that only one of the N–H of the 1*H*-pyrazolo[3,4-*b*]pyridine core makes a hydrogen bond to the hinge region, while the two other nitrogens do not. The nitrogen deletion on the heteroaromatic core yielded the corresponding 1*H*-pyrrolo[2,3-*b*]pyridine (**125b**) and 1*H*-indole (**125c**) keeping the substitutions at C3 and C6 (Figure 9).²⁴² While the pyrrolo[2,3-*b*]pyridine core (**125b**) lost potency against all three Pims (3–7-fold), the indole core compound (**125c**) was able to retain the potency against the target while being completely inactive (> 25 μ M) against the other three kinases tested. The replacement of phenolic motif at C6 of (**125c**) was, however, a highly challenging effort and drove the investigation towards developing alternative substitution patterns on the scaffold.

Based on the X-ray structure, the C5 position of the azaindazole core points towards Lys67 and a favorable interaction could be attained with a hydrogen-bond acceptor substituent. Several X-ray crystal structures of inhibitors bound to Pim-1 effectively take advantage of this interaction. One of these compounds, such as 5-aminopyrimidine-substituted benzo[*c*]isoxazole (**126**) (Figure 9) has nanomolar affinity for Pim-1 ($K_i = 91$ nM).²⁴⁰ Substituents at the C5 position placed on the more kinase selective indole scaffold yielded a series of heteroaromatic compounds, of which 2-pyrazine and 3-pyridine (**127**) analogs were the most potent (Figure 9).

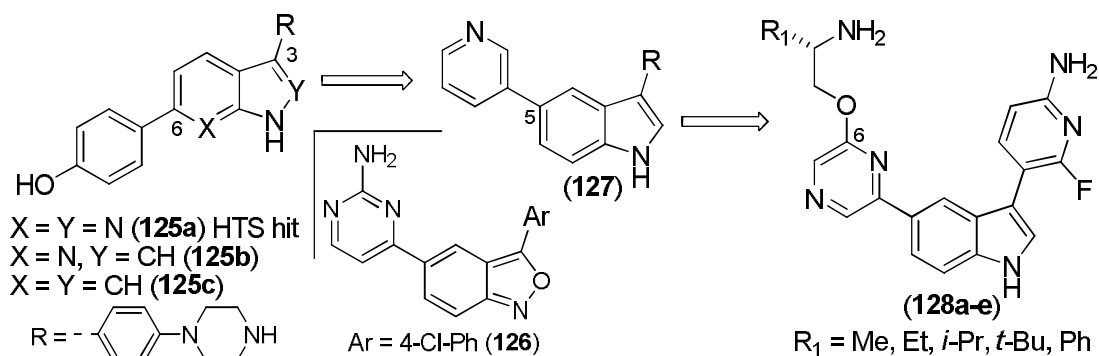


Figure 9. Development of a novel indole-based inhibitor against Pim kinases.

Replacement of the C3-phenylpiperazine with the 2-fluoroaminopyridine ring and introduction of either rigid or flexible basic amino substitutions at C6 of the pyrazine ring yielded very potent inhibitors (Figure 9), reaching the limits of detection of the biochemical assay as found for methyl-analog (**128a**) (IC_{50} Pim-1: <2 nM, Pim-2: 56 nM, Pim-3: <2 nM).²⁴² When R_1 was replaced with ethyl in (**128b**) a two-fold improvement (Pim-2: 26 nM) was observed. The Pim-2 potency suffered as the substituent grew larger as shown for isopropyl and *tert*-butyl groups (**128c–128d**). The phenyl moiety of (**128e**) was, however, well-tolerated, showing the highest affinity of all compounds against Pim-1, Pim-2, and Pim-3 (<2 nM, 10 nM, <2 nM, respectively). The *tert*-butyl analog (**128c**) was further profiled and found to display high selectivity over a panel of 30 other protein kinases (>10 μM).

Pyrrolocarbazoles

Pyrrolo[2,3-*a*]carbazoles have been identified recently as a new scaffold for potent Pim kinase inhibitors.^{243,244} Compound (**129a**, DHPCC-9) (Figure 10A), substituted at the C3 position by a formyl group, exhibited a potent and selective inhibition of all Pim kinases when tested toward a panel of 66 protein kinases, with a high activity against Pim-3 ($IC_{50} = 10$ nM).²⁴³ Recently, (**129a**) was reported to slow down migration and invasion of cancer cells derived from either prostate cancer or squamocellular carcinoma patients, thus represents an attractive compound for drug development to inhibit the invasiveness of Pim-overexpressing cancer cells.²⁴⁵

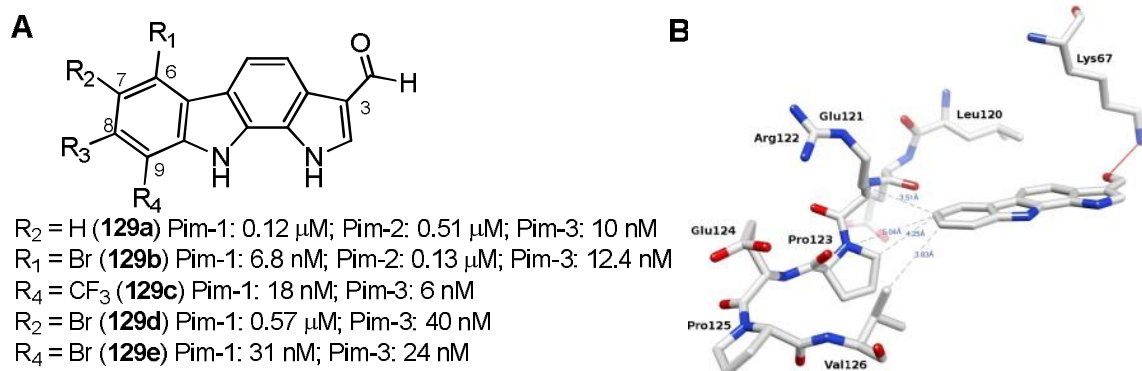
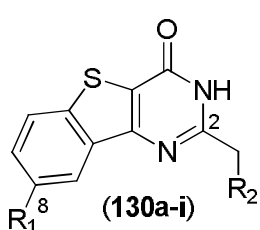


Figure 10. A) Pyrrolo[2,3-*a*]carbazoles (**129a–e**). IC_{50} values for Pim-1, 2 and 3 in brackets. B) Interatomic distances (\AA) between C7 and C8 positions of pyrrolocarbazole (**129a**) and Pim-1 kinase hinge residues (PDB code 3JPV). The hydrogen bond between the formyl group and the Lys67 side chain is indicated in red.²⁴⁴

When the phenyl ring was further substituted with a bromine atom at various positions, compound (**129b**)²⁴⁴ (Figure 10A) bearing a Br atom at C6, was reported to be the most potent inhibitor of Pim kinases in the series, with a 17-fold higher activity toward Pim-1 compared to (**129a**). The best Pim-3 inhibitor was, however, the analog (**129c**), with a CF₃ substituent at C9 (IC₅₀ = 6 nM).²⁴⁴ The diversely C6–C9 phenyl ring-substituted analogs (**129a–e**, Figure 10A) were evaluated for their *in vitro* antiproliferative potencies toward three cancer cell lines (PA1, PC3, and DU145) and a fibroblast primary culture, revealing IC₅₀ values in the low micromolar range.^{243,244} The crystal structure of Pim-1 complexed with (**129a**) was determined, revealing a non-ATP mimetic binding mode with no hydrogen bonds formed with the kinase hinge region (Figure 10B).²⁴⁴

Benzothienopyrimidin-4-ones

Tao *et al.*,²⁴⁶ from the Abbott Laboratories, recently reported a series of 69 benzothienopyrimidinones (**130**, Figure 11) as novel and potent Pim kinase inhibitors that do not only inhibit all three Pim kinases at subnanomolar concentrations but also exhibit excellent kinase selectivity. The reported inhibitors efficiently interrupted the phosphorylation of BAD in both leukemia and prostate adenocarcinoma cell lines (K562 and LnCaP-Bad, respectively), indicating that their potent biological activities are mechanism-based. In the comprehensive search for a pan-Pim kinase inhibitor, the initial SAR study of the 2-position of the pyrimidone ring gave compound (**130a**, Figure 11), with a 3-hydroxyphenyl substituent pose high affinity for Pim-1, but only modest affinity for Pim-2 (K_i = 0.9 nM, 147 nM, respectively).



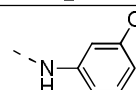
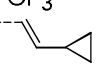
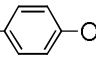
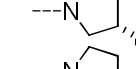
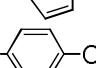
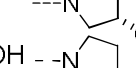
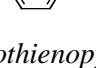
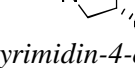
Comp.	R ₁	R ₂	Pim-1	Pim-2	Pim-3 (nM)
(130a)	Cl		0.9	147	
(130b)	Br	-NMe ₂	5	16	
(130c)	H	-NMe ₂	296	238	
(130d)	CF ₃	-NMe ₂	11	36	
(130e)		-NMe ₂	1	2	0.2
(130f)		-NMe ₂	2	3	0.5
(130g)	Ph		3	10	0.3
(130h)			5	3	<0.1
(130i)			0.7	2	0.4

Figure 11. Some members of the benzothienopyrimidin-4-one library with K_i values in table.

The subsequent SAR study of the phenyl ring at C8 showed that the introduction of a simple halogen atom (**130b**, R₁ = Cl; **130c**, R₁ = Br), or alkyl group (**130d**, R₁ = CF₃) dramatically increased the affinity. The hydrophobic cyclopropylvinyl group in (**130e**) further increased the Pim-1 and Pim-2 inhibition to a single-digit nanomolar level. The same was observed in analogs with five- and six-member aromatic rings at C8 (**130f–i**).²⁴⁶ Combination of the (*S*)-3-hydroxypyrrolidinyl group at the 2-position with the *p*-phenolic group at 8-position resulted in the compound (**130i**, Figure 11), with most potent inhibition of all three Pim kinases and over 1000-fold higher affinity for Pim-1 and Pim-3 over 15 other kinases.²⁴⁶ Another potent analog (**130f**) is highly bioavailable, exhibiting

bioavailability of 76% with oral dosing. It has shown inhibition of the growth of K562 cells ($EC_{50} = 1.7 \mu\text{M}$) and low nanomolar K_i values against Pim-1, Pim-2 and Pim-3 (2, 3, and 0.5 nM, respectively). Further ADME profiling suggested a long half-life in human and mouse liver microsomes, in addition to good permeability, modest protein binding, and no considerable CYP inhibition below $20 \mu\text{M}$ concentration.²⁴⁶

Pyrazinyl cinnamic acids

In 2009, the group of Morwick²⁴⁷ from Boehringer Ingelheim Pharmaceuticals reported a comprehensive study of pyrazinyl carboxylic acid inhibitors of Pim-2 kinase. A high-throughput screen hit (**131a**, Figure 12) showed an unconventional binding mode to Pim-1, as revealed by X-ray crystallography. The X-ray data illustrated that the inhibitor binds to the highly negatively charged cleft between two lobes of Pim-1 and reveals the unusual lack of hinge binding. The carboxyl group of the inhibitor forms a salt bridge with a bound Mg^{2+} that in turn forms a salt bridge with Glu89 from the αC helix.²⁴⁷ Additionally, the carboxyl group of the inhibitor forms a hydrogen bond directly with Lys67. The basic nitrogen of the homopiperazine (1,4-diazepane) group is located in a region aligned with three acidic residues (Asp131, Asp128 and Glu171) and forms water-mediated hydrogen bonds with two of them. (**131a**) is highly selective within the kinase family, and shows similar potency for both Pim-1 and Pim-2 (IC_{50} 57 nM and 40 nM, respectively). The compound has a good solubility and acceptable cell permeability with a good half-life in human liver microsomes, and no CYP inhibition below $30 \mu\text{M}$.²⁴⁷ A complete removal of the cinnamic acid portion generated an inactive compound, suggesting that the cinnamic acid fragment contributes more significantly to the potency than the homopiperazine. The bioisosteric tetrazole (**131b**) can apparently engage the network of interactions observed for the carboxylic acid to some extent. It has a potency within 4-fold that of a hit compound (**131a**).

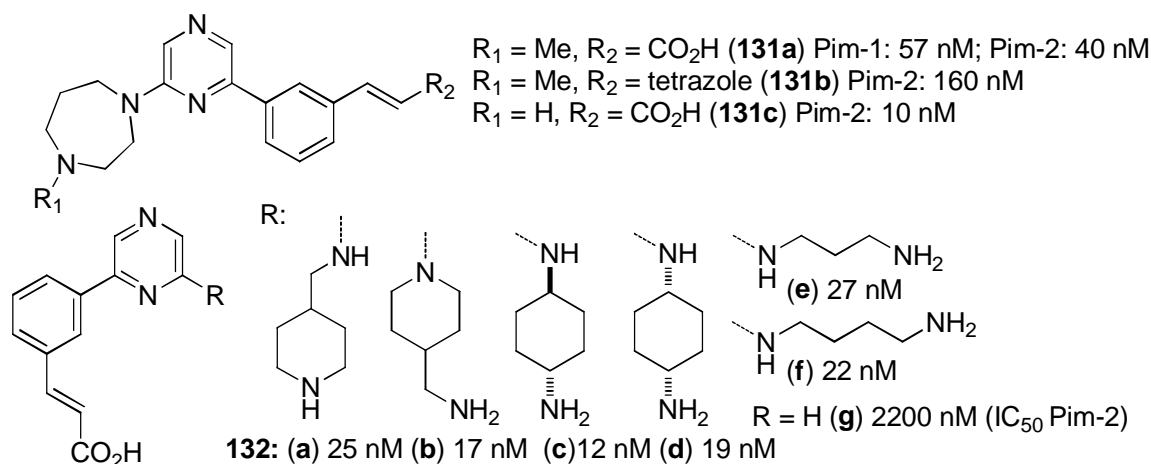


Figure 12. Disubstituted pyrazine cinnamic acids by Boehringer Ingelheim Pharmaceuticals.

Removal of the methyl substituent from the distal amine of (**131a**) gave secondary amine (**131c**) with a low nanomolar affinity for Pim-2 ($IC_{50} = 10 \text{ nM}$).²⁴⁷ Among cyclic six-membered analogs (**132a–d**) and acyclic diamines (**132e–f**) (Figure 12), the compound (**132c**) with a *trans*-cyclohexane-1,4-diamino substituent showed the most potent Pim-2 inhibition. The removal of the basic diamino fragment resulted in compound (**132g**), which is significantly less potent against Pim-2. The same authors responded to claims concerning the α,β -conjugated cinnamic acid moiety, which may potentially act as a Michael acceptor,

enhancing the affinity of (**131a**) by covalent modification of the protein. The reversible binding mode of (**131a**) for Pim-1 was evaluated by a time-dependent assay with varying concentrations of ATP, where the results suggested a reversible binding mode. The X-ray structure of (**131a**) confirmed this observation, as an examination of the area near the β -carbon to the acid revealed no nucleophilic residues within bonding distance to the protein.²⁴⁷

Benzofuran-2-carboxylic acids

In 2011, Xiang *et al.* from Genzyme Corp. identified benzofuran-2-carboxylic acids (Figure 13) as Pim-1 inhibitors by fragment-based screening.²⁴⁸ The X-ray crystal structure of compound (**133**) bound to Pim-1 shows the salt bridge interaction of 2-carboxyl group with Lys67 and the hydrophobic interactions of the C5 Br-substituent surrounded by the hydrophobic pocket of the Pim-1 hinge region. The authors replaced the 5-bromo substituent of compound (**133**) with an extended linker fragment containing a basic heterocyclic moiety to capture additional interactions with acidic amino acid residues (Asp128 and Glu171) in the ribose binding region, while maintaining the benzofuran-2-carboxylic acid framework unchanged. An appropriate distance between the terminal amino group and the benzofuran core appeared to be critical in achieving high potency. The most potent of this series, *meta*-substituted pyrazine compound (**134**), with a primary aliphatic amino substituent, had IC₅₀ values of 53 nM for Pim-1 and 21 nM for Pim-2. The compound (**134**) shares obvious structural similarities with pyrazinyl cinnamic acids (**131–132**), reported the Morwick group²⁴⁷ (*vide supra*).

C5 bromo analogs carrying a basic moiety at the C7 position of the benzofuran framework were also studied (Figure 13). The nature of the linker does not seem to be very important; however, the basicity of the nitrogen center of the terminal amine is a significant factor impacting the potency, as evidenced by comparing the Pim-1 and Pim-2 inhibition of compounds with terminal piperidine, to compounds with terminal pyridine. Replacing the amino group with a hydroxy group diminishes the activity. The X-ray crystal structure analysis of analog (**135a**) showed that the concise and rigid *cis*-diaminocyclohexyl ring possessed an ideal shape to position the terminal amino residue in the right distance and orientation, allowing for strong interactions with Asp128 and Glu171.

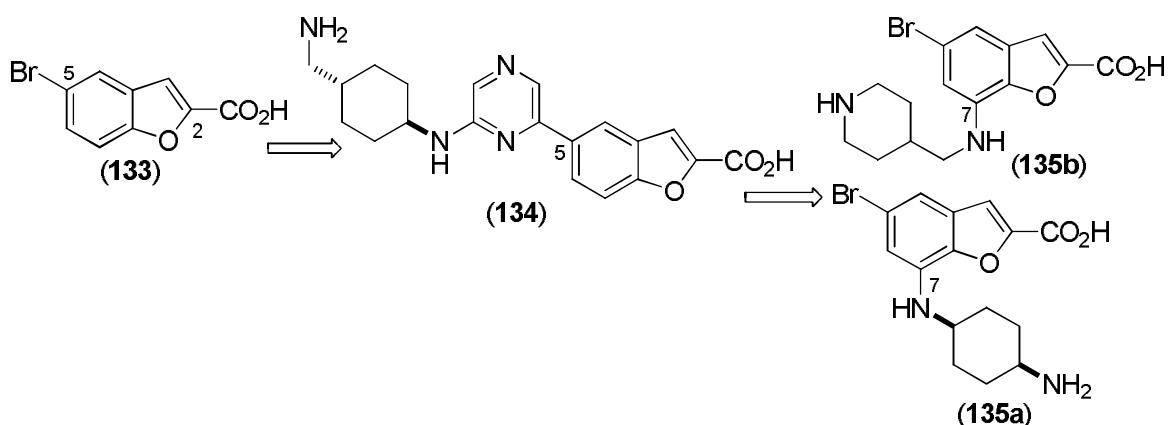


Figure 13. Genzyme's benzofurancarboxylic acids as Pim-1 and Pim-2 inhibitors.

The compound (**135a**) is capable of strong binding and inhibition of both Pim-1 and Pim-2 as demonstrated by IC₅₀ values of 1.0 nM and 4.0 nM, respectively. Terminal piperidine analog (**135b**) (IC₅₀ = 20 nM for Pim-1) was tested using an Ambit 442 kinase panel (at 100

nM concentration). Under these conditions, in addition to Pim-1, Pim-2, and Pim-3, only three non-Pim kinases were inhibited (>50% of the binding), which indicates the good selective nature of this structural class against the Pim kinase family. Both compounds (**135a**, **135b**) were inactive against a set of five CYP isozymes, demonstrated adequate aqueous solubility, and were moderately stable in rat and human liver microsome metabolic stability assays.

(5-Arylfuran-2-yl)methylene indolin-2-ones

In 2011, Cylene Pharmaceuticals reported a high-throughput screening (HTS) hit compound (**136**) (Figure 14) containing an oxindole group as an inhibitor of Pim-1 kinase ($IC_{50} = 386$ nM).²⁴⁹ The inhibitor shows some structural features similar to pyrazinyl cinnamic acids (**131–132**) (*vide supra*). A SAR study resulted in a series of 19 analogs (**137**), including variation of the carboxylic acid moiety with aliphatic basic amines (R_1), incorporation of nitrogen atoms to the *m*-substituted phenyl ring (X_1 , X_2) and various halogen substituents (R_2), and substitution around the indole ring (R_4) and the (*E*)-alkene (R_3). This led to a discovery of (**138**) (Figure 14), a novel pan-Pim kinase inhibitor with high efficiency (IC_{50} Pim-1: 5 nM, Pim-2: 25 nM, Pim-3: 16 nM) and moderate pharmacokinetic profile. The authors showed that compound (**138**) was Pim-selective, since only Pim-1, Pim-2, Pim-3, and Flt-3, of the 107 screened kinases were, inhibited by more than 80% (at 0.5 μ M concentration).²⁴⁹ The antiproliferative activity of (**138**) was examined against a panel of cell lines derived from human solid tumors and hematological malignancies, where it demonstrated robust antiproliferative potencies against all cell lines tested. Cell lines derived from acute leukemias were the most sensitive. In addition, in combination with chemotherapeutics, compound (**138**) exhibited synergistic antiproliferative activity and displayed significant *in vivo* efficacy in acute myeloid leukemia (MV-4-11) and prostate adenocarcinoma (PC3) human xenograft models representing the diseases, where Pim kinases have been shown to play an important role.

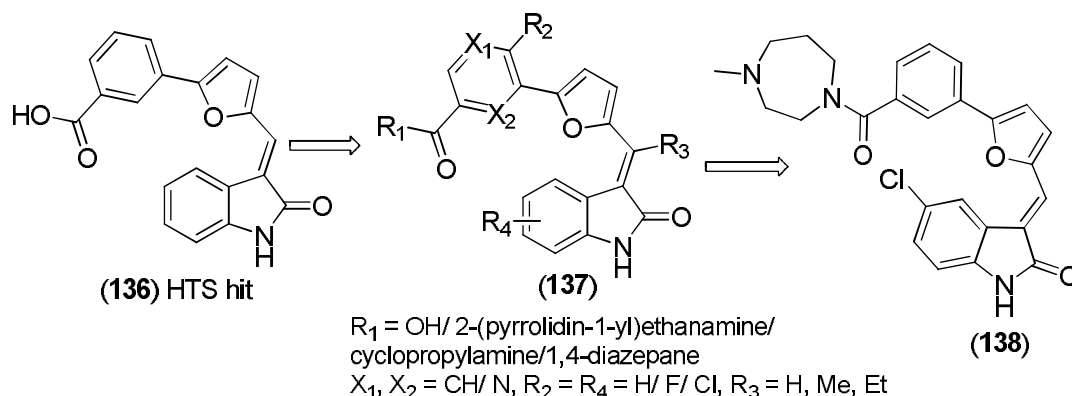


Figure 14. Development of pan-Pim kinase inhibitor by Cylene Pharmaceuticals.

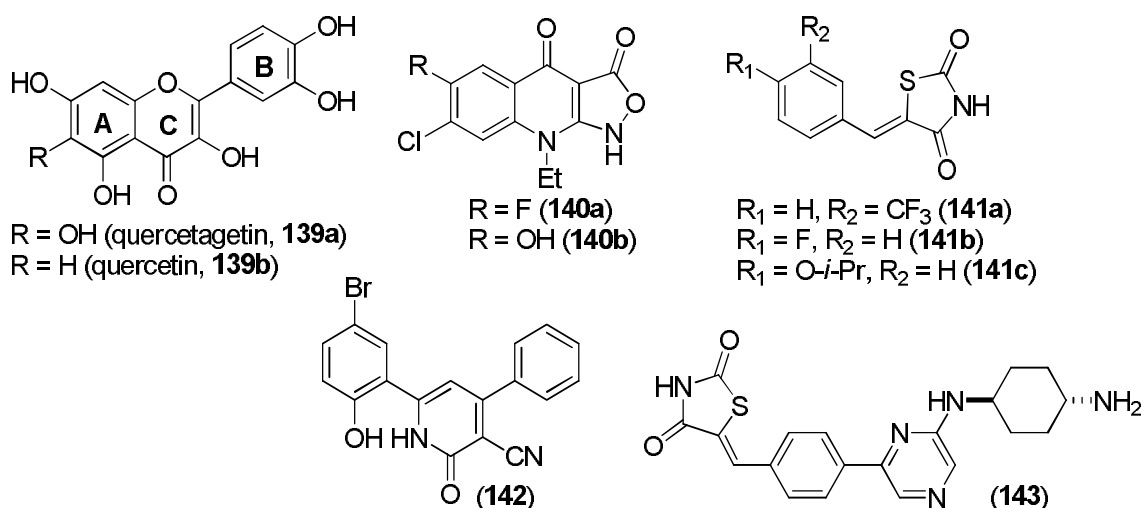
Miscellaneous Pim inhibitors

Among the naturally occurring plant-derived flavonoids, quercetagenin (**139a**) shows moderate affinity for Pim-1 ($IC_{50} = 340$ nM).²⁵⁰ However, quercetagenin has been identified as a highly selective inhibitor of Pim-1 over Pim-2 and other serine-threonine kinases (e.g. PKC and PKA), with both *in vitro* assays and in cell cultures. The X-ray crystal structure of (**139a**) bound to the ATP-binding site of Pim-1 shows that the compound orients the B ring inside the pocket.²⁴⁹ The hydroxy group of the C ring in (**139a**) makes a canonical hydrogen

bond with backbone carbonyl oxygen of the hinge residue Glu121. Another flavonol quercetin (**139b**), a non-specific inhibitor of protein kinases and other enzymes, is reported to have nanomolar inhibition against Pim-1 ($IC_{50} = 43$ nM).²²⁸ A much weaker affinity was reported ($IC_{50} = 1.1$ μ M) by Holder *et al.*²⁵⁰ for the same compound (**139b**), however.

The HTS hit (**140a**), containing an isoxazoloquinoline-3,4-dione core was reported to be a potent inhibitor for Pim-1 and Pim-2 kinases ($K_i = 22$ nM and 174 nM, respectively).²⁵¹ Synthesis of a small library, and installation of a hydroxy group on the phenyl ring of the core resulted in the most potent inhibitor (**140b**), with a potential to form a key hydrogen bond interaction with the hinge region and K_i values of 2.5 and 43.5 nM against Pim-1 and Pim-2, respectively, and displayed an activity profile with a high degree of selectivity among a panel of 22 kinases.²⁵¹

Aryl-substituted thiazolidine-2,4-dione (**141a**) was identified by screening to be a Pim-1 inhibitor.²⁵² Computational lead optimization led to the synthesis of a library of substituted thiazolidine-2,4-diones, where the most potent compound (**141b**) showed an IC_{50} of 13 nM for Pim-1 and compound (**141c**) showed an IC_{50} value of 20 nM for Pim-2. Despite high potency against Pim-1 and 2, the screened compounds were unable to inhibit Pim-3 efficiently.



Series of substituted pyridones were reported as potent inhibitors of Pim-1 kinase.²⁵³ The diaryl-substituted pyridine (**142**) inhibits Pim-1 at 50 nM (IC_{50}) *in vitro*. The X-ray structure of (**142**) with Pim-1 showed a large hydrogen bond network between the carbonyl group on the pyridine ring, Lys67, Phe187, and two water molecules. An additional weak hydrogen bond between the aromatic hydrogen on the phenol ring and the main carbonyl chain of Glu121 contributes to the stabilization of the molecules.²⁵³

Finally, Genzyme Corp. recently published a highly potent compound derived from a fragment-based drug design program. In this program, the analysis of nuances of fragment binding of known Pim-inhibitors led to the synthesis of a compound (**143**) with an impressive IC_{50} of 467 pM.²⁵⁴

Summary of the natural and synthetic compounds targeting Pim kinases

Only few natural products have been identified as Pim kinase inhibitors, including staurosporine, bis(indolyl)maleimides, and flavonoids. While staurosporine (**93**), BIM-1 (**119**), and quercetin (**139b**) inhibit Pim kinases potently, they lack selectivity by inhibiting

a variety of other protein kinases, thus leaving the therapeutic usefulness of such compounds unclear. Synthetic compounds with selective Pim inhibition have emerged, however, especially within last 5 years (*vide infra*).

Staurosporine-mimicking ruthenium complexes such as (**121a–b**) have shown to be highly effective Pim kinase inhibitors with excellent kinase selectivity. These complexes seem to behave like “regular” organic compounds without displaying metal-related cytotoxicities. The importance of these compounds was further demonstrated in the elucidation of the crystal structure of Pim-2 kinase with an organoruthenium complex (*rac*-**120a**).

In a class of imidazo and triazolopyridazines, several potent and selective Pim-1 inhibitors have been developed. For example, compound (**122a**) has *in vitro* antileukemic potential shown in various cell line models and in AML patients’ samples. Another heterocyclic compound (**129a**, DHPCC-9) with a pyrrolo[2,3-*a*]carbazole structure is reported to be a potent inhibitor of Pim-3 ($IC_{50} = 10$ nM) and has recently shown to slow down migration and invasion of cancer cells, thus represents an attractive compound for drug development to inhibit invasiveness of Pim-overexpressing cancer cells.

Within the last 2–3 years, the pharmaceutical industry has shown an emerging interest in Pim kinases, and several pharmaceutical companies have launched Pim inhibitors with novel scaffolds combined with high potency and kinase selectivity. In 2009, SuperGen (now Astex Pharmaceuticals) developed imidazo[1,2-*b*]pyridazine (**122b**, SGI-1776) with a reported low nanomolar affinity for Pim-1 ($IC_{50} = 7.0$ nM). SGI-1776 advanced to phase I clinical trials, and therefore became the first clinical-stage investigational drug specifically targeting Pim kinases.

In the same year, Abbott Laboratories discovered benzothienopyrimidinones (**130**) as a novel class of Pim inhibitors possessing low nanomolar K_i values against all three Pim kinases while maintaining kinase selectivity. Multiple compounds exhibited potent antiproliferative activity in cell cultures with submicromolar EC_{50} values and pharmacokinetic studies suggested that these Pim inhibitors are highly bioavailable.

In 2009, Boehringer Ingelheim Pharmaceuticals reported a comprehensive study of pyrazinyl cinnamic acids (**131–132**) as efficient inhibitors of Pim-2 kinase. One of the studied analogs (**131c**), with a low nanomolar ($IC_{50} = 10$ nM) affinity for Pim-2, showed good aqueous solubility, acceptable permeability, and a good half-life in human liver microsomes.

In 2011, Cylene Pharmaceuticals developed indolin-based novel pan-Pim kinase inhibitors. The compound (**138**) displays high potency in mechanistic and antiproliferative cellular assays and shows synergistic antiproliferative activity in combination with chemotherapeutics. In addition, (**138**) showed significant *in vivo* efficacy in two xenograft models representing the diseases, where Pim kinases have been shown to play an important role.

In 2011, Genzyme Corp. identified benzofuran-2-carboxylic acids as selective Pim-1 inhibitors. The most potent compound (**135a**) is able to inhibit Pim-1 and Pim-2 with single-digit IC_{50} values (1.0 nM and 4.0 nM, respectively). In 2012, the same company published very potent compound (**143**) showed impressive IC_{50} of 467 pM for Pim-1.

Although no PIM kinase inhibitor has successfully reached in the clinical use yet, the intense effort of many groups to develop potent and selective inhibitors of PIM kinases will obviously lead to clinically useful drugs.

3 Aims of the study

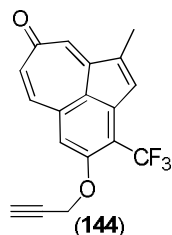
The objective of this study was to synthesize various six-membered compounds, including both carbo and heterocyclic ring systems, with possible interesting biological properties. Both solid- and solution-phase methods were studied.

The more specific aims of the research were

- to study and develop a practical synthetic method for the aza Diels-Alder reaction between polymer-bound diene and N=N azadienophiles on solid-phase including synthesis of hexahydrocinnoline derivatives (**I**);
- to synthesize 4-aminoguaiazulene and utilize it in a preparation of heterocyclic benzo[*cd*]azulenes (**II**);
- to design and synthesize a model compound targeted to the C1 domain of PKC and evaluate its biological activity. In the synthetic study, the cascade of two Diels-Alder cycloadditions was used as the key reaction in a construction of the tricyclic framework of the model compound (**III**);
- to synthesize novel benzo[*cd*]azulene derivatives and to study their capability of inhibiting Pim kinases (**IV**).

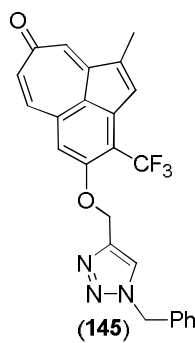
4 Experimental

A detailed presentation of the materials, synthetic, and analytical methods can be found in the original publication **III**, and in the supporting information for original publications **I**, **II**, and **IV**. The supporting information for original publications **I**, **II**, and **IV** is not included in this thesis. This material is available from the author or via the Internet at <http://pubs.acs.org> for original publication **I** (56 pages), and at <http://www.sciencedirect.com/> for original publication **II** (9 pages). The experimental procedures and analytical data for the unpublished compounds are presented in this chapter.



(144) **1-Methyl-4-(prop-2-yn-1-yloxy)-3-(trifluoromethyl)-8H-benzo[cd]azulen-8-one (144).**

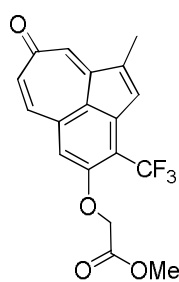
Troponone (**48c**) (0.10 g, 0.36 mmol) was dissolved in acetone (10 mL), then powdered potassium carbonate (0.10 g, 0.81 mmol, 2.3 equiv) and propargyl bromide (80 wt % in toluene, 90 μ L, 0.81 mmol, 2.3 equiv) were added to the reaction mixture. The resulting mixture was stirred at ambient temperature for 2 days. TLC analysis of the reaction mixture showed the formation of a yellow product and the disappearance of an orange starting material. EtOAc (10 mL) and water (5 mL) were added, and phases were separated. The aqueous phase was extracted with EtOAc (2 \times 10 mL) and the combined organic phases were dried over anhydrous Na₂SO₄, filtered, and evaporated to dryness. The obtained crude product was purified by column chromatography on silica gel (eluent: EtOAc/*n*-hexane 1:1) to give (**144**) (69 mg, 61%) as a yellow solid. M. p. 161–163 °C; ¹H NMR (300 MHz, CDCl₃): δ 7.28 (H, d, *J* = 12.6 Hz), 7.04 (1H, m), 7.02 (1H, d, *J* = 2.4 Hz), 6.98 (1H, s), 6.89 (1H, dd, *J* = 2.4 Hz, 12.6 Hz), 4.88 (2H, d, *J* = 2.1 Hz), 2.60 (1H, t, *J* = 2.1 Hz), 2.24 (3H, d, *J* = 1.5 Hz) ppm; ¹³C NMR (75 MHz, CDCl₃): δ 188.1, 157.1, 148.9, 144.6, 143.5, 138.6, 137.6, 134.4, 131.2, 131.1 (q, *J* = 4.8 Hz), 127.4, 123.7 (q, *J* = 273.0 Hz), 115.5, (q, *J* = 32.0 Hz), 112.2, 77.3, 77.1, 57.2, 13.0 ppm; Anal. calc. for C₁₈H₁₁F₃O₂ (316.07): C, 68.36; H, 3.51. Found: C, 68.09; H, 3.29; LC–MS: [M+H]⁺ *m/z* 317.



(145) **4-[(1-Benzyl-1H-1,2,3-triazol-4-yl)methoxy]-1-methyl-3-(trifluoromethyl)-8H benzo[cd]azulen-8-one (145).**

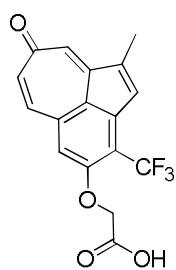
Alkyne (**144**) (94 mg, 0.30 mmol) was dissolved in a mixture of DMF–H₂O (4:1, 5 mL) and benzyl bromide (43 μ L, 0.36 mmol, 1.15 equiv), sodium azide (65 mg, 0.36 mmol, 1.15 equiv), then an aqueous 1.0 M solution of CuSO₄ (0.07 mmol, 70 μ L, 0.2 equiv) and sodium ascorbate (29 mg, 0.14 mmol, 0.5 equiv) were added. The reaction mixture was

irradiated in a microwave reactor at 120 °C for 35 min. The resulting precipitate was washed with dilute aqueous ammonia solution (3 × 10 mL) and after drying, the obtained crude product was purified by column chromatography on silica gel (eluent: EtOAc/*n*-hexane 3:1) to give **(145)** (42 mg, 31%) as a yellow solid. M. p. 251 °C (decomp.); ¹H NMR (300 MHz, DMSO-*d*₆): δ 8.30 (1H, s), 7.57 (1H, s), 7.55 (H, d, *J* = 12.9 Hz), 7.40–7.28 (4H, m), 7.05 (1H, s), 6.98 (1H, dd, *J* = 2.4 Hz), 6.86 (1H, dd, *J* = 2.4 Hz, 12.9 Hz), 5.64 (2H, s), 5.40 (2H, s) 2.23 (3H, s) ppm; ¹³C NMR (75 MHz, DMSO-*d*₆): δ 186.9, 157.2, 147.7, 145.0, 142.3, 142.0, 138.5, 137.2, 136.0, 134.6, 130.9, 129.9, 128.7, 128.7, 128.1, 127.8, 127.8, 125.6, 124.8, 123.6 (q, *J* = 273.0 Hz), 113.0 (q, *J* = 31.0 Hz), 113.0, 62.9, 52.8, 12.4 ppm; Anal. calc. for C₂₅H₁₈F₃N₃O₂ (449.14): C, 66.81; H, 4.04; N, 9.35. Found: C, 66.54; H, 3.89; N, 9.16; GC-MS: [M]⁺ *m/z* 449.



(146) Methyl 2-[[1-methyl-8-oxo-3-(trifluoromethyl)-8H-benzo[cd]azulen-4-yl]oxy]acetate (146).

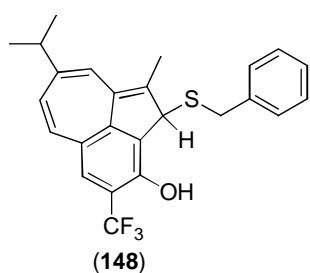
Troponone (**48c**) (0.10 g, 0.36 mmol) was dissolved in acetone (8 mL), then powdered potassium carbonate (0.10 g, 0.36 mmol) and methyl bromoacetate (102 μL, 1.08 mmol, 3.0 equiv) were added to the reaction mixture. The resulting mixture was stirred at ambient temperature for 3 days. TLC analysis of the reaction mixture showed the formation of a yellow product and the disappearance of an orange starting material. EtOAc (10 mL) and water (5 mL) were added and phases were separated. The aqueous phase was extracted with EtOAc (2 × 10 mL) and the combined organic phases were dried over anhydrous Na₂SO₄, filtered, and evaporated to dryness. The obtained crude product was purified by column chromatography on silica gel (eluent: EtOAc/cyclohexane 1:1) to give **(146)** (60 mg, 48%) as bright yellow needles. M. p. 177–179 °C; ¹H NMR (300 MHz, CDCl₃): δ 7.22 (H, d, *J* = 12.6 Hz), 7.05 (1H, m), 7.02 (1H, d, *J* = 2.4 Hz), 6.88 (1H, dd, *J* = 2.4 Hz, 12.6 Hz), 6.68 (1H, s), 4.81 (2H, s), 3.83 (3H, s), 2.25 (3H, s) ppm; ¹³C NMR (75 MHz, CDCl₃): δ 188.0, 168.2, 157.5, 148.8, 144.8, 143.7, 138.3, 137.7, 134.4, 131.3, 131.1 (q, *J* = 5.0 Hz), 127.6, 123.4 (q, *J* = 273.0 Hz), 115.4, (q, *J* = 32.0 Hz), 114.4, 66.2, 52.7, 12.9 ppm; Anal. calc. for C₁₈H₁₃F₃O₄ (350.08): C, 61.72; H, 3.74. Found: C, 61.46; H, 3.51; LC-MS: [M+H]⁺ *m/z* 351.



(147) 2-[[1-Methyl-8-oxo-3-(trifluoromethyl)-8H-benzo[cd]azulen-4-yl]oxy]-acetic acid (147).

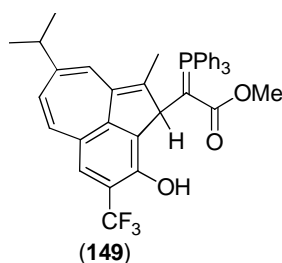
To a solution of methyl ester **(146)** (97 mg, 0.28 mmol) in THF–methanol–acetone–water (2:2:2:1) (15 mL) at room temperature, lithium hydroxide hydrate (18 mg, 0.42 mmol, 1.5

equiv) was added, and the resulting mixture was stirred at room temperature until TLC analysis indicated complete consumption of the starting material (90 min). EtOAc (20 mL) and brine (10 mL) were added and the resulting mixture was acidified with aqueous 1 M HCl (5 mL). Layers were separated and the aqueous phase was extracted with EtOAc (2 × 10 mL). The organic phase was dried over anhydrous Na₂SO₄, filtered, and the solvents were removed on a rotary evaporator to yield (**147**) as orange crystals (90 mg, 96%) without a need for further purification. M. p. 270–271 °C (decomp.); ¹H NMR (300 MHz, DMSO-*d*₆): δ 13.19 (1H, br s), 7.55 (H, d, *J* = 12.6 Hz), 7.32 (1H, s), 7.17–7.07 (1H, m), 7.00 (1H, d, *J* = 2.4 Hz), 6.84 (1H, dd, *J* = 2.4 Hz, 12.6 Hz), 4.95 (2H, s), 2.25 (3H, d, *J* = 1.2 Hz) ppm; ¹³C NMR (75 MHz, DMSO-*d*₆): δ 186.9, 169.0, 157.1, 147.5, 144.9, 142.3, 138.3, 137.1, 134.5, 130.8, 129.9 (q, *J* = 4.6 Hz), 125.6, 123.6 (q, *J* = 273.0 Hz), 113.0, (q, *J* = 31.0 Hz), 112.3, 65.4, 12.3 ppm; Anal. calc. for C₁₇H₁₁F₃O₄ (336.06): C, 60.72; H, 3.30. Found: C, 60.90; H, 3.29; LC–MS: [M+H]⁺ *m/z* 337.



(±)-2-(Benzylthio)-8-isopropyl-1-methyl-4-(trifluoromethyl)-2H-benzo[cd]azulen-3-ol (148).

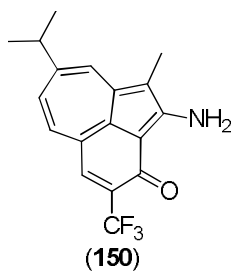
Benzo[*cd*]azulen-3-one (**36c**) (100 mg, 0.33 mmol) was dissolved in anhydrous ethanol (4 mL) and benzylthiol (85 μL, 0.66 mmol, 2 equiv) was added. The reaction mixture was stirred at room temperature under argon atmosphere until TLC analysis indicated the complete consumption of the green starting material (1.5 h) and formation of an orange product. The reaction mixture was evaporated to constant weight on a rotary evaporator and the obtained crude product was purified by column chromatography on silica gel (eluent: EtOAc/*n*-hexane 1:8) to give (**148**) as an orange solid (118 mg, 81%). M. p. 114–116 °C (dec.); ¹H NMR (300 MHz, CDCl₃): δ 7.31 (1H, m), 7.23–7.12 (3H, m), 7.08 (1H, d, *J* = 1.8 Hz), 7.06 (1H, m), 7.01 (1H, s), 5.99 (1H, d, *J* = 12.6 Hz), 5.90 (1H, s), 5.50 (1H, dd, *J* = 1.8 Hz, 12.6 Hz), 4.30 (1H, s), 3.32 (1H, d, *J* = 13.2 Hz), 3.22 (1H, d, *J* = 13.2 Hz), 2.28 (1H, septet, *J* = 6.9 Hz), 1.81 (3H, d, *J* = 0.9 Hz), 1.09 (6H, d, *J* = 6.9 Hz) ppm; ¹³C NMR (75 MHz, CD₂Cl₂): δ 152.2, 149.7, 144.8, 139.3, 137.8, 134.5, 132.5, 130.5, 129.5, 129.5, 128.9, 128.9, 128.0, 127.7, 127.7, 125.8, 124.3 (q, *J* = 271 Hz), 122.3, 115.6 (q, *J* = 31 Hz), 53.1, 38.7, 32.7, 22.2, 22.1, 11.4 ppm; Anal. calc. for C₂₅H₂₃F₃OS (428.14): C, 70.07; H, 5.41. Found: C, 69.79; H, 5.30.



(±)-Methyl 2-(3-hydroxy-8-isopropyl-1-methyl-4-(trifluoromethyl)-2H-benzo[cd]azulen-2-yl)-2-(triphenylphosphoranylidene)acetate (149).

To a solution of methyl (triphenylphosphoranylidene)acetate (110 mg, 0.33 mmol, 1.5 equiv) in anhydrous THF (5 mL) a solution of benzo[*cd*]azulen-3-one (**36c**) (75 mg, 0.25

mmol, 1.0 equiv) in THF (3 mL) was added at $-15\text{ }^{\circ}\text{C}$ under argon atmosphere. After 15 min, the cold bath was removed, and the reaction mixture was allowed to warm up to room temperature. TLC analysis indicated the complete consumption of green starting material and formation of a bright yellow product (90 min). EtOAc (20 mL) and water (10 mL) were added, and phases were separated. The aqueous phase was extracted with EtOAc (2×10 mL) and the combined organic phases were dried over anhydrous Na_2SO_4 , filtered, and evaporated to dryness. The crude product was purified by column chromatography on silica gel (eluent: EtOAc/Cyclohexane 1:5) to give (**149**) as a light-orange powder (112 mg, 70%). Some material was lost during the purification since the product is unstable in acidic media. M. p. $142\text{--}144\text{ }^{\circ}\text{C}$ (dec.); ^1H NMR (300 MHz, C_6D_6): δ 11.16 (1H, br s), 7.54–7.40 (6H, m), 7.10–6.94 (10H, m), 5.62 (1H, d, $J = 12.3$ Hz), 5.17 (1H, s), 5.09 (1H, dd, $J = 1.8$ Hz, 12.3 Hz), 4.88 (1H, d, $J = 28.2$ Hz), 3.02 (3H, s), 1.93 (1H, septet, $J = 6.9$ Hz), 1.38 (3H, d, $J = 1.2$ Hz), 0.93 (6H, d, $J = 6.9$ Hz) ppm; ^{13}C NMR (75 MHz, acetone- d_6): δ 175.5 (d, $J = 12$ Hz), 153.6, 150.8, 142.0, 138.5, 137.3, 136.4, 134.4 (d, $J = 10$ Hz) $\times 3$, 133.1 (d, $J = 12$ Hz) $\times 6$, 133.2, 129.3 (d, $J = 12$ Hz) $\times 9$, 128.2 (q, $J = 5$ Hz), 126.4, 125.7 (q, $J = 270$ Hz), 124.7, 122.7, 114.3 (q, $J = 30$ Hz), 51.5 (d, $J = 12$ Hz), 50.4, 38.4, 38.2 (d, $J = 118$ Hz), 22.1, 21.8, 13.0 ppm; Anal. calc. for $\text{C}_{39}\text{H}_{34}\text{F}_3\text{O}_3\text{P}$ (638.22): C, 73.34; H, 5.37. Found: C, 73.49; H, 5.11; HRMS-ESI m/z : calc. for $\text{C}_{39}\text{H}_{34}\text{F}_3\text{O}_3\text{P}$ $[\text{M}+\text{H}]^+$: 639.2276, found 639.2136.



2-Amino-8-isopropyl-1-methyl-4-(trifluoromethyl)-3H-benzo[cd]-azulen-3-one (150).

Benzo[cd]azulen-3-one (**36c**) (100 mg, 0.33 mmol) was dissolved in methanol (8 mL) and hydroxylamine hydrochloride (184 mg, 2.65 mmol, 8 equiv) and ammonium acetate (205 mg, 2.65 mmol, 8 equiv) were added. The reaction mixture was stirred for 3 days under argon atmosphere. TLC analysis indicated a formation of a polar product. EtOAc (20 mL) and saturated solution of sodium hydrogencarbonate (10 mL) were added and phases were separated. The aqueous phase was extracted with EtOAc (2×10 mL), and the combined organic phases were dried over anhydrous Na_2SO_4 , filtered and evaporated to dryness. The crude product was purified by column chromatography on silica gel (eluent: EtOAc/*n*-hexane 1:2) to give (**150**) as a dark, brownish-green solid (40 mg, 38%). M. p. $237\text{ }^{\circ}\text{C}$; ^1H NMR (300 MHz, $\text{DMSO-}d_6$): δ 9.03 (1H, br s), 8.77 (1H, br, s), 8.13 (1H, s), 7.63 (1H, s), 7.61 (1H, dd, $J = 1.5$ Hz, 11.7 Hz), 7.16 (1H, dd, $J = 1.5$ Hz, 11.7 Hz), 3.10 (1H, septet, $J = 6.9$ Hz), 2.25 (3H, s), 1.30 (6H, d, $J = 6.9$ Hz) ppm; ^{13}C NMR (75 MHz, CDCl_3): δ 174.9, 163.9, 155.1, 146.5, 141.0, 137.3, 134.4, 130.9 (q, $J = 28$ Hz), 128.5, 125.7, 123.4, 123.3 (q, $J = 272$ Hz), 112.3, 109.1, 40.3, 24.4, 24.4, 7.8 ppm; Anal. calc. for $\text{C}_{18}\text{H}_{16}\text{F}_3\text{NO}$ (319.12): C, 67.70; H, 5.05; N, 4.39. Found: C, 66.37; H, 4.88; N, 3.98; HRMS-ESI m/z : calc. for $\text{C}_{18}\text{H}_{16}\text{F}_3\text{NO}$ $[\text{M}+\text{H}]^+$: 320.1262, found 320.1262.

5 Results and discussion

The overall findings of this thesis work are described in this chapter, including the synthesis of six-membered nitrogen-containing heterocyclic cinnoline derivatives by Diels-Alder reaction on solid-phase (Chapter 5.1), and the synthesis of a model compound targeted to the C1 domain of PKC by Diels-Alder methodology (Chapter 5.2). Chapter 5.3 focuses on the synthesis of new guaiazulene derivatives; synthesis of 4-aminoguaiazulene and its δ -lactam derivatives (5.3.1) and synthesis of tricyclic benzo[*cd*]azulene derivatives as selective and potent Pim kinase inhibitors (Chapter 5.3.2).

5.1 Synthesis of hexahydrocinnolines by aza Diels-Alder reaction

Cinnoline (**151**) (1,2-diazanaphthalene) is a heteroaromatic compound and isosteric to either quinoline or isoquinoline. Therefore, many synthesized cinnoline compounds are designed as analogs of the previously obtained quinoline or isoquinoline derivatives.²⁵⁵ Cinnoline itself shows antibacterial activity against *Escherichia coli*.²⁵⁵ While cinnoline derivatives have not been found in nature, the cinnoline moiety, and its various structural modifications, can be found in several pharmaceutically interesting compounds (Figure 15). Cintazone (**152**), for example, is a nonsteroidal anti-inflammatory agent, and cinoxacin (**153**) is a synthetic antimicrobial agent, both related to oxolinic and nalidixic acids and used in urinary tract infections. Certain cinnoline-related compounds are useful as antianxiety and antihypertensive agents. The Porco group has demonstrated the usefulness of the epoxyquinol scaffold in the synthesis of a structurally diverse chemical library,²⁵⁶ structurally resembling the hexahydro-1,2,4-triazolocinnoline-3,5-diones synthesized in this study. Some members of the epoxyquinol library, such as compound (**154**) (Figure 15), specifically inhibited an induction of human heatshock protein (HSP 72) with IC_{50} value of 1.5 μ M.²⁵⁶ From a 168-member oxime library, the extended urazole compound (**155**) (Figure 15) inhibited the growth of human small-cell lung carcinoma cell line (A549) with an IC_{50} value of 6.2 μ M.²⁵⁷

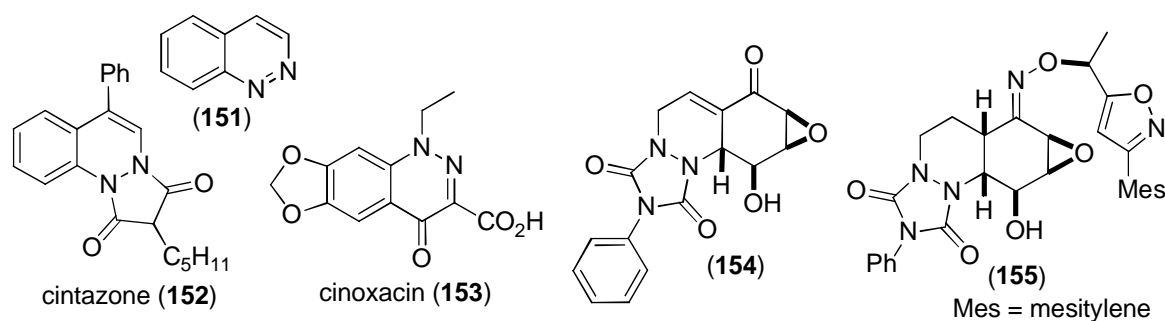
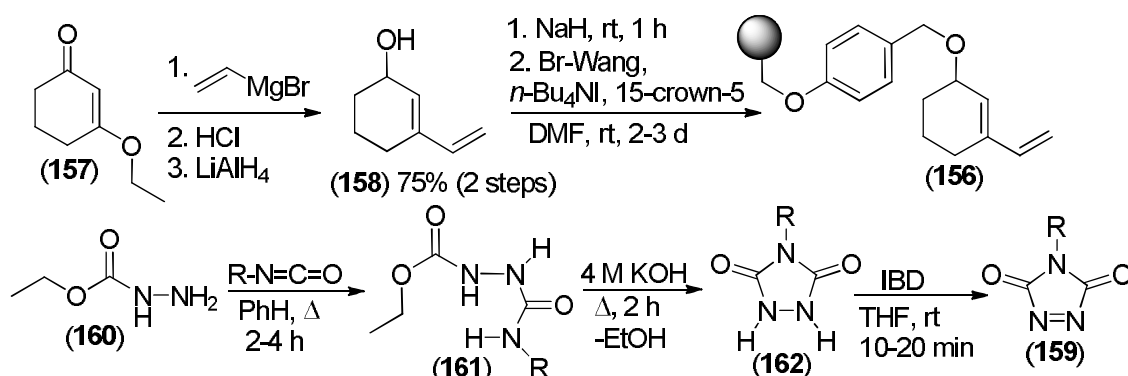


Figure 15. Cinnoline and some biologically active cinnoline derivatives.

As part of these studies on polymer-supported pericyclic reactions for preparing biologically interesting compounds, a practical synthetic method for the preparation of hexahydrocinnolines was developed. The synthesis of polymer-bound diene (**156**) (Scheme 16) commences with the facile Grignard reaction of readily available 3-ethoxycyclohex-2-enone (**157**) and vinylmagnesium bromide. This was followed by a reduction of the corresponding ketone with $LiAlH_4$ in diethyl ether resulting in allylic alcohol (**158**) (75% over two steps). The hydroxy group of (**158**) was used as an anchor for coupling with the

polymeric support. After the deprotonation of the secondary alcohol (**158**) with sodium hydride, the resulting anion was linked with the commercially available bromo-Wang resin in the presence of tetra-*n*-butylammonium iodide and a catalytic amount of 15-crown-5 in THF which secured effective loading (Scheme 16). The residual bromide left on the resin (**158**) was determined by the volumetric Volhard method, with no residual bromide found. As mentioned in Chapter 2, TADs (1,2,4-triazole-3,5-diones) (**159**) are known to be excellent hetero dienophiles in the Diels-Alder reaction, since the lower LUMO energy of the N=N bond, in contrast to the corresponding C=C bond, in alkenes makes the reactions proceed more rapidly and often at ambient temperatures.

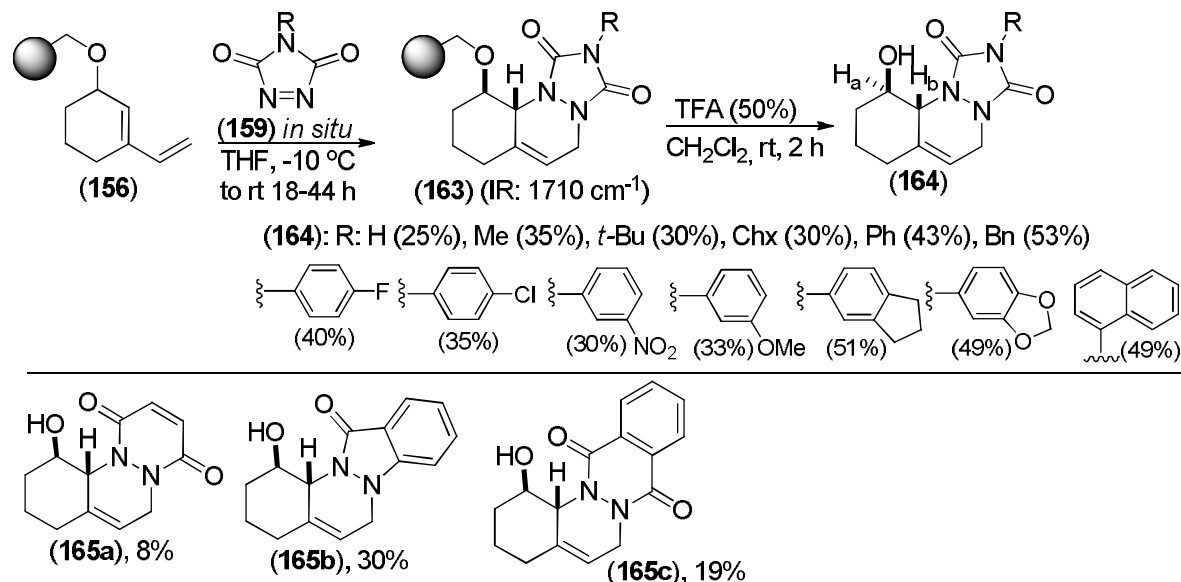
The commercial availability of the urazoles was restricted during this study. However, the preparation of urazoles by condensing *N*-alkyl or *N*-aryl isocyanates and ethyl hydrazide carboxylate (**160**), followed by cyclization of intermediate (**161**) in a basic medium (KOH/H₂O) turned out to be relatively straightforward (Scheme 16). Purification by recrystallization gave conveniently *N*-substituted urazoles (**162**), which can be stored as bench-stable azadienophilic precursors. Several oxidizing agents, including fuming nitric acid, lead peroxide, manganese dioxide, lead(IV) acetate, *tert*-butyl hypochlorite, and dinitrogen tetroxide, have been reported for the generation of *N*-substituted TADs (**159**).²⁵⁸ However, all of these reagents, except dinitrogen tetroxide, form byproducts that are difficult to remove or are too reactive toward sensitive azo compounds. Hypervalent iodine oxidation with iodobenzene diacetate (IBD) was reported to be a mild and non-acidic way for formation of (**161**).²⁵⁸ Intensive and rapid color change of the urazoles (**162**) (from colorless to dark red/violet) during IBD oxidation *in situ* indicates the formation of highly reactive dienophile species (**159**).



Scheme 16. Preparation of diene and dienophiles: synthesis of polymer-bound 3-vinyl-2-cyclohexen-1-ol and 1,2,4-triazole-3,5-diones.

Commercially available *N*-phenyl-1,2,4-triazole-3,5-dione was found to participate effectively in the hetero Diels-Alder reaction with polymer-bound diene (**156**) at a temperature as low as -78 °C. The [4+2]-cycloaddition reaction was monitored by FT-IR spectroscopy, where the appearance of a strong characteristic carbonyl band at 1710 cm⁻¹ in (**163**) (Scheme 17) revealed formation of the cycloadduct. The use of a higher reaction temperature (-10 °C vs -78 °C) did not show any difference in the stereoselectivity of the Diels-Alder reaction. In a similar fashion, the *in situ* generated *N*-aryl and *N*-alkyl TADs (**159**) participated in the aza Diels-Alder reaction, and the formed hexahydrocinnoline derivatives were cleaved from the resin in a traceless manner. Trifluoroacetic acid-mediated cleavage of the benzylic ether bond produced tricyclic cinnoline derivatives (**164**) as secondary alcohols. *N*-Aryl TADs gave slightly better yields (30–53%) compared to the *N*-alkyl TADs generated *in situ* from the corresponding *N*-alkyl urazoles (26–35%). The

stereochemistry of single diastereomeric cycloadducts (**164**) was determined by ^1H NMR studies, which showed that allylic proton H_b resonates as a doublet ($^3J_{\text{H}_a\text{-H}_b} = 8\text{--}10$ Hz). This, together with a broad ddd (doublet of doublet of doublets) of homoallylic methine proton H_a indicates that protons H_a and H_b are *trans* to each other (Scheme 17), as was reported previously for the corresponding solution-phase reaction product (**164**, R = Ph).²⁵⁹



Scheme 17. *Aza Diels-Alder on solid-phase: synthesis of cinnoline derivatives (164–165). Isolated yields of cinnolines (164) after three reaction steps in brackets.*

The scope of the method was extended by using other types of carbonylazo compounds as cyclic azadienophiles. Indazolinone, maleic hydrazide, phthalhydrazide, and pyrazolidine-3,5-dione were oxidized by IBD or lead (IV) acetate to the corresponding aza compounds and allowed to react with polymer-supported diene (**156**). The polymer-bound heterocycles were released from the resin, as their corresponding alcohols, by treatment with TFA to give tri and tetracyclic products (**165a–c**) (Scheme 17) up to moderate yields (8–30%) and with the same stereochemistry as for compounds (**164**) (^1H NMR). Compound (**165b**) was isolated as a single regio and stereoisomer. The carbonyl group of the indazolone moiety was located on the same side as the hydroxy group of the cyclohexanol ring and proven by X-ray crystallography (**165b**).

5.2 Synthesis of a tricyclic model compound targeting PKC C1b

By using the X-ray crystal structure of the PKC δ C1b domain combined with molecular modeling, (3-aminodecahydro-1,4-methanonaphthalen-2-yl)methanol (**166a**) was discovered as a novel C1 domain ligand. Docking simulations suggested that (**166a**) would be well accommodated in the PKC δ binding site (Figure 16). As illustrated in Figure 2, phorbol 13-*O*-acetate binds inside a groove on the PKC δ surface, forming a network of five hydrogen bonds.¹⁴⁹ This network involves two hydroxy and one carbonyl groups from phorbol 13-*O*-acetate that interact with the main chain amide and side chain hydroxy groups of Thr242, the main chain amide and carbonyl groups of Gly253, and the main chain carbonyl group of Leu251 from the protein. Similar interactions are suggested by the

docking simulations, whereby the hydroxy group of (**166a**) interacts with the main chain amide and side chain hydroxy groups of Thr242, and the amino group of (**166a**) accepts hydrogen bonds from both the carbonyl group of Leu251 and from that of Gly253.

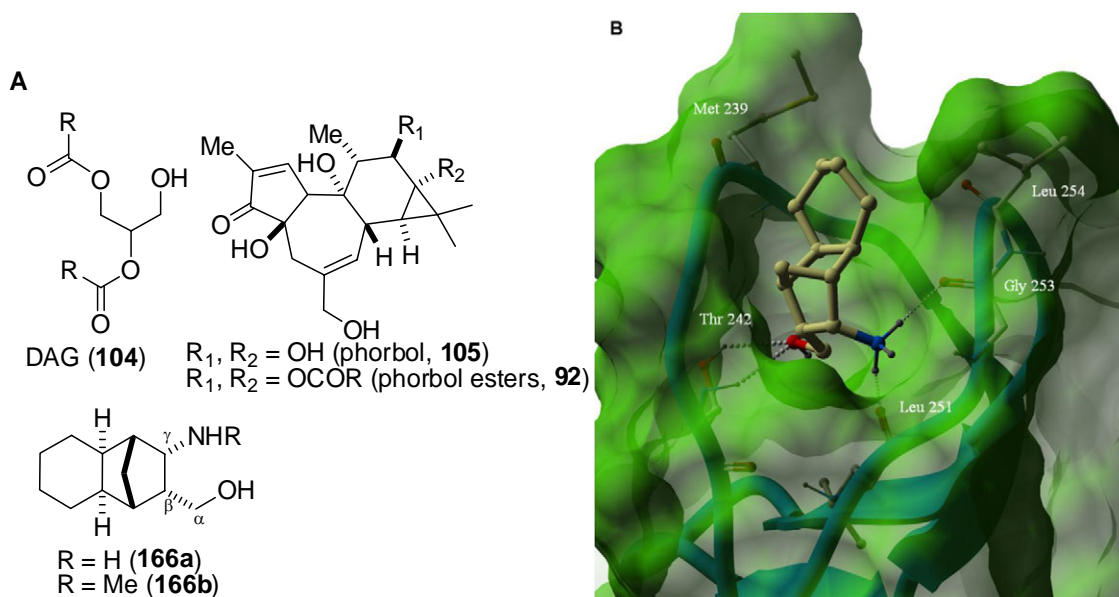
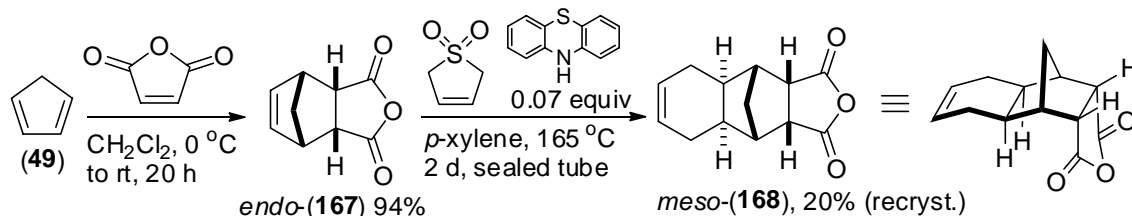


Figure 16. *A*) Structures of 1,2-diacylglycerol (DAG, **104**), phorbols (**105**, **92**) and γ -amino alcohols (**166a–b**). *B*) (**166a**) docked in the crystal structure of the PKC δ C1b domain¹⁴⁸ The C1b domain is represented as a transparent green surface and the secondary structure colored cyan. The hit compound (**166a**) and the residues are presented in ball and stick representation and colored by atom type. Hydrogen bonds are shown as white spheres. The figure was created using ICM-Browser (version3.7-2a, MolSoft L.L.C.).

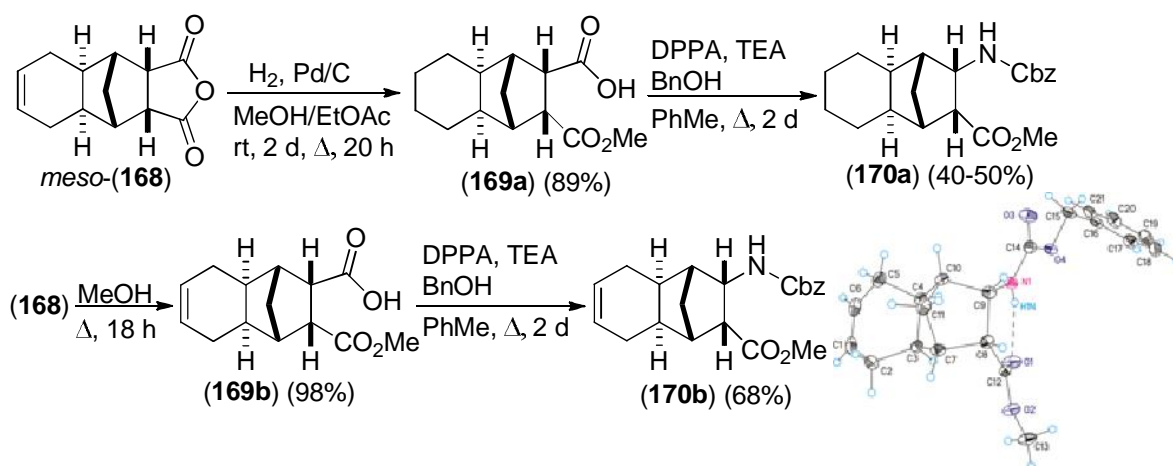
The synthetic endeavor of constructing the decahydronaphthalene core started from a known *endo*-norbornen-5,6-*cis*-dicarboxylic anhydride (**167**)³³ that is preparable in high yield from cyclopentadiene (**49**) and maleic anhydride (Scheme 18). The compound (**167**) was used as a dienophile for the next/subsequent [4+2]-cycloaddition reaction with 1,3-butadiene, generated *in situ* from its 3-sulfolene precursor in the presence of 0.07 equiv of phenothiazine as a chemical stabilizer. Under the forcing reaction conditions (160–170 °C, sealed tube, 2 d) the non-activated double bond of (**167**) undergoes the D-A cycloaddition with 1,3-butadiene to give the bridged tricyclic *meso*-anhydride (**168**)²⁶⁰ (Scheme 18).



Scheme 18. The tandem Diels-Alder sequence to construct the six continuous stereocenters of *meso*-anhydride (**168**)²⁶⁰ via *endo*-(**167**).

Up to 20% yield was produced (the crude product *exo/endo*-ratio ~ 4:1 by GC-MS) in multigram scale, and importantly as a single diastereomer after a single recrystallization from acetone. *Meso*-anhydride (**170**) presented the desired *exo*-stereochemistry in the fused cyclohexene ring as reported previously by Alder *et al.*²⁶⁰

The anhydride (**168**) was subjected to a one-pot catalytic hydrogenation and methanolysis step (H_2 , Pd/C, EtOAc/MeOH, Δ , 3 d) to give the ester (**169a**) with a completely reduced decahydronaphthalene core, isolated as a single diastereomer in high yield (89%, Scheme 19). Methanolysis of alkene (**168**) produced (**169b**) nearly quantitatively (98%, Scheme 19). The key reaction in the introduction of the amino functionality in (**169a–b**) was the use of the modified Curtius-Schmidt rearrangement reaction. The carboxylic acid (**169a**) was first converted into the corresponding isocyanate via an acyl azide intermediate using diphenylphosphoryl azide (DPPA).²⁶¹ A one-pot reaction in the presence of triethylamine and benzyl alcohol gave carbamate (**170a**) in moderate yield (40–50%) after chromatographic purification (Scheme 19). However, when (**169b**), bearing a cyclohexene moiety was subjected to the same Curtius-Schmidt rearrangement conditions, the Cbz-amine (**170b**) was isolated in higher yield (68%), and more importantly, as a solid reaction product. This, in turn, enabled us to carry out its single crystal X-ray structure analysis, which unambiguously confirmed the chemical structure of (**170b**) in the solid state (Scheme 19).

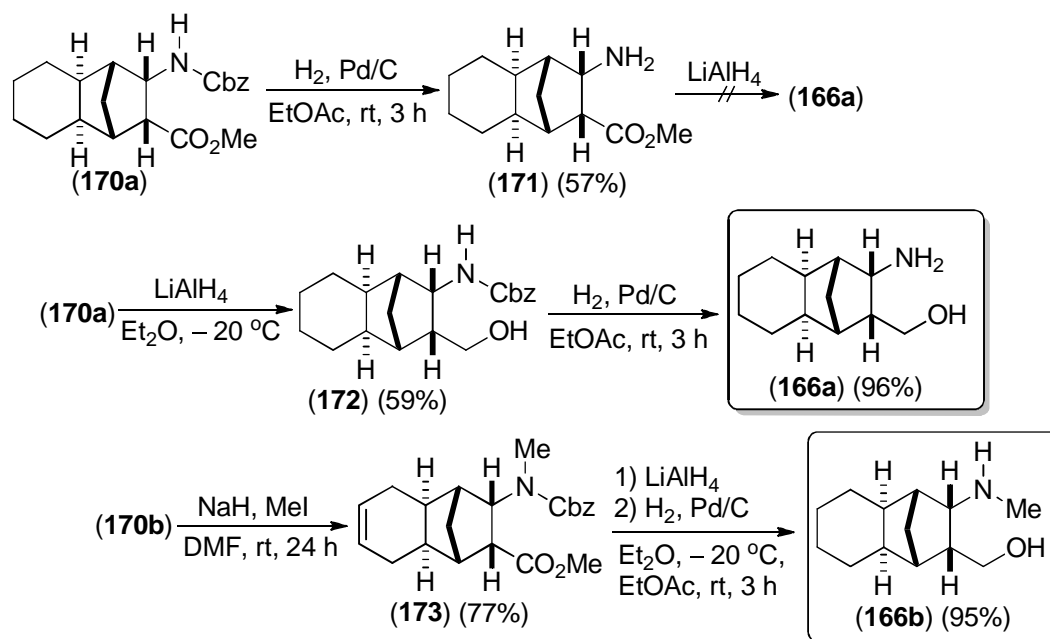


Scheme 19. One-pot Curtius-Schmidt rearrangement of hemiesters (**169a–b**) to the Cbz-protected amines (**170a–b**). ORTEP diagram of the molecular structure of (**170b**).

The removal of the Cbz-protection group of compound (**170a**) by catalytic hydrogenation (H_2 , Pd/C, EtOAc, 2–3 h) gave the corresponding amine (**171**) (57%, Scheme 20). Subsequent reduction with LiAlH_4 , however, was not successful, since the incomplete reaction was followed by purification difficulties. Therefore, the order of synthetic sequence was reversed. The reduction of the methyl ester in (**170a**) with LiAlH_4 was conducted at low temperature (-50 to -20 °C) since the nucleophilic intramolecular side reaction (formation of the cyclic carbamate by elimination of benzyl alcohol) was found to take place at ambient temperature. At this time the primary alcohol (**172**) was obtained in 59% yield after column chromatography on SiO_2 (Scheme 20). The final catalytic hydrogenation step reduced the fused cyclohexene ring and removed the carboxybenzyl group (H_2 , Pd/C, EtOAc, rt, 3 h, Scheme 20) giving (\pm)-*cis*-(3-aminodecahydro-1,4-methanonaphthalen-2-yl)methanol (**166a**) as a pure compound.

To convert the amino functionality of (**166a**) to a more hydrophobic one, its *N*-methyl derivative (**166b**) was synthesized, since the C1 domain is thought to be partly buried in the membrane bilayer during PKC activation.^{149,151} The direct *N*-monomethylation of primary amines is known to be a difficult task in preparative synthetic chemistry, and harsh reaction conditions, poor yields, and low selectivity are the major limitations of direct *N*-methylation reactions of primary amines. However, the use of the Cbz-protection group in (**170b**)

allowed its *N*-monomethylation under mild conditions. Deprotonation of (**170b**) with NaH in DMF, followed by treatment with iodomethane, gave the *N*-methyl derivative (**173**) (77%) without affecting the *cis*, *endo* relationship of the carboxymethyl and Cbz-amino groups (Scheme 20). The Cbz-protected γ -aminomethyl alcohol was obtained conveniently from the parent alkene (**173**) under the same reaction conditions used for the preparation of the compound (**172**), and it was subjected to the catalytic hydrogenation without further purification. (\pm)-[*cis*-3-(Methylamino)decahydro-1,4-methanonaphthalen-2-yl]methanol (**166b**) was isolated and converted to the hydrochloride salt (2 M HCl in Et₂O) in 90% yield (over 2 steps).



Scheme 20. Synthesis of γ -amino alcohols (**166a** and **166b**) by the successive reduction and catalytic hydrogenation sequence.

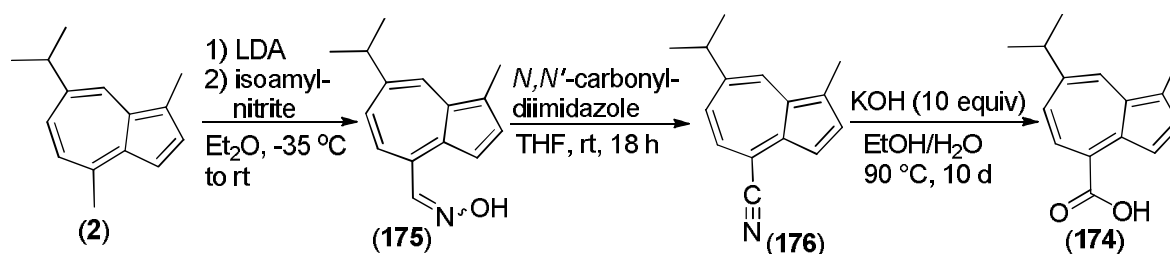
The synthesized (3-aminodecahydro-1,4-methanonaphthalen-2-yl)methanols (**166a–b**) were assayed for binding to the C1 domain of recombinant human PKC α and PKC δ using a filtration method in a 96-well plate format. Crude cell lysates of *Baculovirus*-infected *Sf* 9 cells were used as the source for PKC in the assay; lysate from uninfected *Sf* 9 cells did not exhibit phorbol ester binding (data not shown). The compounds were tested at a concentration range of 0.3–20 μ M. The results revealed that (**166a** and **166b**) were unable to displace [20-³H]phorbol-12,13-dibutyrate from PKC α and PKC δ (data not shown). Further work is being conducted in an effort to modify the synthesized compounds.

5.3 Synthesis of new guaiazulene derivatives

5.3.1 Synthesis of 4-aminoguaiazulene and its δ -lactam derivatives

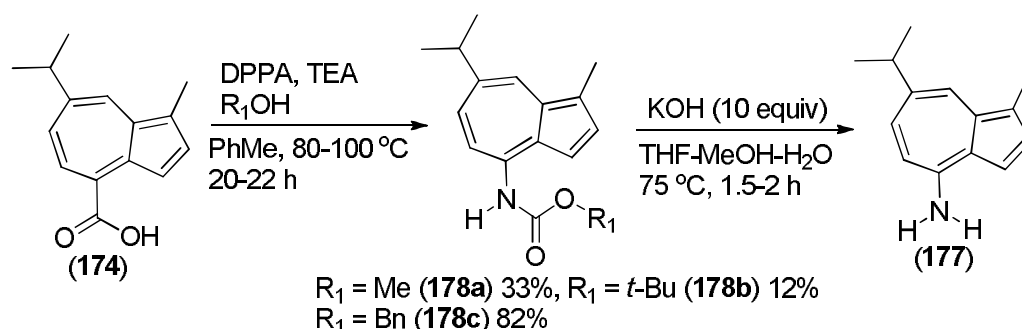
During the course of these studies, the introduction of a heteroatom into this structure was considered in order to modify the guaiazulene structure. This modification would be

especially interesting as nitrogen-substituted azulene derivatives are scarcely documented in the literature. Therefore, a method for nitrogen insertion into the 4-position of the guaiazulene (**2**) seven-membered ring was developed. This approach offered the possibility of synthesizing a number of new heterocyclic azulene derivatives. Modification of the 4-position of guaiazulene (**2**) is feasible due to the enhanced acidity of the C–H bond in its methyl group, a procedure that reflects a common strategy in the field of azulene chemistry. Aumüller has previously utilized this strategy for the three-step synthesis of 7-isopropyl-1-methylazulene-4-carboxylic acid (**174**)²⁶² starting from (**2**) (Scheme 21). Treatment of guaiazulene (**2**) with LDA, followed by addition of isoamyl nitrite, yields *N*-oxime (**175**) in modest yield (28%); however, the subsequent dehydration with *N,N*-carbonyldiimidazole yields nitrile (**176**) in nearly quantitative conversion. The nitrile (**176**) tolerates harsh reaction conditions and can therefore be subjected to strong basic conditions (KOH, 10 equiv) under prolonged heating in refluxing EtOH/H₂O-mixture (90 °C, 10 days), where the two-step hydrolysis *via* a primary amide intermediate finally gives the carboxylic acid (**174**) (Scheme 21).



Scheme 21. Preparation of 7-isopropyl-1-methylazulene-4-carboxylic acid (**174**).²⁶⁴

This crystalline and stable aryl carboxylic acid (**174**) was used as a starting material for the synthesis of nitrogen-substituted azulene derivatives. The key reaction in the preparation of amine (**177**) was the use of the modified Curtius-Schmidt rearrangement. The carboxylic acid (**174**) was first converted into the corresponding isocyanate *via* an acyl azide intermediate using diphenylphosphoryl azide (DPPA).²⁶¹ A one-pot reaction in the presence of triethylamine and an alcohol gave carbamates (**178a–c**) in variable yields (Scheme 22). For example, when methanol and *tert*-butyl alcohol were used, the yields were only moderate (12–33%). However, in the case of benzyl alcohol the reaction proceeded well, and benzyl (7-isopropyl-1-methylazulen-4-yl)carbamate (**178c**) was isolated in high yield (82%) after silica gel column chromatography. Subsequent deprotection of the Cbz-protected amine of (**178c**) turned out to be challenging, as standard methods, such as catalytic hydrogenation or acidic hydrolysis with HBr, suffered from the participation of the azulene moiety in numerous side reactions. Removal of the benzyl carbamate protective group was achieved in the presence of potassium hydroxide in an aqueous solution of THF and MeOH. When compound (**178c**) was heated with KOH in THF–MeOH–H₂O, the color of the reaction mixture changed quickly from blue to deep purple. The hydrolysis was complete in 1–1.5 h (TLC monitoring) and 7-isopropyl-1-methylazulen-4-amine (**177**) (Scheme 22) was isolated in good yield (76%) after column chromatography on silica gel. Amine (**177**) was found to be relatively stable when stored under an inert atmosphere in a refrigerated toluene solution (~0.10 mM).

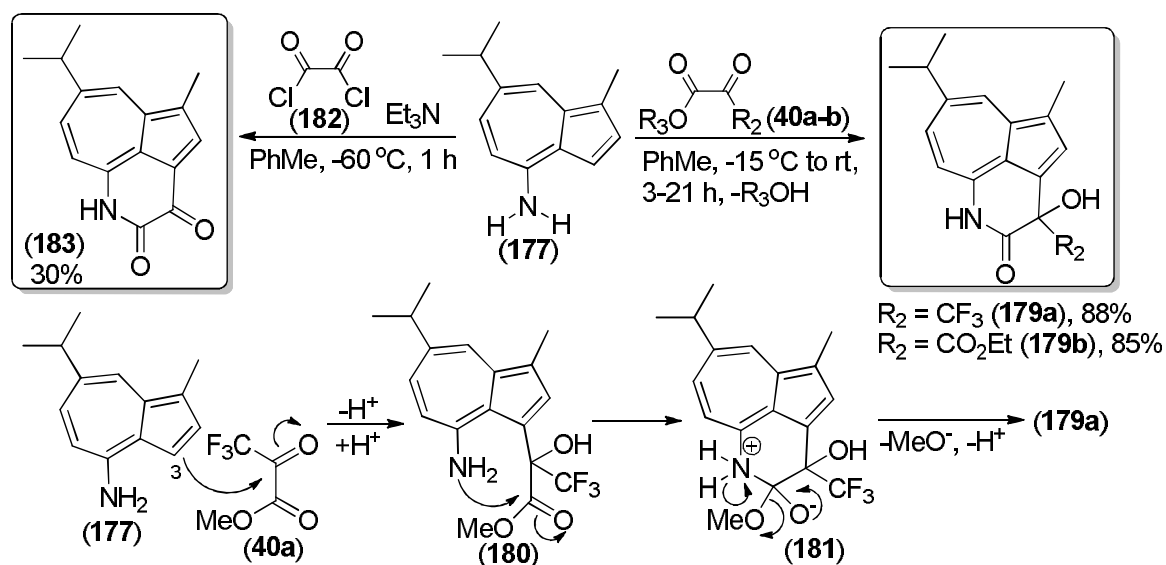


Scheme 22. Synthesis of 4-aminoguaiazulene (**177**) from the known carboxylic acid (**174**).

In agreement with previous work in our laboratory³², 7-isopropyl-1-methylazulene-4-amine (**177**) reacted with various 1,2-dicarbonyl compounds (**40a–b**) (Scheme 23). The cascade reactions yielded δ -lactams under mild reaction conditions without the need for a catalyst and produced a new six-membered ring fused to the azulene aromatic system. The one-pot reaction between (**177**) and methyl 3,3,3-trifluoropyruvate (**40a**) proceeded efficiently and yielded δ -lactam (**179a**) in 88% yield after purification by column chromatography. Theoretically, this reaction could have led to two regioisomeric products, but only one product was isolated. The azulenyl amine reacts in a similar fashion to that reported for the pure hydrocarbon guaiazulene.³²

The high nucleophilicity of the guaiazulenes electron-rich 3-position ensures that electrophilic substitution of this carbon atom is the predominant reaction between (**177**) and (**40a**) to yield (**180**) (Scheme 23), this is followed by a ring closure to furnish (**181**). Finally, the elimination of methanol produces δ -lactam (**179a**). The regioselectivity is further explained by the high electrophilicity of the central carbon atom of the doubly activated dicarbonyl reagent. The reaction with diethyl ketomalonate (**40b**) is comparable to that of (**40a**) (Scheme 23). Reaction of amine (**177**) at room temperature for 21 h yielded the corresponding lactam (**179b**) in 85% isolated yield after purification by column chromatography. In contrast, these types of cyclizations do not run smoothly with carbonyl reagents being not additionally activated, such as ethyl pyruvate, 2,3-butanedione, and ethyl glyoxylate. In these cases, lactam product was not obtained. However, other very reactive dicarbonyl reagents can be successfully employed, demonstrating that a broader structural variety is accessible by analogous reaction procedures.

For example, we found that a rapid reaction occurs between amine (**177**) and oxalyl chloride (**182**) (Scheme 23). When the reaction temperature was as low as -60 °C and an excess of the tertiary base (Et₃N) was used, compound (**183**) was obtained in moderate (30%) yield after purification by column chromatography. In contrast to the α -hydroxylactams (**179a–b**) the product (**183**) contains a different functional group and is an α -ketolactam.



Scheme 23. Cyclisation of 4-aminoguaiazulene (**177**) to six-membered lactams (**179a–b**, **183**) and proposed reaction mechanism for the formation of (**179a**).

5.3.2 Synthesis of tricyclic benzo[*cd*]azulenes as potential Pim-1 inhibitors

Analysis of the biological effects of new tricyclic benzo[*cd*]azulenes led to their identification as potent and selective inhibitors against Pim family kinases. These compounds inhibit the phosphorylation of Pim substrates and reverse the anti-apoptotic effects of Pim kinases. They also prevent migration of PC-3 prostate cancer cells and significantly suppress the proliferation of lymphoblastoid cell lines infected and immortalized by the Epstein-Barr virus. Therefore, the discovered benzo[*cd*]azulene compounds could be promising Pim-selective inhibitors for both research and therapeutic purposes.

Recently, Aumüller *et al.* developed a facile one-pot method for transformation of guaiazulene derivatives into new tricyclic heptafulvenes (**44**) (Figure 17).³² These compounds have a functionalized and fused six-membered ring on a benzo[*cd*]azulene skeleton. Furthermore, these heptafulvenes (**44**) were prone to oxidative cleavage when treated with a mild oxidant *m*CPBA (*meta*-chloroperoxybenzoic acid), yielding the corresponding tricyclic tropones (**48**) (Figure 17). In addition, the same authors reported a tautomerization reaction that proceeds *via* isomerization of π -bonds across the azulene moieties of tricyclic benzo[*cd*]azulen-3-ones (**36**) derived from the parent 4,5-dihydrobenzo[*cd*]azulen-3-ones (**35**).³¹ This efficient synthetic route produced heptafulvenes (**39**) (Figure 17) with a regioisomeric substitution pattern on the aromatic six-membered ring.³¹

Benzo[cd]azulenes are selective inhibitors against Pim family kinases

Six of the previously reported compounds (Figure 17) were used at 10 μ M concentrations against a panel of 71 different protein kinases and screened for residual kinase activities less than 50%.²⁶³ The results are presented in Table 1 of manuscript **IV** (appendix). Two of the tested compounds (**44a** and **36c**) significantly reduced the *in vitro* activities of Pim family members, especially Pim-1 and Pim-3 (Table 1 of manuscript **IV**). Compound (**44a**) showed clearly more selectivity than (**36c**), but also had some inhibitory activity against

PRAK (p38-regulated/activated protein kinase), p38g (mitogen-activated protein kinase) and some DYRK (dual specificity tyrosine-phosphorylation-regulated kinase) family members. Compounds (**48a**) and (**184**) were also active against Pim-1 and Pim-3 and demonstrated more selectivity than (**44a**). Interestingly, the structurally similar compounds (**44e**) and (**36b**) showed hardly any activity in *in vitro* kinase assays. It should be mentioned that the resulted screening gives only rough estimation on the kinase specificity of the compounds.

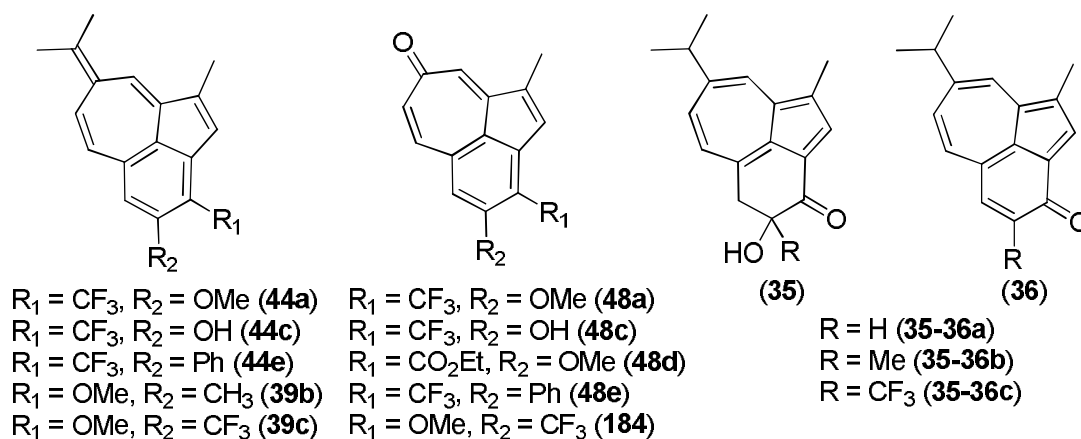
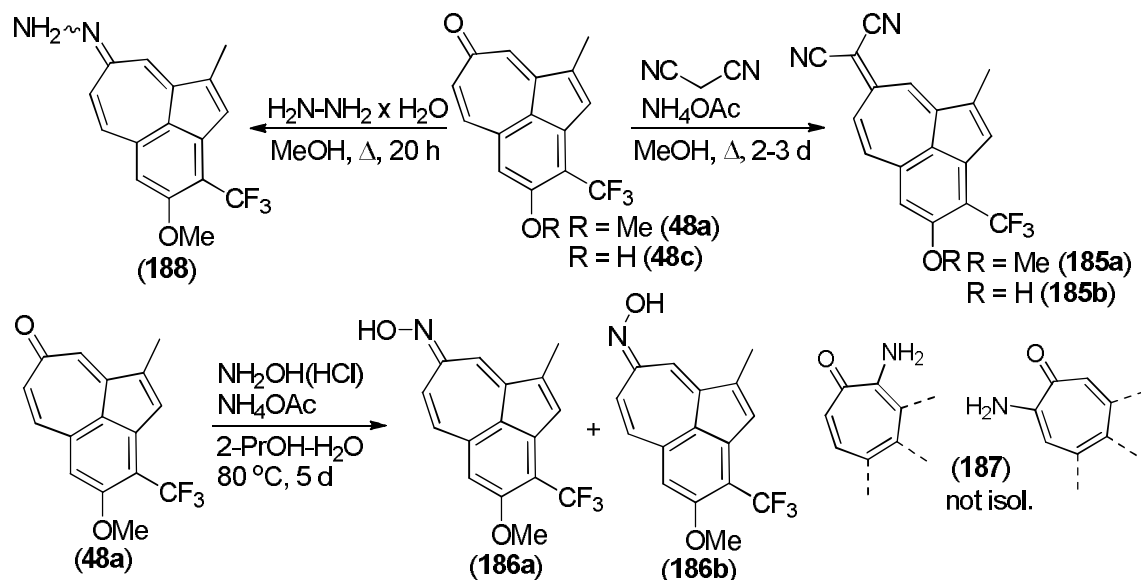


Figure 17. Some of the benzo[cd]azulenes and benzo[cd]azulen-3-ones by Aumüller *et al.*^{31,32}

Synthesis of new benzo[cd]azulene derivatives: Modification of the carbonyl functionality

The promising results on Pim kinase inhibition in multiple cell-based assays led to a further modification of the azulenes, heptafulvenes, and tropones presented in Figure 17. The aim was to develop derivatives that would be even more potent as Pim kinase inhibitors than previously reported benzo[cd]azulenes. Troponone (**48a**)³² was used as a key intermediate, since it was easily prepared in high yield (82%) from the parent heptafulvene (**44a**) and accessible to chemical modification through its carbonyl group. In addition, it was shown to be a potential and Pim selective kinase inhibitor. The exocyclic C=C double bond was restored in a single transformation, when (**48a**) was subjected to the Knoevenagel condensation with malononitrile. The reaction was catalyzed by ammonium acetate and gave highly conjugated dicyanoheptafulvene (**185a**) in 45% yield (MeOH, reflux, 2–3 d, Scheme 24). An analogous two-step synthesis of similar dinitrile system is reported *via* ethoxytropylium fluoroborate.²⁶⁴ The electron withdrawing cyano groups are known to have a stabilizing effect on heptafulvenes. The crystalline product (**185a**) can be stored at room temperature over a prolonged period and shows good chemical stability in aqueous solutions. Demethylation of the aryl methyl ethers on tropones (**48a**, **184**) was found to be unsuccessful under standard conditions (BBr_3 , 2–4 equiv, CH_2Cl_2 , rt, 2–8 h). Therefore the free phenol analog (**48c**)³² (Figure 17) was synthesized and subjected to the Knoevenagel condensation (malononitrile, MeOH, reflux, 4 d) to give the phenolic dinitrile (**185b**) (Scheme 24). The carbonyl group of (**48a**) was transformed into the oxime functionality by treating it with hydroxylamine hydrochloride in the presence of ammonium acetate in a mixture of isopropanol–water (3:1) for a prolonged time (5 d, 80 °C, Scheme 24). Two stereoisomers were separated by a careful column chromatography on silica gel followed by recrystallization (EtOAc/*n*-Hex) to give pure *Z* and *E* isomers (NMR, NOE assignment) of oximes (**186a**) (42%, yellow needles) and (**186b**) (29%, orange needles). Under these reaction conditions, no 2-aminotropone derivatives (**187**) (Scheme 24) were formed, as has

been previously reported for the tropone itself to produce a mixture of products.²⁶⁵ The analogous reaction for (**48a**) in the presence of hydrazine monohydrate (MeOH, reflux, 20 h) (Scheme 24) yields hydrazone product (**188**) as an inseparable *E/Z*-mixture. Again none of the 2-amino-substituted products were isolated, which is in contrast to the previous observations in the related tropone systems.²⁶⁵



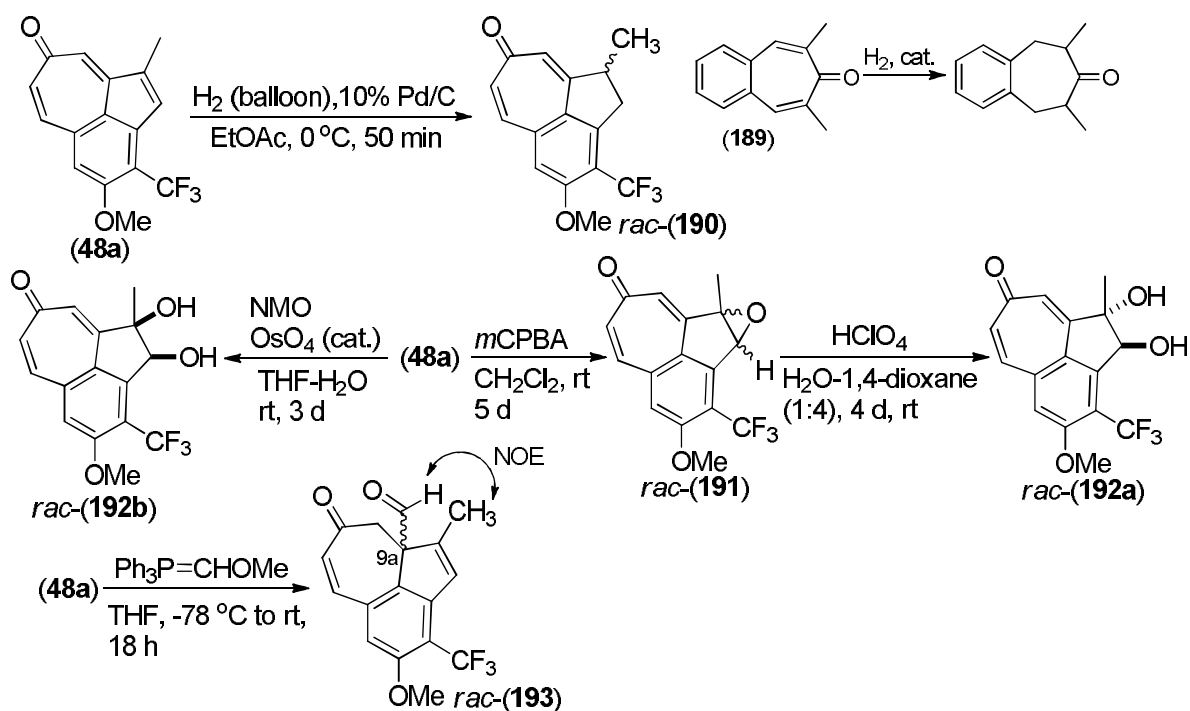
Scheme 24. Modification of tropone carbonyl function in synthesis of new derivatives.

Derivatization of the double bond of the five-membered ring

Catalytic hydrogenation of (**48a**) gave one main product after chromatographic isolation. Instead of reduction of the C=C double bonds in the seven-membered ring as reported for the similar 3,4-fused benzotropone (**189**),²⁶⁵ it was found that the double bond in the five-membered ring of (**48a**) was more susceptible to catalytic hydrogenation, when the reaction conditions were carefully controlled (Scheme 25, H₂, 10% Pd/C, EtOAc, 0 °C, 50 min). The racemic non-planar compound (**190**) was obtained in 40% yield.

The double bond in a five-membered ring showed regioselectivity towards oxidation when tropone (**48a**) was treated with an excess of *m*CPBA for a prolonged reaction time (3 equiv, rt, 5 d) giving the racemic epoxide (**191**) (Scheme 25) as a main product in 42% yield after column chromatography. The epoxide in (**191**) was prone to the acid-catalyzed ring opening (perchloric acid) to give *trans*-diol (**192a**) (Scheme 25) in high yield (89% after column chromatography). The corresponding *cis*-diol (**192b**) was synthesized directly from the alkene (**48a**) by using a catalytic amount of osmium tetroxide (OsO₄) and *N*-methylmorpholine *N*-oxide (NMO) as a co-oxidant. The diols (**192a–b**) showed improved solubility in protic solvents and were colorless compared to the previously synthesized strongly colored tropones (yellow/orange).

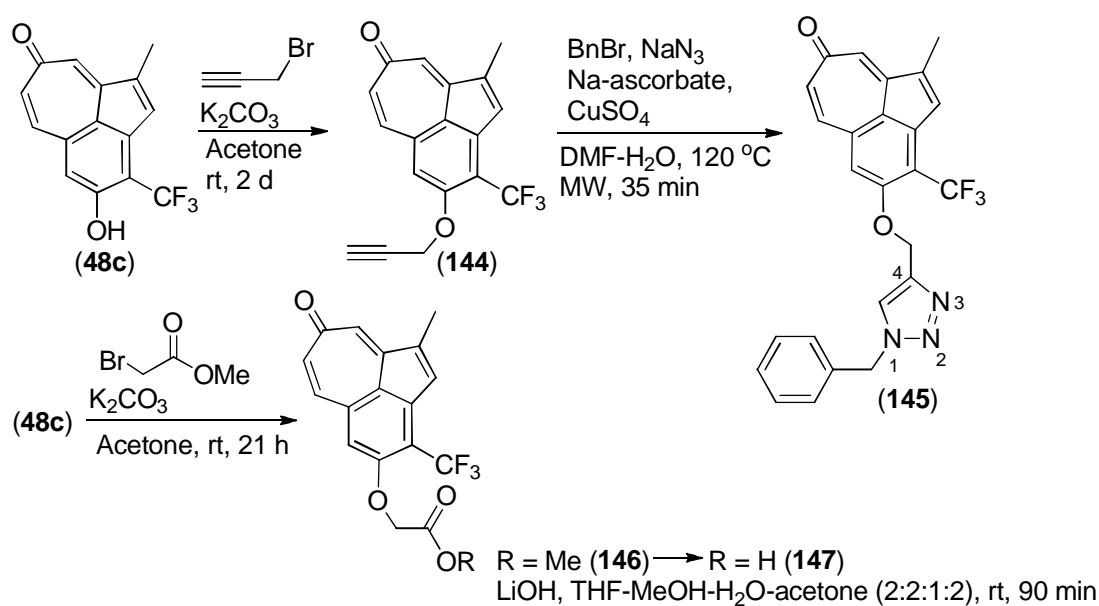
In the presence of phosphonium ylides the α,β -unsaturated ketone moiety of tropone (**48a**) was found to undergo 1,4-conjugate addition reaction instead of the expected Wittig reaction (Scheme 25). The low temperature (–78 °C) addition of ylide (methoxymethylene)triphenylphosphorane to (**48a**) gave one main product (**193**) in 38% yield after aqueous acidic work-up and chromatographic purification. Extensive 2D NMR (HMBC, HSQC, and NOESY) analysis unveiled that (**193**) had an unexpected structure of a non-planar quaternary aldehyde at carbon C9a (Scheme 25).



Scheme 25. Reduction and oxidation reactions of the five-membered ring in benzo[cd]azulenes and an example of the regioselective 1,4-conjugate addition.

Functionalization of the phenolic 4-position

The phenolic 4-position of benzo[cd]azulene (**48c**) is easily accessible for the attachment of various functional groups under mild reaction conditions. For example, propargylation of the phenol (**48c**) (K₂CO₃, propargyl bromide, acetone, rt, 48 h) gave terminal alkyne (**144**)²⁶⁶ (Scheme 26) in 62% yield, which was used in microwave-assisted, copper-catalyzed azide alkyne cycloaddition²⁶⁷ (Scheme 26, one-pot: BnBr, NaN₃, CuSO₄, Na-ascorbate, DMF-H₂O, 4:1, MW, 35 min) to give a tropone analog (**145**)²⁶⁶ as a single 1,4-regioisomeric product with the 1,2,3-triazole side chain.



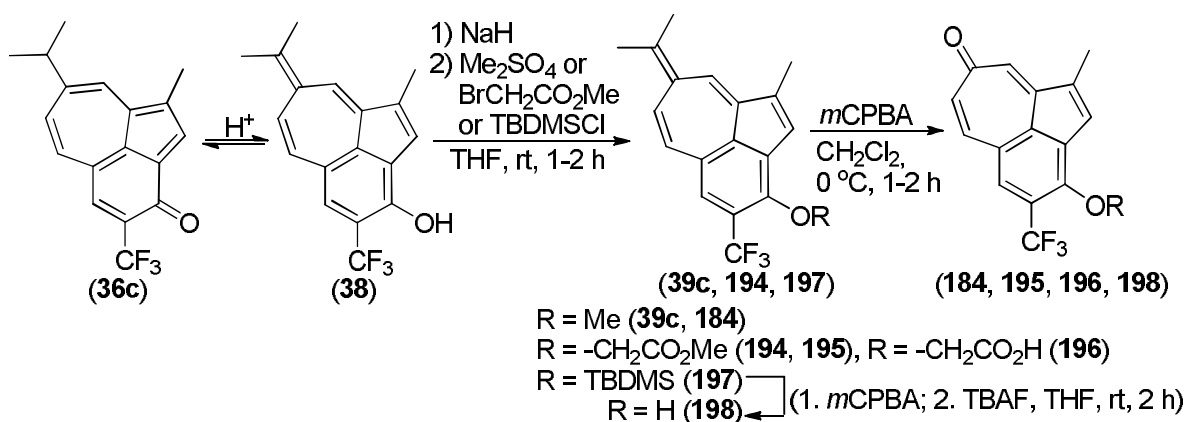
Scheme 26. Functionalization of the phenolic 4-position.

Several known Pim-1 inhibitors take advantage of the interaction with the positively charged amino residue of Lys67 on the binding pocket of Pim-1. Therefore, negatively charged carboxylate residue was attached to the benzo[*cd*]azulene framework to possibly make an ionic interaction with Lys67. This was achieved by deprotonation of phenol (**48c**) with potassium carbonate followed by treatment with methyl bromoacetate to give acetate (**146**)²⁶⁶ as a crystalline solid (Scheme 26). Hydrolysis of (**146**) with LiOH in THF–MeOH–H₂O–acetone gave the tricyclic acetic acid derivative (**147**)²⁶⁶ in 96% yield.

Functionalization of the 3-position of benzo[*cd*]azulene-3-ones

In this study, benzo[*cd*]azulene-3-one (**36c**) was synthesized from guaiazulene (**2**) with a 4-step procedure.³¹ The acid-catalyzed tautomerization reaction of (**36c**) presented in Chapter 2 produces heptafulvene (**39c**) as a trifluoromethyl ether in high yields after *in situ* *O*-methylation of the 3-position. In a similar manner, the enolization of (**36c**), followed by a treatment with methyl bromoacetate, yields a new heptafulvene (**194**)²⁶⁸ with a glycolate side chain on the 3-position (63% yield) (Scheme 27). Both heptafulvenes (**39c**, **194**) were further modified by oxidizing them with *m*CPBA. Novel tropone methyl ether (**184**) was isolated in high yield (85%) as a regioisomer of the heptafulvene **48c** (Scheme 27). Oxidation of (**194**) gave acetate (**195**), which was hydrolyzed under the same conditions as (**146**) (*vide infra*) to give a novel tropone derivative (**196**)²⁶⁸ with the acetic acid residue now on the 3-position and as a regioisomer of (**147**).

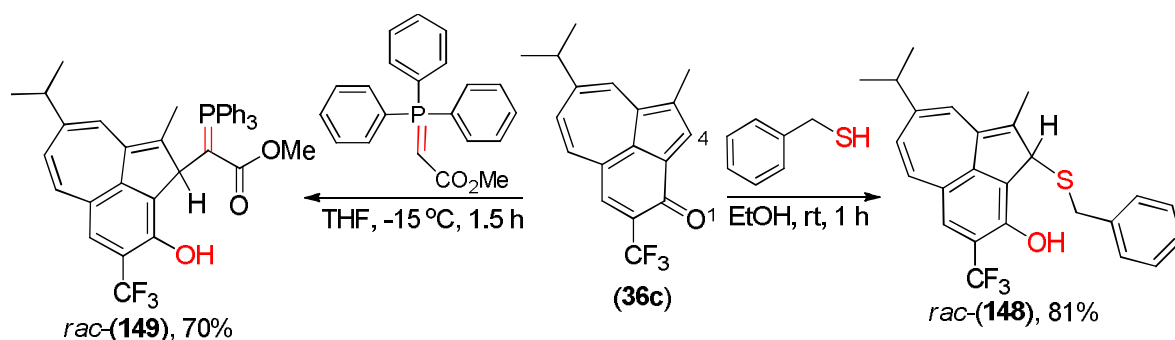
The isolation of the phenol (**38**) of benzo[*cd*]azulene-3-one (**36c**) (Scheme 27) is not possible since the reverse nature of a tautomerization reaction and therefore phenolic products cannot be synthesized. The demethylation of the aryl methyl ethers on tropones (**48a**, **184**) to phenolic products with standard reagent (BBr₃) is also inefficient. However, to overcome this problem, a cleavable phenolic tautomer could be trapped as a silyl enol ether. This strategy was demonstrated in the efficient two-step synthesis, where the phenol tautomer (**38**) is generated first *in situ* (HCl, cat., THF, rt, 20 min) and, after deprotonation, derivatized by silylation (NaH, 5 equiv and TBDMSCl 2.5 equiv, rt, 2–3 h) to give (**197**) in high 84% yield (Scheme 27). This allowed the *m*CPBA oxidation of the *exo*-double bond of heptafulvene (**197**), followed by a removal of the TBDMS-protection group by a 1.0 M solution of TBAF (tetrabutylammonium fluoride) in THF (1.2 equiv, THF, rt, 2 h) to finally give the troponoyl phenol (**198**) (Scheme 27) as a regioisomer of the benzo[*cd*]azulene (**48c**).



Scheme 27. Use of the acid-catalyzed tautomerization reaction in synthesis of regioisomeric benzo[*cd*]azulenes.

Nucleophilic conjugate addition reactions of benzo[*cd*]azulen-3-one

The utilization of benzo[*cd*]azulen-3-one (**36c**) was not only restricted in synthesis of new regioisomeric heptafulvenes and tropones. Benzo[*cd*]azulen-3-one (**36c**) was discovered to undergo efficient and regioselective 1,4 and 1,6-conjugate addition reactions with various soft and hard nucleophiles (Scheme 28).²⁶⁶ In an interesting example, the sulfur nucleophile (benzylthiol) reacts preferentially to the five-membered ring of benzo[*cd*]azulen-3-one (**36c**). Thus a regioselective 1,4-attack yields benzylthiol-substituted phenolic benzo[*cd*]azulene (**148**) (Scheme 28). Despite the fact that product (**148**) is prone to decomposition when exposed to an acidic environment (SiO₂) in the purification by column chromatography, it is isolable in high 81% yield.²⁶⁶



Scheme 28. 1,4-Conjugate-addition reactions of benzo[*cd*]azulen-3-one to phenolic products.

Interestingly, the carbonyl group of benzo[*cd*]azulen-3-one (**36c**) did not undergo a typical Wittig reaction, but rather a conjugate addition reaction in the presence of methoxycarbonyl and nitrile-group stabilized phosphonium ylides. These preliminary studies of a reaction between (**36c**) and (triphenylphosphoranylidene)acetonitrile yielded a complex mixture of products (TLC). However, when benzo[*cd*]azulen-3-one (**36c**) was allowed to react with methyl (triphenylphosphoranylidene)acetate in anhydrous THF (-15 °C to rt, 1.5 h), the green starting material disappeared completely with formation of a single reaction product (**149**) (Scheme 28).²⁶⁶ The phosphine compound (**149**) was isolated as a yellow solid in 70% yield, although some of the material was lost during the purification by column chromatography since (**149**) is unstable in acidic media.

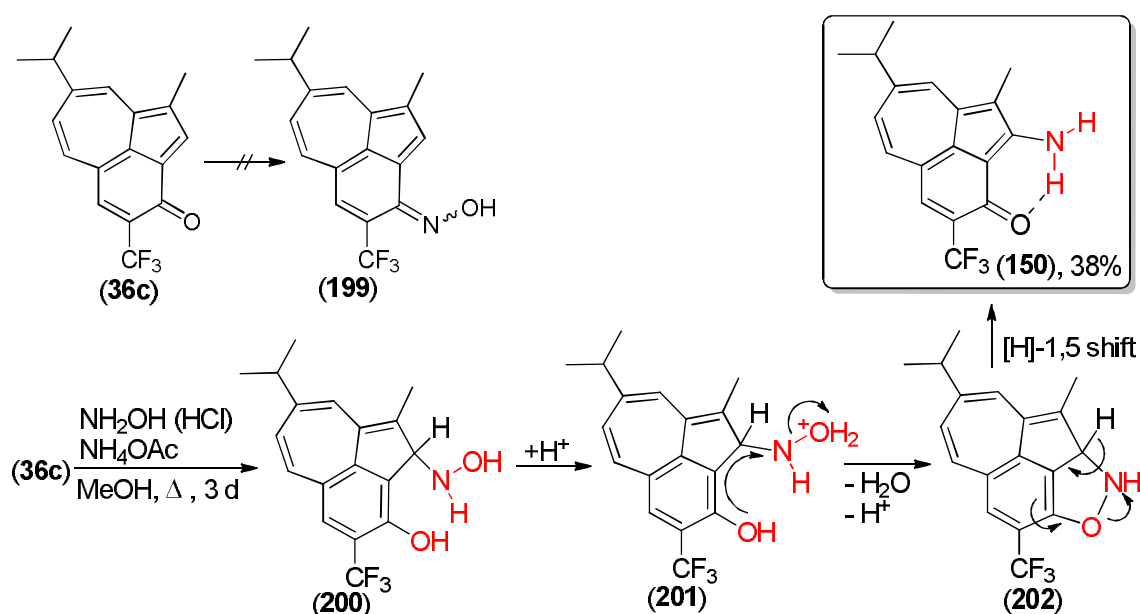
These two examples of conjugate addition reactions were performed at ambient temperature or even below 0 °C and they proceeded well even without any added catalyst to produce new types of tricyclic non-planar structures with a phenolic functionality on a benzo[*cd*]azulene skeleton

The reactivity of benzo[*cd*]azulen-3-one (**36c**) towards oxygen nucleophiles was also studied, but a reaction between phenol and (**36c**) failed to give any products. Benzo[*cd*]azulen-3-one (**36c**) even showed resistance to react in the presence of an excess of more nucleophilic oxygen species, such as phenolate anion (phenol, K₂CO₃, EtOH, rt) under prolonged reaction time (24 h) resulting only in partially decomposed starting material.²⁶⁶

During the attempts to manipulate benzo[*cd*]azulen-3-one (**36c**), the chemical behavior of its carbonyl group was found to have some odd qualities. A condensation reaction between ketone (**36c**) and hydroxylamine was assumed to give *N*-oxime reaction products (**199**) *via* the conventional 1,2-addition reaction (Scheme 29). However, when (**36c**) was heated in the presence of hydroxylamine hydrochloride (8 equiv) and ammonium acetate in

refluxing methanol for 3 days (Scheme 29), the isolated reaction product was not an oxime, despite the identical molecular weights of two products (LC-MS: $[M+H]^+$ m/z 320). It is assumed that hydroxylamine undergoes 1,4-conjugate addition to the 2-position of benzo[*cd*]azulen-3-one (**36c**) to give the initial phenolic intermediate (**200**) (Scheme 29). Protonation of the hydroxy moiety on the NHOH-group in slightly acidic reaction media is followed by an intramolecular attack of the phenolic hydroxy of (**201**) to the nitrogen atom. This leads to the scission of the labile N-O single bond as water is eliminated out and to the formation of the transient five-member heterocyclic (isoxazole) ring in (**202**) (Scheme 29). In the final step, a 1,5-hydrogen shift of a methine proton in (**202**) restores the carbonyl group of benzo[*cd*]azulen-3-one and releases the amino group to the 2-position by opening the intermediate five-member ring. 2-Aminobenzo[*cd*]azulen-3-one (**150**)²⁶⁶ is isolated as a main reaction product in 38% yield after column chromatography (Scheme 29).

According to the ¹H NMR studies, the NH₂ group of (**150**) gives two separate signals and can therefore be distinguished (DMSO-*d*₆: δ 9.03 and 8.77 ppm). The two separate signals are rationalized to be a result of a lack of free rotation around C-NH₂ bond, caused by a likely intramolecular hydrogen-bond (dashed line) between N-H and C=O in the benzo[*cd*]azulen-3-one (**150**) (Scheme 29). The presence of a carbonyl carbon at the 3-position of product (**150**), rather than a tautomeric phenol structure, was proven by the ¹³C NMR spectra, where the chemical shifts of the C=O of product (**150**) and starting material (**36c**) were identical (δ 174.9 ppm).²⁶⁶ The constitution of compound (**150**) was further confirmed by its high-resolution mass spectra (HRMS-ESI m/z : calc. for C₁₈H₁₆F₃NO $[M+H]^+$: 320.1262, found 320.1262).



Scheme 29. A tentative reaction mechanism for the formation of 2-aminobenzo[*cd*]azulen-3-one.

Further *in vitro* and cell-based characterization of benzo[*cd*]azulenes

To define the efficacy of the synthesized compounds, *in vitro* kinase assays were performed with bacterially produced human Pim-1 protein, to measure its residual activity. To confirm the preliminary results shown in Table 1 of manuscript **IV** (appendix), the previously synthesized compounds were used as controls. All the previously tested compounds resulted

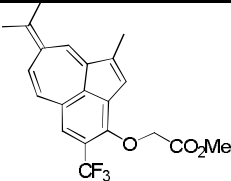
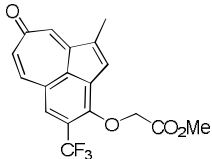
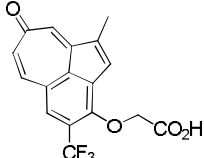
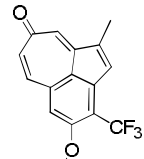
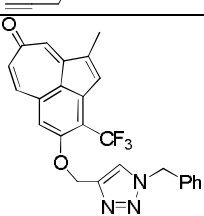
in very similar residual Pim-1 activities to those presented in Table 1 (manuscript **IV**). To qualify whether benzo[*cd*]azulenes can enter the cell and inhibit intracellular Pim kinase activity, the cell-based assays were carried out. In these assays, FDCP1-derived cell lines that had been stably transfected with either neomycin (FD/Neo) or the 44 kD isoform of Pim-1 (FD/Pim44) were used. In these assays a potent Pim inhibitor would reduce the survival of FD/Pim44 cells to the level of FD/Neo control cells, but would not have severe cytotoxic effects. The metabolic activity of the cells was measured to quantify the effects of the benzo[*cd*]azulenes on cell viability.

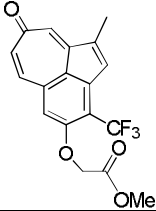
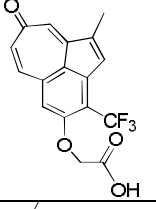
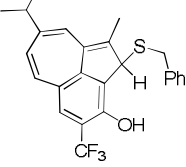
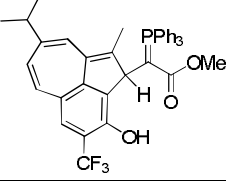
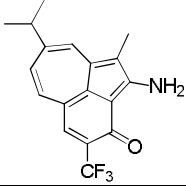
In these assays benzo[*cd*]azulenes (**44a**) and (**184**) reduced the metabolic activity of FD/Pim44 cells to the level of FD/Neo cells. By contrast, structurally similar compounds (**36b**) and (**44e**) remained ineffective in these assays. While (**36c**) initially displayed no efficacy, additional experiments with newly prepared and freshly dissolved sample demonstrated its high potency, but also cytotoxicity, which is why heptafulvene (**44a**) and tropone (**184**) were used in further biological assays (data not shown).

The calculation EC₅₀ (effective concentrations) values for (**44a**) and (**184**) showed nearly similar concentrations in both FD/Neo (5.2 and 6.9 μM) and FD/Pim44 (3.2 and 6.1 μM) cell lines, respectively.

The results of *in vitro* activities and cell viabilities are presented in Table 2 of manuscript **IV**. Compounds not included in the manuscript **IV** are listed in Table 2 (*vide infra*).

Table 2. Residual Pim-1 kinase activity (%) and cell viability (%) in the presence of benzo[*cd*]azulenes (10 μM and 0.5–5.0 μM, respectively).

Structure	Compound, ref.	Residual Pim-1 activity	Residual viability of FD/Neo cells	Residual viability of FD/Pim44 cells
	(194) ²⁶⁸	59	–	–
	(195) ²⁶⁸	87	–	–
	(196) ²⁶⁸	67	–	–
	(144) ²⁶⁶	119	–	–
	(145) ²⁶⁶	58	–	–

	(146) ²⁶⁶	113	–	–
	(147) ²⁶⁶	67	–	–
	(148) ²⁶⁶	28	32 (0.5 μM)	58 (0.5 μM)
	(149) ²⁶⁶	26	38 (1.5 μM)	35 (1.5 μM)
	(150) ²⁶⁶	37	62 (5.0 μM)	48 (5.0 μM)

Structure–activity relationships of benzo[cd]azulenes and conclusions

The results from *in vitro* activities and cell-based assays were used for structure-activity relationship studies (Table 2, manuscript **IV**). In the heptafulvenic series compound (**44a**) with the trifluoromethyl and methoxy substituents on 3- and 4-positions displayed a promising residual Pim-1 kinase activity of 43%. In addition, (**44a**) was even more effective against Pim-3 (residual activity of 30%). The regioisomeric heptafulvene (**39c**) was nearly as active against Pim-1 (residual activity 46%). In cell-based assays, compound (**44a**) reduced the metabolic activity of FD/Pim44 cells (cell viability 65%) without affecting of the FD/Neo control cells. By contrast, the regioisomeric heptafulvene (**39c**) was completely ineffective in these assays and rather showed some signs of off-target cytotoxicity (FD/Neo 74%, FD/Pim44 97%). The free 4-phenol analog (**44c**) was discovered to be the most potent compound of heptafulvene series, with low residual Pim-1 activity (29%). Its chemical instability however excluded it out from the cellular assays. Replacement of hydroxy functionality in (**44c**) with a phenyl ring in (**44e**) increased residual Pim-1 activity to 59%. Regardless of moderate *in vitro* activity, compound (**44e**) displayed any potency on cellular assays. The heptafulvene (**194**) with an oxyacetate side showed moderate inhibition (residual activity 59%). The necessity of the trifluoromethyl substituent on the phenyl ring in effective inhibition of Pim-1 kinase was demonstrated by replacing it with a methyl group in (**39b**) with a complete loss of inhibitory activity.

The tropones (**48a**) and (**184**) oxidized from the parent heptafulvenes (**44a**) and (**39c**)

were both slightly less potent with (residual activities of 74% and 58%, respectively). Later during the cellular assays it was recognized that tropone (**48a**) showed signs of non-specific cytotoxicity by affecting both the FD/Neo and FD/Pim44 cells (80%, 81%, respectively). However, its regioisomer (**184**) efficiently impaired the pro-survival advantage of Pim-1 overexpression in FD/Pim44 cells (69%) without any effects on FD/Neo cells. Due to the presence of modifiable carbonyl functionality and better chemical stability compared to the corresponding heptafulvenes, tropones were selected for further modifications.

Alkylation of the 3- and 4-positions gave tropones (**144**) and (**146**) but with no inhibitory activity at all. The triazole-functionalized tropone (**145**) showed more effective inhibition (residual Pim-1 activity of 58%), however, being only partly soluble to DMSO solvent. The regioisomeric carboxylic acids (**147** and **196**) showed only moderate residual Pim-1 activities (both 67%). When the trifluoromethyl substituent of (**48a**) was switched to an ethoxycarbonyl group in (**48d**), the kinase inhibitory activity was again completely lost (residual Pim-1 activity 98%). Tropone (**48c**) with a phenolic residue at 4-position was the most potent compound synthesized with residual Pim-1 activity of only 11%. Despite very promising *in vitro* kinase activity; in cell-based assays (**48c**) was disappointingly far less effective and showed signs of off-target cytotoxicity (FD/Neo 85%, FD/Pim44 83%). By contrast, its regioisomer (**198**) synthesized in this study was far less potent with residual Pim-1 activity of 65%.

The five-membered ring of (**48a**) was subjected for further modifications where the epoxide (**191**) showed moderate activity (residual activity 65%). The *cis*- and *trans*-diols (**192b**) and (**192a**) demonstrated slightly better *in vitro* activities against Pim-1 (residual activities 55% and 69%, respectively). However, it should be mentioned that both of these compounds showed a great improvement of solubility into protic solvents. The non-planar alkane (**190**) regioselectively hydrogenated from (**48a**) was completely inactive. However, the quaternary aldehyde (**193**) with a non-planar structure, proved to be a potent inhibitor of Pim-1 (residual activity 34%). In the cell-based assays it unfortunately showed obvious signs of non-specific cytotoxicity (FD/Neo, FD/Pim44, both 64%).

The troponoyl carbonyls on the 8-position of tropones (**48a**) and (**48c**) were further modified. The malonitrile derived heptafulvenes (**185a**) and (**185b**) resulted in moderate to effective (residual activities 60% and 41%, respectively) residual Pim-1 activities. Despite of dicyanoheptafulvene (**185a**) only moderate *in vitro* activity, it displayed similar properties as (**44a**) and (**184**) and efficiently impaired the pro-survival advantage of Pim-1 overexpression in FD/Pim44 cells (viability 61%) However, (**185a**) also affected the Neo expressing control cells (78%). By contrast, the more *in vitro* potent phenolic (**185b**) was completely inefficient in cell-based assays (FD/Pim44 93%).

The oximes (**186b**) and (**186a**) were assayed separately as pure *Z*- and *E*-isomers, but were not found to be potent against Pim-1 (residual kinase activities 82% and 71%). Similarly, the hydrazide (**188**) (mixt. of *Z/E* isomers) showed only moderate inhibitory activity (64%).

In the series of benzo[*cd*]azulen-3-ones, (**35c**) was only modestly active (residual Pim-1 activity 74%) and (**35b**) ineffective (92%). The dehydrated 4-methyl analog (**36b**) was also ineffective (92%) but (**36a**) with no substituent at 4-position was moderately effective (62%). Compound (**183**) representing the group of heterocyclic azulene derivatives showed moderate residual activity (59%). The CF₃-substituted compound (**36c**) showed moderate inhibition against Pim-1, but was surprisingly potent when tested against Pim-3 (residual activities 51% and 24%, respectively). However, on cell-based assays it dramatically reduced the cell viabilities of both cell lines (FD/ Neo 6%, FD/Pim44 3%). It is conceivable that the observed high activity of the benzo[*cd*]azulen-3-one **4c** in cell-based assays results

from its enhanced reactivity with various nucleophiles.²⁶⁶ The more detailed study will be published in due course. Moreover, (**36c**) was found to be a potent inhibitor of Pim-3 kinase with a residual activity of 24%.²⁶³ The azulene compounds derived from benzo[*cd*]azulen-3-one (**36c**) were tested against Pim-1. The 2-amino benzo[*cd*]azulen-3-one (**150**) showed potent residual *in vitro* activity against Pim-1 (37%). The two phenolic compounds (**148**, **149**) were even more efficient with residual activities of 28% and 26%, respectively.²⁶⁶ In the preliminary cellular assays compounds (**148**, **149** and **150**) reduced efficiently the cell viabilities of both cell lines even at 0.5 μ M concentration. The detailed results covering synthesis and biological potency of these compounds will be published later in an individual article.

The SAR analysis indicated that the presence of CF₃-substituent on the phenyl ring plays an essential role in the effective inhibition of Pim-1 kinase. Moreover, phenolic structure on benzo[*cd*]azulenes was important for effective Pim-1 inhibition; exemplified in (**48c**), (**148**), (**149**) and (**185b**) with the most efficient *in vitro* inhibitory activities.

Intriguingly, the *in vitro* results of benzo[*cd*]azulenes did not always correlate with their efficacy in cell-based assays. While the tropone (**48c**) very potently inhibited Pim-1 activity *in vitro*, it was less efficient in cells and also showed some signs of cytotoxicity. By contrast, (**184**) displayed only mild effects *in vitro*, but was still almost as effective as (**44a**) in cell-based assays. The same fashion was seen within dicyano-derived heptafulvenes (**185a**) and (**185b**), where the less *in vitro* active (**185a**) was the second most effective compound in cell-based assays of the whole study.

Ongoing development of additional benzo[*cd*]azulene derivatives is expected to further improve their efficacy as Pim-selective kinase inhibitors and putative anti-tumor drug candidates.

6 Summary and conclusions

A practical solid-phase method for the preparation of biologically interesting heterocyclic six-membered compounds by the aza Diels-Alder reaction was developed. A variety of hexahydrocinnoline derivatives and related compounds were synthesized by this approach (I). The availability of carbonylazo dienophiles was restricted, during the study, since only one single compound (4-phenyl-1,2,4-triazole-3,5-dione) was commercially available. Therefore, a convenient two-step synthetic procedure was used in a parallel fashion to introduce the urazole compounds as bench-stable precursors of 1,2,4-triazole-3,5-diones in high yields. The semicyclic diene 3-vinyl-cyclohexen-1-ol was prepared for the study over two steps, followed by its efficient loading *via* benzyl ether to the commercially available bromo-Wang resin. The aza Diels-Alder reaction between polymer-bound diene and *in situ* generated *N*-aryl and *N*-alkyl 1,2,4-triazole-3,5-diones was performed at ambient temperature with no added catalyst. The subsequent acid-mediated cleavage of the benzylic C–O bond of the resin-bound cycloadducts took place in a traceless manner, with no sign of linker being detected. The typical isolated yields were modest, ranging from 8 to 53% over three reaction steps. Some of the cycloadditions were carried out in a parallel fashion. The cleaved cycloadducts were typically purified by column chromatography to ensure the high purity, although some of the reactions gave rather pure crude products. The stereochemistry of single diastereomeric cycloadducts was determined by ¹H NMR spectroscopy and the results were consistent to those reported from solution-phase reactions.

The hetero Diels-Alder method was successfully transformed to polymeric support. The advantages of a solid-phase method were in the isolation and purification of the resin, and the use excess reagents to help to drive the equilibrium towards the products. However, the major drawback of the developed method was the restricted access to multiple derivatization sites on both diene and dienophile components of the Diels-Alder reaction, which led to products with limited variation on the substituent sites.

Some of the compounds were screened against a panel of 71 different protein kinases. The selected cycloadducts showed no significant kinase inhibition; however, these compounds could be used in the future as templates to diversify their chemical structures since these transformations are likely to provide access to even more functionalized heterocyclic compounds.

Utilization of the known X-ray crystal structure of the PKC δ C1b domain combined with molecular modeling led to a discovery of (3-aminodecahydro-1,4-methanonaphthalen-2-yl)methanol (**166a**) as a new C1 domain ligand (III). Various synthetic strategies and methods were attempted, including two Diels-Alder routes for the construction of the decahydronaphthalene core. Under the forcing reaction conditions, the bridged tricyclic *meso*-anhydride (**168**) was synthesized with its six continuous stereocenters, and in 20% yield, after some reaction optimization. The anhydride (**168**) was accessible in multigram scale and importantly as a single *exo*-diastereomer after recrystallization. The Curtius-Schmidt rearrangement reaction was used for the installation of amino functionality to carboxylic acids derived from the anhydride (**168**). The single crystal X-ray structure analysis confirmed the chemical structure of the key intermediate (**170b**). The reduction of methyl ester, followed by a catalytic hydrogenation step, completed the synthesis of (\pm)-*cis*-(3-aminodecahydro-1,4-methanonaphthalen-2-yl)methanol (**166a**). The Cbz-protecting group was utilized in the synthesis of the *N*-methyl derivative (**166b**).

Despite a successful preparation of the decahydronaphthalene core of γ -amino alcohols with the correct stereochemistry, the drawback of this synthetic route was the lack of

convenient generation of derivatives of (**168**) by the selected Diels-Alder route. The most disappointing fact was that the (3-aminodecahydro-1,4-methanonaphthalen-2-yl)methanols (**166a**, **166b**) were unable to displace [20-³H]phorbol-12,13-dibutyrate from PKC α and PKC δ , and therefore left the benefit of these compounds as PKC C1b ligands unclear. While both γ -amino alcohols were prepared and tested as racemates, synthesis of optically pure ligands may be achieved by desymmetrization of *meso*-anhydride (**168**) by asymmetric methanolysis. Further work is being conducted in an effort to modify the synthesized compounds.

En route to new guaiazulene derivatives, we became interested in introducing a heteroatom into this structure. Therefore, a method for nitrogen insertion into the 4-position of the guaiazulene seven-membered ring was developed (II). This approach offered the possibility of synthesizing a number of new heterocyclic azulene derivatives. The aryl carboxylic acid (**174**) was converted to benzyl (7-isopropyl-1-methylazulen-4-yl)carbamate (**176c**) in high yield (82%) by the Curtius rearrangement reaction. The removal of the Cbz-protecting group under basic reaction conditions gave 7-isopropyl-1-methylazulen-4-amine (**177**) as a new aminoazulene derivative. Amine (**177**) can be purified by column chromatography on silica gel and is relatively stable when stored in a refrigerated solution under an inert atmosphere. The cascade reactions between (**177**) and various 1,2-dicarbonyl compounds yielded δ -lactams (**179a–b**) under mild reaction conditions without the need for a catalyst and produced a new heterocyclic six-membered ring fused to the azulene aromatic system. While only two δ -lactam products were synthesized in this study, the yields were high with a formation of single regioisomers. The cyclizations failed with carbonyl reagents that are not additionally activated (e.g. ethyl pyruvate, 2,3-butanedione, and ethyl glyoxylate). However, other very reactive dicarbonyl reagents such as oxalyl chloride can be used, as demonstrated in the synthesis of α -keto lactam (**183**). Further work is being conducted in an effort to expand the scope of the reaction and to investigate the biological properties of these compounds as potential inhibitors of Pim protein kinases.

Recently, some of the benzo[*cd*]azulenes synthesized in our laboratory were characterized as selective Pim inhibitors when screened against a panel of 71 protein kinases. In addition, we found that treatment with benzo[*cd*]azulenes significantly slows down migration of adherent cancer cells derived from either prostate cancer or squamocellular carcinomas. Based on the promising results on Pim kinase inhibition in multiple cell-based assays, further modification of the azulenes, heptafulvenes, and tropones was conducted with the aim of developing new derivatives of the original benzo[*cd*]azulene compounds (IV). Variation of multiple positions around the benzo[*cd*]azulene core was achieved, including manipulation of the troponoyl carbonyl function, derivatization of the double bond on the five-membered ring, and functionalization of the both 3 and 4 positions of the phenyl ring. Introduction of regioisomeric tropones and heptafulvenes of the most promising compounds was achieved.

The most striking results of the whole study were obtained in the attempts to manipulate the carbonyl function of benzo[*cd*]azulen-3-one (**36c**). It was discovered that compound (**36c**) undergoes an efficient and regioselective 1,4-addition reactions with various soft and hard nucleophiles. In an interesting example, sulfur nucleophile (benzylthiol) leads to preferable 1,4-attack to the five-membered ring of (**36c**) to produce (**148**). The single phenolic reaction product (**148**) is isolable as high as 81% yield, despite the fact that it is prone to decomposition during the purification by column chromatography on SiO₂.

Interestingly, benzo[*cd*]azulen-3-one (**36c**) did not undergo a typical Wittig reaction but rather a conjugate addition reaction in the presence of a phosphonium ylide. Likewise in product (**148**), the nucleophilic addition took place at the five-membered ring and gave triphenylphosphonium ylide-substituted benzo[*cd*]azulene (**149**) as a sole reaction product. When heated in the presence of hydroxylamine, the ketone carbonyl of the compound (**36c**) did not follow the expected 1,2-addition reaction to give the *N*-oxime products. Instead, hydroxylamine undergoes a surprising 1,4-conjugate addition to the five-member ring of benzo[*cd*]azulen-3-one (**36c**). This leads to the scission of the N-O single bond as water is eliminated followed by the subsequent 1,6-hydrogen shift, which restores the carbonyl function and gives 2-aminobenzo[*cd*]azulen-3-one (**150**) as a main reaction product.

These three examples of conjugate addition reactions were performed at ambient temperature or even below 0 °C (except **150**) and they worked well, even without any added catalyst, to produce a new type of tricyclic phenolic benzo[*cd*]azulenes. These results with detailed biological properties will be published in the future.

Structure-activity studies of benzo[*cd*]azulenes revealed that the trifluoromethyl substituent on the phenyl ring plays an essential role in the effective inhibition of Pim-1 kinase. This was demonstrated with compounds bearing alternative arene substituent patterns, such as found in the methyl and ethoxycarbonyl analogs (**39b**) and (**44d**), both being completely inactive compounds. This study also showed that the presence of phenolic hydroxy on the six-membered ring of benzo[*cd*]azulenes was important for its effective activity. Tropone (**48c**), azulenes (**44c**), (**148**) and (**149**) and heptafulvene (**185b**), all carrying a phenol as a common structural feature, showed the most efficient inhibitory *in vitro* inhibitory activity against Pim-1. By contrast, the regioisomeric tropone (**198**) showed only modest efficiency as compared to the above mentioned compounds.

The benzo[*cd*]azulenes detailed in this study were found to be useful research compounds as potential Pim-selective kinase inhibitors. Attempts to crystallize Pim-1 with benzo[*cd*]azulene compound for the X-ray structure determination are under way. Information from the possible X-ray crystal structure, combined with new synthetic methods developed in this study, will be valuable tools in further development of promising scaffolds of small molecule therapies against Pim-overexpressing invasive tumors and other tumorigenic disorders in the future.

References

**

1. Ružička, L. Multimembered rings, higher terpene compounds and male sex hormones. Nobel lecture, 12 December **1945**. http://www.nobelprize.org/nobel_prizes/chemistry/laureates/1939/ruzicka-lecture.pdf (accessed August 28, 2012).
2. Kekulé, A. Sur la constitution des substances aromatiques. *Bull. Soc. Chim. Fr.* **1865**, 3, 98–110.
3. Rapson, W. S.; Robinson, R. Experiments on the synthesis of substances related to the sterols. Part II. A new general method for the synthesis of substituted cyclohexenones. *J. Chem. Soc.* **1935**, 1285–1288.
4. Wieland, P.; Miescher, K. Über die Herstellung mehrkerniger Ketone. *Helv. Chim. Acta* **1950**, 33, 2215–2228.
5. Majetich, G.; Behnke, M.; Hull, K. A stereoselective synthesis of (±)-nootkatone and (±)-valencene via an intramolecular sakurai reaction. *J. Org. Chem.* **1985**, 50, 3615–3618.
6. Scheerer, J.R.; Lawrence, J.F.; Wang, G.C.; Evans, D.A. Asymmetric synthesis of salvinorin A, a potent K opioid receptor agonist. *J. Am. Chem. Soc.* **2007**, 129, 8968–8969.
7. Oppolzer, W.; Snieckus, V. Intramolecular ene reactions in organic synthesis. *Angew. Chem. Int. Ed.* **1978**, 17, 476–486.
8. Johnson, W. S. Biomimetic polyene cyclizations. *Angew. Chem. Int. Ed.* **1976**, 15, 9–17.
9. Abe, I.; Rohmer, M.; Prestwich, G. D. Enzymatic cyclization of squalene and oxidosqualene to sterols and triterpenes. *Chem. Rev.* **1993**, 93, 2189–2206.
10. Jasperse, C. P.; Curran, D. P.; Fevig, T. L. Radical Reactions in Natural Product Synthesis. *Chem. Rev.* **1991**, 91, 1237–1286.
11. Nicolaou, K. C.; Petasis, N. A.; Uenishi, J.; Zipkin, R. E. The endiandric acid cascade. Electrocyclizations in organic synthesis. 2. Stepwise, stereocontrolled total synthesis of endiandric acids C-G. *J. Am. Chem. Soc.* **1982**, 104, 5557–5558.
12. DeGraffenreid, M. R.; Bennett, S.; Caille, S.; Gonzalez-Lopez de Turiso, F.; Hungate, R. W.; Julian, L. D.; Kaizerman, J. A.; McMinn, D. L. Sun, D.; Yan, X.; Powers, J. P. An efficient and scalable one-pot double michael addition-Dieckmann condensation for the synthesis of 4,4-disubstituted cyclohexane β-keto esters. *J. Org. Chem.* **2007**, 72, 7455–7458.
13. Fürstner, A. Olefin metathesis and beyond. *Angew. Chem. Int. Ed.* **2000**, 39, 3012.
14. Deiters, A.; Martin, S. F. Synthesis of oxygen- and nitrogen-containing heterocycles by ring-closing metathesis. *Chem. Rev.* **2004**, 104, 2199–2238.
15. White, J. D.; Hrnčiar, P.; Stappenbeck, F. Asymmetric total synthesis of (+)-codeine via intramolecular carbenoid insertion. *J. Org. Chem.* **1999**, 64, 7871–7884.
16. Piesse, S.; Hebd, C. R. *Séances Acad. Sci.* **1863**, 57, 1016.
17. Plattner, P. A.; Pfau, A. S. Zur Kenntnis der flüchtigen Pflanzenstoffe. IV. Über die Konstitution der Azulene. *Helv. Chim. Acta* **1937**, 20, 224–232.
18. Zahradník, R. Electronic structure and properties of non-alternant hydrocarbons. *Angew. Chem. Int. Ed.* **1965**, 4, 1039–1050.
19. Boekelheide, V.; Smith, C. D. A study of the synthesis and properties of 2H-benz[cd]azulene and related compounds. *J. Am. Chem. Soc.* **1966**, 88, 3950–3958.

**

20. Hafner, K.; Schaum, H. Cycloheptatrieno-indene. *Angew. Chem. Int. Ed.* **1963**, *2*, 95–96.
21. Gibson, W. K.; Leaver, D.; Roff, J. E.; Cumming, C. W. Synthesis of cycl[3.3.2]azinones and benz[*cd*]azulenones. *J. Chem. Soc. Chem. Commun.* **1967**, 214–215.
22. Hafner, K.; Rieper, W. New synthesis of 2*H*-benzazulenes. *Angew. Chem. Int. Ed.* **1970**, *9*, 248.
23. Balduzzi, S.; Mueller-Bunz, H.; McGlinchey, M. J. A convenient synthetic route to benz[*cd*]azulenes: versatile ligands with the potential to bind metals in an η^5 , η^6 , or η^7 fashion. *Chem.–Eur. J.* **2004**, *10*, 5398–5405.
24. Nair, V.; Anilkumar, G. Cycloaddition reactions of heptafulvenes: an overview. *Synlett* **1998**, *9*, 950–957.
25. Abe, N.; Morita, T.; Takase, K. The synthesis and properties of 7*H*-naphth[3,2,1-*cd*]azulen-7-ones. *Tetrahedron Lett.* **1973**, *14*, 4755–4758.
26. Abe, N.; Morita, T.; Takase, K. Synthesis and some properties of 7*H*-naphth[3,2,1-*cd*]azulen-7-ones and related compounds *J. Chem. Soc. Perkin Trans. 1* **2001**, 1353–1358.
27. Morita T.; Abe, N.; Takase, K. The synthesis and properties of 3*H*-benz[*cd*]azulen-3-ones. *Formosan Sci.* **1996**, *49*, 25–29.
28. Abe, N.; Morita, T.; Takase, K. *Tetrahedron Lett.* **1974**, *13*, 3621–3624.
29. Neidlein, R.; Kramer, W. Heterocyclic and carbocyclic 12- π - and 14- π -Systems, 47th communication¹. Synthesis of 7,9-dimethyl-4,5-dihydro-3*H*-benz[*cd*]azulene-3-one and 7,9-dimethyl-3*H*-benz[*cd*]azulene-3-one. A simple synthesis of azulenopseudophenalenon. *Helv. Chim. Acta* **1982**, *65*, 280–285.
30. Neidlein, R.; Kramer, W.; Krotz, R. Syntheses of azulenopseudophenalenone (3*H*-benz[*cd*]azulene-3-one) and azulenohydroxypseudophenalenone (4,5-dihydro-3*H*-benz[*cd*]azulene-3,5-dione). *Arch. Pharm.* **1984**, *317*, 984–995.
31. Aumüller, I. B.; Yli-Kauhaluoma, J. Synthesis and tautomerization of benzo[*cd*]azulen-3-ones. *Org. Lett.* **2011**, *13*, 1670–1673.
32. Aumüller, I. B.; Yli-Kauhaluoma, J. Benzo[*cd*]azulene skeleton: azulene, heptafulvene, and tropone derivatives. *Org. Lett.* **2009**, *11*, 5363–5365.
33. Nissilä, T.; Backman, N.; Kolmonen, M.; Leinonen, A.; Kiriazis, A.; Yli-Kauhaluoma, J.; Sainiemi, L. T.; Kostianen, R.; Franssila, S.; Ketola, R. Rotating multipillar array electrospray ionization-mass spectrometry for rapid analysis and high-throughput screening. *Int. J. Mass Spectrom.* **2012**, *310*, 65–71.
34. Diels, O.; Alder, K. *Justus Liebigs Ann. Chem.* **1928**, *460*, 98–122.
35. Boger, D. L. Chapter 4.3: [4+2] Cycloadditions: Heterodiene Additions. In *Comprehensive Organic Synthesis*; Trost, B. M., Fleming, I., Paquette, L. A., Eds.; Pergamon Press: Oxford, **1991**; Vol. 5, pp. 451–512.
36. Taticchi, F. A. *Dienes in the Diels-Alder reaction*. John Wiley & Sons: New York, **1990**.
37. Martin, J. G.; Hill, R. K. Stereochemistry of the Diels-Alder reaction. *Chem. Rev.* **1961**, *61*, 537–562.
38. Oppolzer, W. Intramolecular Cycloaddition reactions of *ortho*-quinodimethanes in organic synthesis. *Synthesis* **1978**, 793–802.
39. Funk, R. L.; Vollhardt, K.P.C. *Chem. Soc. Rev.* **1980**, *9*, 41–61.
40. Nicolaou, K. C.; Barnette, W. E, Ma, P. A remarkably simple, highly efficient, and stereoselective synthesis of steroids and other polycyclic systems. Total synthesis of

**

- estra-1,3,5(10)-trien-17-one via intramolecular capture of *O*-quinodimethanes generated by cheletropic elimination of SO₂. *J. Org. Chem.* **1980**, *45*, 1463–1470.
41. Funk, R.L.; Vollhardt, K.P.C. Transition-Metal-Catalyzed Alkyne Cyclizations. A cobalt-mediated total synthesis of *dl*-estrone. *J. Am. Chem. Soc.* **1980**, *102*, 5253–5261.
 42. Afarinkia, K.; Vinader, V.; Nelson, T.; Posner, G. H. Diels-Alder cycloadditions of 2-pyrones and 2-pyridones. *Tetrahedron* **1992**, *48*, 9111–9171.
 43. Boger, D. L. Diels-Alder reactions of heterocyclic azadienes: scope and applications. *Chem. Rev.* **1986**, *86*, 781–793.
 44. Sauer, J.; Wiest, H. Diels-Alder additions with "inverse" electron demand. *Angew. Chem. Int. Ed.* **1962**, *1*, 269.
 45. Che, D.; Siegl, J.; Seitz, G. Synthesis of chiral 2-(20-pyrrolidinyl) pyridines from (*S*)- and (*R*)-proline: potential ligands of the neuronal nicotinic acetylcholine receptors. *Tetrahedron Asymm.* **1999**, *10*, 573–585.
 46. Pindur, U.; Lutz, G.; Otto, C. Acceleration and selectivity enhancement of Diels-Alder reactions by special and catalytic methods. *Chem. Rev.* **1993**, *93*, 741–761.
 47. Gleiter, R.; Merger, R. Chapter 8. In *Modern Acetylene Chemistry*. VCH, Weinheim, **1995**, pp. 285–319.
 48. Hoffmann, R. W. *Dehydrobenzene and Cycloalkynes*, Academic Press, New York, **1967**, pp. 208–236 and 343–356.
 49. Barlett, P. D.; Ryan, M. J.; Cohes, S. G. *J. Am. Chem. Soc.* **1942**, *64*, 2649–2653.
 50. Kelly, T. R.; De Silva, H.; Silva, R. A. Unidirectional rotary motion in a molecular system. *Nature* **1999**, *401*, 150–152.
 51. Deem, M. L. Cyclopropanes as reagents for synthesis – cycloaddition reactions with cyclopropenes. *Synthesis* **1972**, 675–691.
 52. Wittig, G.; Ludwig, R. T. Triptycen aus Antrachen und Dehydrobenzol. *Angew. Chem.* **1956**, *68*, 40.
 53. Weinreb, S. M. Chapter 4.2. Heterodienophile additions to Dienes. In *Comprehensive Organic Synthesis*; Trost, B. M., Fleming, I., Paquette, L. A., Eds.; Pergamon Press: Oxford, **1991**; Vol. 5, pp. 401–449.
 54. Alder, K. *Neuere Methoden der Preparativen Organischen Chemie*, Verlag Chemie, Berlin, **1943**, pp. 251–412.
 55. Gillis, B. T.; Hagarty, J. D. The reaction of 4-phenyl-1,2,4-triazoline-3,5-dione with conjugated dienes. *J. Org. Chem.* **1967**, *32*, 330–333.
 56. Rádl, S. 1,2,4-Triazoline-3,5-diones. *Adv. Heterocycl. Chem.* **1997**, *67*, 119–205.
 57. Moody, C. J. Azodicarbonyl compounds in heterocyclic synthesis. *Adv. Heterocycl. Chem.* **1982**, *30*, 1–45.
 58. Alder, K.; Stein, G. Untersuchungen über den Verlauf der Diensynthese. *Angew. Chem.* **1937**, *50*, 510–519.
 59. Alder, K.; Schumacher, M. Über den sterischen verlauf von dien-synthesen mit acyclischen dienen. *trans, trans-, cis, trans-* und *cis, cis-*1,4-diphenyl-butadien. *Justus Liebigs Ann. Chem.* **1951**, *571*, 87–107, Über den sterischen Verlauf von Dien-Synthesen mit acyclischen Dienen. Das Verhalten von *trans, trans-, cis-* und *cis, trans-*4-phenyl-butadien-1-carbonsäure-methylester bei der Dien-Synthese, 108–122, Über den sterischen verlauf von dien-synthesen mit acyclischen dienen. *trans, trans-* und *trans, cis-*1-phenyl-4-methyl-butadien, 123–137.
 60. Sauer, J. Diels-Alder-Reaktionen: Zum Reaktionsmechanismus. *Angew. Chem.* **1967**, *79*, 76–94.

**

61. Sankararaman, S. Chapter 3: Cycloaddition Reactios. In *Pericyclic Reactions – A Textbook*. Wiley, Germany, **2005**.
62. Corey, E. J.; Danheiser, R. L.; Chandrasekaran, S.; Siret, P.; Keck, G. E.; Gras, J. -L. Stereospecific total synthesis of gibberellic acid. A key tricyclic intermediate. *J. Am. Chem. Soc.* **1978**, *100*, 8031–8034.
63. Fleming, I. Chapter 4. In *Frontier Orbitals and Organic Chemical Reactions*, John Wiley, New York, **1976**, pp. 114–142.
64. Merrifield, R. B. Solid phase peptide synthesis. I. The synthesis of a tetrapeptide *J. Am. Chem. Soc.* **1963**, *85*, 2149–2154.
65. Früchtel, J. S.; Jung, G. Organic chemistry on solid supports. *Angew. Chem. Int. Ed.* **1996**, *35*, 17–42.
66. Wilson, S. R.; Czarnik, A. W. *Combinatorial Chemistry*, Wiley–Interscience, New York, **1997**.
67. Lorschach, B. A.; Kurth, M. J. Carbon-carbon bond forming solid-phase reactions. *Chem. Rev.* **1999**, *99*, 1549–1581.
68. Nicolaou, K. C.; Winssinger, N.; Pastor, J.; Ninkovic, S.; Sarabia, F.; He, Y.; Vourloumis, D.; Yang, Z.; Li, T.; Giannakakou, P.; Hamel, E. Synthesis of epothilones A and B in solid and solution phase. *Nature* **1997**, *387*, 268–272.
69. Nicolaou, K. C.; Winssinger, N.; Vourloumis, D.; Ohshima, T.; Kim, S.; Pfefferkorn, J.; Xu, J.-Y.; Li, T. Solid and solution phase synthesis and biological evaluation of combinatorial sarcodictyin libraries. *J. Am. Chem. Soc.* **1998**, *120*, 10814–10826.
70. Yli-Kauhaluoma, J. Diels-Alder reactions on solid support. *Tetrahedron* **2001**, *57*, 7053–7071.
71. Sun, S.; Murray, W. V. Solid phase Diels-Alder reactions of amino acid derived trienes. *J. Org. Chem.* **1999**, *64*, 5941–5945.
72. Stahl, P.; Kissau, L.; Mazitschek, R.; Giannis A.; Waldmann, H. Natural product derived receptor tyrosine kinase inhibitors: identification of IGF1R, Tie-2, and VEGFR-3 inhibitors. *Angew. Chem. Int. Ed.* **2002**, *41*, 1174–1178.
73. Stahl, P.; Kissau, L.; Mazitschek, R.; Huwe, A.; Furet, P.; Giannis, A.; Waldmann, H. Total synthesis and biological evaluation of the nakijiquinones. *J. Am. Chem. Soc.* **2001**, *123*, 11586–11593.
74. Yoshida, M.; Hedberg, C.; Kaiserc, M.; Waldmann, H. Traceless solid phase synthesis of natural product inspired *cis*-1,2-dehydrodecalins. *Chem. Commun.* **2009**, 2926–2928.
75. Tietze, L. F.; Kettenchou, G. Hetero Diels-Alder reactions in organic chemistry. *Top. Curr. Chem.* **1997**, *189*, 1–120.
76. Ciganek, E. *The Intramolecular Diels-Alder reaction*. *Organic Reactions* **1984**, *32*, 1–374.
77. Smith, M. B. N-dienyl amides and lactams. Preparation and Diels-Alder reactivity. *Org. Prep. Proced. Int.* **1990**, *22*, 315–397.
78. Oppolzer, W. Intramolekulare [4 + 2]- und [3 + 2]-Cycloadditionen in der organischen Synthese. *Angew. Chem.* **1977**, *89*, 10–24.
79. Kagan, H. B.; Riant, O. Catalytic asymmetric Diels-Alder reactions. *Chem. Rev.* **1992**, *92*, 1007–1019.
80. Oppolzer, W. Asymmetric Diels-Alder and ene reactions in organic synthesis. New synthetic methods. *Angew. Chem. Int. Ed.* **1984**, *23*, 876–889.
81. Waldmann, H. Asymmetric hetero Diels-Alder reactions. *Synthesis* **1994**, 535–551.

**

82. Corey, E. J.; Guzman-Perez, A. The catalytic enantioselective construction of molecules with quaternary carbon stereocenters. *Angew. Chem. Int. Ed.* **1998**, *37*, 388–401.
83. Jorgenssen, K. A. Catalytic asymmetric Diels-Alder reactions of carbonyl compounds and imines. *Angew. Chem. Int. Ed.* **2000**, *39*, 3558–3588.
84. Corey, E. J. Catalytic enantioselective Diels-Alder reactions: methods, mechanistic fundamentals, pathways and applications. *Angew. Chem. Int. Ed.* **2002**, *41*, 1650–1667.
85. Evans, D. A.; Johnson, J. S. *Comprehensive Asymmetric Catalysis*, Springer, Berlin, **1999**, Vol. 3, pp. 1177–1235.
86. Nicolaou, K. C.; Snyder, S. A.; Montagnon, T.; Vassilikogiannakis, G. The Diels–Alder reaction in total synthesis. *Angew. Chem. Int. Ed.* **2002**, *41*, 1668–1698.
87. Stocking, E. M.; Williams, R. M. Chemistry and biology of biosynthetic Diels–Alder reactions. *Angew. Chem. Int. Ed.* **2003**, *42*, 3078–3115.
88. Kim, H. J.; Ruzsyczky, M. W.; Choi, S-H.; Liu, Y-N.; Liu, H-W. Enzyme-catalysed [4+2] cycloaddition is a key step in the biosynthesis of spinosyn A. *Nature* **2011**, *473*, 109–112.
89. Ma, S. M.; Li, J. W. -H.; Choi, J. W.; Zhou, H.; Lee, K. K. M.; Moorthie, V. A.; Xie, X.; Kealey, J. T.; Da Silva, N. A.; Vederas, J. C.; Tang, Y. Complete reconstitution of a highly reducing iterative polyketide synthase. *Science* **2009**, *326*, 589–592.
90. Ose, T.; Watanabe, K.; Mie, T.; Honma, M.; Watanabe, H.; Yao, M.; Oikawa, H.; Tanaka, I. Insight into a natural Diels–Alder reaction from the structure of macrophomate synthase. *Nature* **2003**, *422*, 185–189.
91. Kim, R.-R.; Illarionov, B.; Joshi, M.; Cushman, M.; Lee, C. Y.; Eisenreich, W.; Fischer, M.; Bacher, A. Mechanistic insights on riboflavin synthase inspired by selective binding of the 6,7-dimethyl-8-ribityllumazine exomethylene anion. *J. Am. Chem. Soc.* **2010**, *132*, 2983–2990.
92. Manning, G.; Whytel, D. B; Martinez, R.; Hunter, T.; Sudarsanam, S. The protein kinase complement of the human genome. *Science* **2002**, *298*, 1912–1934.
93. Blume-Jensen, P.; Hunter, T. Onkogenic kinase signalling. *Nature* **2001**, *411*, 355–365.
94. Hunter, T. Signaling–2000 and Beyond. *Cell* **2000**, *100*, 113–127.
95. Cohen, P. Protein kinases – the major drug targets of the twenty-first century? *Nat. Rev. Drug Discov.* **2002**, *1*, 309–315.
96. Matthews, D. A.; Gerritsen, M. E. Chapter 1.1: A Brief History of Protein Phosphorylation. In *Targeting Protein Kinases for Cancer Therapy*; John Wiley & Son, Inc.: New Jersey, USA, **2010**; pp. 1–3.
97. Castagna, M.; Takai, Y, Kaibuchi, K.; Sano, K, Kikkawa, U.; Nishizuka Y. Direct activation of calcium-activated, phospholipid-dependent protein kinase by tumor promoting phorbol esters. *J. Biol. Chem.* **1982**, *257*, 7847–7851.
98. Hidaka, H.; Inagaki, M.; Kawamoto, S.; Sasaki, Y. Isoquinolinesulfonamides, novel and potent inhibitors of cyclic nucleotide dependent protein kinase and protein kinase C. *Biochemistry* **1984**, *23*, 5036–5041.
99. Davies, S. P.; Reddy, H.; Caivano, M.; Cohen, P. Specificity and mechanism of action of some commonly used protein kinase inhibitors. *Biochem. J.* **2000**, *351*, 95–105.
100. Omura, S.; Iwai, Y.; Hirano, A.; Nakagawa, A.; Awaya, J.; Tsuchiya, H.; Takahashi, Y.; Masuma, R. A new alkaloid AM-2282 of *Streptomyces* origin taxonomy,

**

- fermentation, isolation and preliminary characterization. *J. Antibiot.* **1977**, *30*, 275–282.
101. Tamaoki, T.; Nomoto, H.; Takahashi, I.; Kato, Y., Morimoto, M., Tomita, F. Staurosporine, a potent inhibitor of phospholipid/Ca²⁺ dependent protein kinase. *Biochem. Biophys. Res. Commun.* **1986**, *135*, 397–402.
102. Link, J. T.; Raghavan, S.; Gallant, M.; Danishefsky, S. J.; Chou, T. C.; Ballas, L. M. Staurosporine and *ent*-staurosporine: The first total syntheses, prospects for a regioselective approach, and activity profiles. *J. Am. Chem. Soc.* **1996**, *118*, 2825–2842.
103. Bush, J. A.; Long, B. H.; Catino, J. J.; Bradner, W. T.; Tomita K. Production and biological activity of rebeccamycin, a novel antitumor agent. *J. Antibiot.* **1987**, *40*, 668–678.
104. Anizon, F.; Belin, L.; Moreau, P.; Sancelme, M.; Voldoire, A.; Prudhomme, M.; Ollier, M.; Sevère, D.; Riou, J. F.; Bailly, C.; Fabbro, D.; Meyer T. Syntheses and biological activities (topoisomerase inhibition and antitumor and antimicrobial properties) of rebeccamycin analogues bearing modified sugar moieties and substituted on the imide nitrogen with a methyl group. *J. Med. Chem.* **1997**, *40*, 3456–3465.
105. Bailly, C.; Riou, J. F.; Colson, P.; Houssier, C.; Rodrigues-Pereira, E.; Prudhomme, M. DNA cleavage by topoisomerase I in the presence of indolocarbazole derivatives of rebeccamycin. *Biochemistry* **1997**, *36*, 3917–29.
106. Takahashi, I.; Kobayashi, E.; Asano, K.; Yoshida, M.; Nakano, H. UCN-01, a selective inhibitor of protein kinase C from *Streptomyces*. *J. Antibiot.* **1987**, *40*, 1782–1784.
107. Fabbro, D.; Ruetz, S.; Bodis, S. PKC412, a protein kinase inhibitor with a broad therapeutic potential. *Anticancer Drug Res.* **2000**, *15*, 17–28.
108. Fischer, T.; Stone, R. M.; Deangelo, D. J.; Galinsky, I.; Estey, E.; Lanza, C.; Fox, E.; Ehninger, G.; Feldman, E.J.; Schiller, G. J.; Klimek, V. M.; Nimer, S. D.; Gilliland, D. G.; Dutreix, C.; Huntsman-Labed, A.; Virkus, J.; Giles, F. J. Phase IIB Trial of oral midostaurin (PKC412), the FMS-like tyrosine kinase 3 receptor (FLT3) and multi-targeted kinase inhibitor, in patients with acute myeloid leukemia and high-risk myelodysplastic syndrome with either wild-type or mutated FLT3. *J. Clin. Oncol.* **2010**, *28*, 4339–4345.
109. Jirousek, M. R.; Gillig, J. R.; Gonzalez, C. M.; Heath, W. F.; McDonald, J. H. 3; Neel, D. A., Rito, C.J.; Singh, U.; Stramm, L.E.; Melikian-Badalian, A.; Baevsky, M.; Ballas, L. M.; Hall, S. E.; Winneroski, L. L.; Faul, M. M. (S)-13-[(dimethylamino)methyl]-10,11,14,15-tetrahydro-4,9:16, 21-dimetheno-1H, 13H-dibenzo[e,k]pyrrolo[3,4-h][1,4,13]oxadiazacyclohexadecene-1,3(2H)-dione (LY333'531) and related analogues: isozyme selective inhibitors of protein kinase C beta. *J. Med. Chem.* **1996**, *39*, 2664–2671.
110. Jirousek, M. R.; Gillig, J. R.; Neel, D. A.; Rito, C. J.; O'Bannon, D.; Heath, W. F.; McDonald III, J. H.; Faul, M. M.; Winneroski, L. L.; Melikian-Badalian, A.; Baevsky, M.; Ballas, L. M.; Hall, S. E. Synthesis of bisindolylmaleimide macrocycles. *Bioorg. Med. Chem. Lett.* **1995**, *36*, 2093–2096.
111. Engel, G. L.; Farid, N. A.; Faul, M. M.; Richardson, L. A.; Winneroski, L. L. Salt form selection and characterisation of LY 333531 mesylate monohydrate. *Int. J. Pharm.* **2000**, *198*, 239–247

**

112. Huwe, A.; Mazitschek, R.; Giannis, A. Small molecules as inhibitors of cyclin-dependent kinases. *Angew. Chem. Int. Ed.* **2003**, *42*, 2122–2138.
113. Knighton, D. R.; Zheng, J.; Ten Eyck, L. F.; Ashford, V. A.; Xuong, N-H.; Taylor, S. S.; Sowadski, J. M. Crystal structure of the catalytic subunit of cyclic adenosine monophosphate-dependent protein kinase. *Science* **1991**, *253*, 407–414
114. Borel, J. F.; Feurer, C.; Gubler, H. U.; Stähelin, H. Biological effects of cyclosporin A: a new antilymphocytic agent. *Agents Actions* **1976**, *6*, 468–75.
115. Kino, T.; Hatanaka, H.; Hashimoto, M.; Nishiyama, M.; Goto, T.; Okuhara, M.; Kohsaka, M.; Aoki, H.; Imanaka, H. FK-506, a novel immunosuppressant isolated from a Streptomyces. I. Fermentation, isolation, and physico-chemical and biological characteristics. *J. Antibiot.* **1987**, *40*, 1249–55.
116. Liu, J.; Farmer, J. D. Jr; Lane, W. S.; Friedman, J.; Weissman, I.; Schreiber, S. L. Calcineurin is a common target of cyclophilin–cyclosporin A and FKBP FK506 complexes. *Cell* **1991**, *66*, 807–815.
117. Vézina, C.; Kudelski, A.; Sehgal, S. N. Rapamycin (AY-22,989), a new antifungal antibiotic. I. Taxonomy of the producing streptomycete and isolation of the active principle. *J. Antibiot.* **1975**, *28*, 721–726.
118. Heitman, J.; Movva, N. R.; Hall, M. N. Targets for cell cycle arrest by the immunosuppressant rapamycin in yeast. *Science* **1991**, *253*, 905–909.
119. Buchdunger, E.; Zimmermann, J.; Mett, H.; Meyer, T.; Müller, M.; Druker, B. J.; Lydon, N. B. Inhibition of the Abl protein-tyrosine kinase *in vitro* and *in vivo* by a 2-phenylaminopyrimidine derivative. *Cancer Res.* **1996**, *56*, 100–104.
120. Schindler, T.; Bornmann, W.; Pellicena, P.; Miller, W. T.; Clarkson, B.; Kuriyan, J. Structural mechanism for STI-571 inhibition of abelson tyrosine kinase. *Science* **2000**, *89*, 1938–1942.
121. Al-Obeidi, F. A.; Lam, K. S. Development of inhibitors for protein tyrosine kinases. *Oncogene* **2000**, *19*, 5690–5701
122. Rusnak, D. W.; Lackey, K.; Affleck, K. The effects of the novel, reversible epidermal growth factor receptor/ ErbB-2 tyrosine kinase inhibitor, GW2016, on the growth of human normal and tumor-derived cell lines *in vitro* and *in vivo*. *Mol. Cancer Ther.* **2001**, *1*, 85–94.
123. Rabindran, S. K.; Discafani, C. M.; Rosfjord, E. C.; Baxter, M.; Floyd, M. B.; Golas, J.; Hallett, W. A.; Johnson, B. D.; Nilakantan, R.; Overbeek, E.; Reich, M. F.; Shen, R.; Shi, X.; Tsou, W.-R.; Wang, Y.-F.; Wissner, A. antitumor activity of HKI-272, an orally active, irreversible inhibitor of the HER-2 tyrosine kinase. *Cancer Res.* **2004**, *64*, 3958–3965.
124. Newton, A. C. Protein kinase C: structural and spatial regulation by phosphorylation, cofactors, and macromolecular interactions. *Chem. Rev.* **2001**, *101*, 2353–2364.
125. Nishizuka, Y. The role of protein kinase C in cell surface signal transduction and tumour promotion. *Nature* **1984**, *308*, 693–698.
126. Nishizuka, Y. Protein kinase C and lipid signaling for sustained cellular responses. *FASEB J.* **1995**, *9*, 484–496.
127. Battaini, F. Protein kinase C isoforms as therapeutic targets in nervous system disease states. *Pharmacol. Res.* **2001**, *44*, 353–361.
128. Pascale, A.; Amadio, M.; Govoni, S.; Battaini, F. The aging brain, a key target for the future: the protein kinase C involvement. *Pharmacol. Res.* **2007**, *55*, 560–569.

**

129. Olariu, A.; Yamada, K.; Nabeshima, T. Amyloid pathology and protein kinase C (PKC): possible therapeutic effects of PKC activators. *J. Pharmacol. Sci.* **2005**, *97*, 1–5.
130. Alkon, D. L.; Sun, M. K.; Nelson, T. J. PKC signaling deficits: a mechanistic hypothesis for the origins of Alzheimer's disease. *Trends Pharmacol. Sci.* **2007**, *28*, 51–60.
131. Baier, G.; Wagner, J. PKC inhibitors: potential in T cell-dependent immune diseases. *Curr. Opin. Cell Biol.* **2009**, *21*, 262–267.
132. Hayashi, K.; Altman, A. Protein kinase C theta (PKC): a key player in T cell life and death. *Pharmacol. Res.* **2007**, *55*, 537–544.
133. Sabri, A.; Steinberg, S. F. Protein kinase C isoform-selective signals that lead to cardiac hypertrophy and the progression of heart failure. *Mol. Cell. Biochem.* **2003**, *251*, 97–101.
134. Churchill, E.; Budas, G.; Vallentin, A.; Koyanagi, T.; Mochly-Rosen, D. PKC isozymes in chronic cardiac disease: possible therapeutic targets? *Annu. Rev. Pharmacol. Toxicol.* **2008**, *48*, 569–599.
135. Chou, W. H.; Messing, R. O. Protein kinase C isozymes in stroke. *Trends Cardiovasc. Med.* **2005**, *15*, 47–51.
136. Basu, A. The potential of protein kinase C as a target for anticancer treatment. *Pharmacol. Ther.* **1993**, *59*, 257–280.
137. Blobe, G. C.; Obeid, L. M.; Hannun, Y. A. Regulation of protein kinase C and role in cancer biology. *Cancer Metastasis Rev.* **1994**, *13*, 411–431.
138. Hofmann, J. Protein kinase C isozymes as potential targets for anticancer therapy. *Curr. Cancer Drug Targets* **2004**, *4*, 125–146.
139. Boije af Gennäs, G.; Talman, V.; Tuominen, R.; Yli-Kauhaluoma, J.; Ekoski, E. Current status and future prospects of C1 domain ligands as drug candidates. *Curr. Top. Med. Chem.* **2011**, *11*, 1370–1392.
140. House, C.; Kemp, B. E. Protein kinase C contains a pseudosubstrate prototope in its regulatory domain. *Science* **1987**, *238*, 1726–1728.
141. Cho, W. Membrane targeting by C1 and C2 domains. *J. Biol. Chem.* **2001**, *276*, 32407–32410.
142. Wang, Q. J.; Bhattacharyya, D.; Garfield, S.; Nacro, K.; Marquez, V. E.; Blumberg, P. M. Differential localization of protein kinase C δ by phorbol esters and related compounds using a fusion protein with green fluorescent protein. *J. Biol. Chem.* **1999**, *274*, 37233–37239.
143. Griner, E. M.; Kazanietz, M. G. Protein kinase C and other diacylglycerol effectors in cancer. *Nat. Rev. Cancer.* **2007**, *7*, 281–294.
144. Duan, D.; Sigano, D. M.; Kelley, J. A.; Lai, C. C.; Lewin, N. E.; Keddi, N.; Peach, M. L.; Lee, J.; Abeyweera, T. P.; Rotenberg, S. A.; Kim, H.; Kim, Y. H.; El Kazzouli, S.; Chung, J. U.; Young, H. A.; Young, M. R.; Baker, A.; Colburn, N. H.; Haimovitz-Friedman, A.; Truman, J. P.; Parrish, D. A.; Deschamps, J. R.; Perry, N. A.; Surawski, R. J.; Blumberg, P. M.; Marquez, V. E. Conformationally constrained analogues of diacylglycerol. 29. Cells sort diacylglycerol-lactone chemical zip codes to produce diverse and selective biological activities. *J. Med. Chem.* **2008**, *51*, 5198–5220.
145. Le Good, J. A.; Ziegler, W. H.; Parekh, D. B.; Alessi, D. R.; Cohen, P.; Parker, P. J. Protein kinase C isotypes controlled by phosphoinositide 3-kinase through the protein kinase PDK1. *Science* **1998**, *281*, 2042–2045.

**

146. Balendran, A.; Biondi, R. M.; Cheung, P. C.; Casamayor, A.; Deak, M.; Alessi, D. R. A 3-phosphoinositide-dependent protein kinase-1 (PDK1) docking site is required for the phosphorylation of protein kinase C ζ (PKC ζ) and PKC-related kinase 2 by PDK1. *J. Biol. Chem.* **2000**, *275*, 20806–20813.
147. Hurley, J. H.; Newton, A. C.; Parker, P. J.; Blumberg, P.M.; Nishizuka, Y. Taxonomy and function of C1 protein kinase C homology domains. *Protein Sci.* **1997**, *6*, 477–80.
148. Zhang, G.; Kazanietz, M. G.; Blumberg, P. M.; Hurley, J. H. Crystal structure of the cys2 activator-binding domain of protein kinase C δ in complex with phorbol ester. *Cell* **1995**, *81*, 917–924.
149. Leonard, T. A.; Rózycki, B.; Saidi, L. F.; Hummer, G.; Hurley, J. H. Crystal structure and allosteric activation of protein kinase C β II. *Cell* **2011**, *144*, 55–66.
150. Hommel, U.; Zurini, M.; Luyten, M. Solution structure of a cysteine rich domain of rat protein kinase C. *Nat. Struct. Biol.* **1994**, *1*, 383–387.
151. Lomize, A. L.; Pogozheva, I. D.; Lomize, M. A.; Mosberg, H. I. The role of hydrophobic interactions in positioning of peripheral proteins in membranes. *BMC Struct. Biol.* **2007**.
152. Kazanietz, M. G. Eyes wide shut: protein kinase C isozymes are not the only receptors for the phorbol ester tumor promoter. *Mol. Carcinog.* **2000**, *28*, 5–11
153. Noble, M. E. M.; Endicott, J. A.; Johnson, L. N. Protein kinase inhibitors: insights into drug design from structure. *Science* **2004**, *303*, 1800–1805.
154. Manning, G.; Whyte, D. B.; Martinez, R.; Hunter, T.; Sudarsanam, S. The Protein kinase complement of the human genome. *Science* **2002**, *298*, 1912–1934.
155. Taylor, S. S.; Radzio-Andzelm, E. Protein kinase inhibition: natural and synthetic variations on a theme. *Curr. Opin. Chem. Biol.* **1997**, *1*, 219–226.
156. Pettit, G. R.; Herald, C. L.; Doubek, D. L.; Herald, D. L. Isolation and structure of bryostatin 1. *J. Am. Chem. Soc.* **1982**, *104*, 6846–6848.
157. Sudek, S.; Lopanik, N. B.; Waggoner, L. E.; Hildebrand, M.; Anderson, C.; Liu, H.; Patel, A.; Sherman, D. H.; Haygood, M. G. Identification of the putative bryostatin polyketide synthase gene cluster from “*Candidatus Edobugula sertula*”, the uncultivated microbial symbiont of the marine bryozoan *Bugula neritina*. *J. Nat. Prod.* **2007**, *70*, 67–74.
158. Keck, G. E.; Poudel, Y. B.; Cummins, T. J.; Rudra, A.; Covell, J. A. Total synthesis of bryostatin 1. *J. Am. Chem. Soc.* **2011**, *133*, 744–747.
159. M. E. Reyland, P. A. Insel, R. O. Messing, E. C. Dempsey, A. C. Newton, D. Mochly-Rosen, A. P. Fields. Protein kinase C isozymes and the regulation of diverse cell responses. *Am. J. Physiol. Lung Cell. Mol. Physiol.* **2000**, *279*, 429–438.
160. Wender, P. A.; Verma, V. A. The design, synthesis, and evaluation of C7 diversified bryostatin analogs reveal a hot spot for PKC affinity. *Org. Lett.* **2008**, *10*, 3331–3334.
161. Hale, K. J.; Hummersone, M. G.; Manaviazar, S.; Frigerio, M. The chemistry and biology of the bryostatin antitumour macrolides. *Nat. Prod. Rep.* **2002**, *19*, 413–453.
162. Schaufelberger, D. E.; Koleck, M. P.; Beutler, J. A.; Vatakis, A. M.; Alvarado, A. B.; Andrews, P.; Marzo, L. V.; Muschik, G. M.; Roach, J.; Ross, J. T.; Lebherz, W. B.; Reeves, M. P.; Eberwein, R. M.; Rodgers, L. L.; Testerman, R. P.; Snader, K. M.; Forenza, S. The large-scale isolation of bryostatin 1 from *bugula neritina* following current good manufacturing practices. *J. Nat. Prod.* **1991**, *54*, 1265–1270.
163. Newman, D. J.; Cragg, G. M. Marine natural products and related compounds in clinical and advanced preclinical trials. *J. Nat. Prod.* **2004**, *67*, 1216–1238.

**

164. Dowlati, A.; Lazarus, H. M.; Hartman, P.; Jacobberger, J. W.; Whitacre, C.; Gerson, S. L.; Ksenich, P.; Cooper, B. W.; Frisa, P. S.; Gottlieb, M.; Murgo, A. J.; Remick, S. C. Phase I and correlative study of combination bryostatin 1 and vincristine in relapsed B-cell malignancies. *Clin. Cancer Res.* **2003**, *9*, 5929–5935.
165. Sun, M.-K.; Hongpaisan, J.; Nelson, T. J.; Alkon, D. L. Post-stroke neuronal rescue and synaptogenesis mediated *in vivo* by PKC in adult brains. *Proc. Natl. Acad. Sci. U.S.A.* **2008**, *105*, 13620–13625.
166. Way, K. J.; Katai, N.; King, G. L. Protein kinase C and the development of diabetic vascular complications. *Diabetic Med.* **2001**, *18*, 945–959.
167. Oz, H. S.; Hughes, W. T.; Rehg, J. E.; Thomas, E. K. Effect of CD40 ligand and other immunomodulators on *Pneumocystis carinii* infection in rat model. *Microb. Pathog.* **2000**, *29*, 187–190.
168. Hongpaisan, J.; Alkon, D. L. A structural basis for enhancement of long-term associative memory in single dendritic spines regulated by PKC. *Proc. Natl. Acad. Sci. U.S.A.* **2007**, *104*, 19571–19576.
169. Sun, M. -K.; Hongpaisan, J.; Alkon, D. L. Post-ischemic PKC activation rescues retrograde and anterograde long-term memory. *Proc. Natl. Acad. Sci. U.S.A.* **2009**, *106*, 14676–14680
170. Etcheberrigaray, R.; Tan, M.; Dewachter, I.; Kuiperi, C.; Van der Auwera, I.; Wera, S.; Qiao, L.; Bank, B.; Nelson, T. J.; Kozikowski, A. P.; Van Leuven, F.; Alkon, D. L. Therapeutic effects of PKC activators in Alzheimer's disease transgenic mice. *Proc. Natl. Acad. Sci. U.S.A.* **2004**, *101*, 11141–11146.
171. Mendola, D. *Drugs from the Sea*, ed. N. Fusetani, Karger, Basel, **2000**, pp. 120–133.
172. Hale, K. J.; Manaviazar, S. New approaches to the total synthesis of the bryostatin antitumor macrolides. *Chem. Asian J.* **2010**, *5*, 704–754.
173. Mutter, R.; Wills, M. Chemistry and clinical biology of the bryostatins. *Bioorg. Med. Chem.* **2000**, *8*, 1841–1860.
174. Wender, P. A.; DeBrabander, J.; Harran, P. G.; Jimenez, J.-M.; Koehler, M. F. T.; Lippa, B.; Park, C.-M.; Siedenbiedel, C.; Pettit, G. R. The practical synthesis of a novel and highly potent analogue of bryostatin. *Proc. Natl. Acad. Sci. U.S.A.* **1998**, *95*, 6624–6629.
175. Wender, P. A.; Brabander, J. D.; Harran, P. G.; Jimenez, J.; Koehler, M. F. T.; Lippa, B.; Park, C.; Shiozaki, M. Synthesis of the first members of a new class of biologically Active bryostatin analogues. *J. Am. Chem. Soc.* **1998**, *120*, 4534–4535.
176. Wender, P. A.; Baryza, J. L.; Bennett, C. E.; Bi, F. C.; Brenner, S. E.; Clarke, M. O.; Horan, J. C.; Kan, C.; Lacote, E.; Lippa, B.; Nell, P. G.; Turner, T. M. The practical Synthesis of a novel and highly potent analogue of bryostatin. *J. Am. Chem. Soc.* **2002**, *124*, 13648–13649.
177. Keck, G. E.; Truong, A. P. Synthetic studies on the bryostatins: synthetic routes to analogues containing the tricyclic macrolactone core. *Org. Lett.* **2005**, *7*, 2153–2156
178. Keck, G. E.; Kraft, M.B.; Truong, A. P.; Li, W.; Sanchez, C. C.; Kedei, N.; Lewin, N. E.; Blumberg, P. M. Convergent assembly of highly potent analogues of bryostatin 1 via pyran annulation: bryostatin look-alikes that mimic phorbol ester function. *J. Am. Chem. Soc.* **2008**, *130*, 6660–6661
179. Keck, G. E.; Poudel, Y. B.; Welch, D. S.; Kraft, M. B.; Truong, A. P.; Stephens, J. C.; Kedei, N.; Lewin, N. E.; Blumberg, P.M. Substitution on the A-ring confers to bryopyran analogues the unique biological activity characteristic of bryostatins and distinct from that of the phorbol esters. *Org. Lett.* **2009**, *11*, 593–596.

**

180. Keck, G. E.; Li, W.; Kraft, M. B.; Kedei, N.; Lewin, N. E.; Blumberg, P. M. The bryostatin 1 A-ring acetate is not the critical determinant for antagonism of phorbol ester-induced biological responses. *Org. Lett.* **2009**, *11*, 2277–2280.
181. Gouiffe`s, D.; Moreau, S.; Helbecque, N.; Bernier, J. L.; Henichart, J. P.; Barbin, Y.; Laurent, D.; Verbist, J. F. Proton nuclear magnetic study of bistramide A, a new cytotoxic drug isolated from *Lissoclinum Bistratum* Sluiter. *Tetrahedron* **1988**, *44*, 451–459.
182. Biard, J. F.; Roussakis, C.; Kornprobst, J. M.; Gouiffes-Barbin, D.; Verbist, J. F.; Cotellet, P.; Foster, M. P.; Ireland, C. M.; Debitus, C. Bistramides A, B, C, D, and K: a new class of bioactive cyclic polyethers from *Lissoclinum bistratum*. *J. Nat. Prod.* **1994**, *57*, 1336–1345.
183. Statsuk, A. V.; Liu, D.; Kozmin, S. A. Synthesis of bistramide A. *J. Am. Chem. Soc.* **2004**, *126*, 9546–9547.
184. Riou, D.; Roussakis, C.; Robillard, N.; Biard, J. F.; Verbist, J. F. Bistramide A-induced irreversible arrest of cell proliferation in a non-small-cell bronchopulmonary carcinoma is similar to induction of terminal maturation. *Biol. Cell.* **1993**, *77*, 261–264.
185. Sauviat, M.-P.; Gouiffes-Barbin, D.; Ecault, E.; Verbist, J.-F. Blockade of sodium channels by bistramide A in voltage-clamped frog skeletal muscle fibres. *Biochim. Biophys. Acta, Biomembr.* **1992**, *1103*, 109–114.
186. Sauviat, M. P.; Verbist, J. F. Alteration of the voltage-dependence of the twitch tension in frog skeletal muscle fibres by a polyether, Bistramide A. *Gen. Physiol. Biophys.* **1993**, *12*, 465–471.
187. Johnson, W. E. B.; Watters, D. J.; Suniara, R. K.; Brown, G.; Bunce, C. M. Bistratene A induces a microtubule-dependent block in cytokinesis and altered stathmin expression in HL60 cells *Biochem. Biophys. Res. Commun.* **1999**, *260*, 80–88.
188. Statsuk, A. V.; Bai, R.; Baryza, J. L.; Verma, V. A.; Hamel, E.; Wender, P. A.; Kozmin, S. A. Actin is the primary cellular receptor of bistramide A. *Nature Chem. Biol.* **2005**, *1*, 383–388.
189. Griffiths, G.; Garrone, B.; Deacon, E.; Owen, P.; Pongracz, J.; Mead, G.; Bradwell, A.; Watters, D.; Lord, J. The polyether bistratene A activates protein kinase C- δ and induces growth arrest in HL60 cells. *Biochem. Biophys. Res. Commun.* **1996**, *222*, 802–808.
190. Stanwell, C.; Gescher, A.; Watters, D. Cytostatic and cytotoxic properties of the marine product bistratene A and analysis of the role of protein kinase C in its mode of action. *Biochem. Pharmacol.* **1993**, *45*, 1753–1761.
191. Rizvi, S. A.; Courson, D. S.; Keller, V. A.; Rock, R. S.; Kozmin, S. A. The dual mode of action of bistramide A entails severing of filamentous actin and covalent protein modification. *Proc. Natl. Acad. Sci. U. S. A.* **2008**, *105*, 4088–4092.
192. Watters, D.; Garrone, B.; Gobert, G.; Williams, S.; Gardiner, R.; Lavin, M. Bistratene A causes phosphorylation of talin and redistribution of actin microfilaments in fibroblasts: possible role for PKC- δ . *Exp. Cell Res.* **1996**, *229*, 327–335.
193. Hecker, E. Cocarcinogenic principles from the seed oil of *Croton tiglium* and from other Euphorbiaceae. *Cancer Res.* **1968**, *28*, 2338–2349.
194. Zechmeister, K.; Brandl, F.; Hoppe, W.; Hecker, E.; Opferkuch, H. J.; Adolf, W. Structure determination of the new tetracyclic diterpene ingenol-triacetate with triple product methods. *Tetrahedron Lett.* **1970**, *11*, 4075–4078.

**

195. Hecker, E. New, toxic and irritant and co-carcinogenic diterpene esters from Euphorbiaceae and from thymelaeacae. *Pure Appl. Chem.* **1977**, *49*, 1423–1431
196. Krauter, G.; Von der Lieth, C. W.; Schmidt, R.; Hecker, E. Structure/activity relationships of polyfunctional diterpenes of the tiglane type. A pharmacophore model for protein-kinase-C activators based on structure/activity studies and molecular modeling of the tumor promoters 12-*O*-tetradecanoylphorbol 13-acetate and 3-*O*-tetradecanoylingenol. *Eur. J. Biochem.* **1996**, *242*, 417–427
197. Nishizuka, Y. The molecular heterogeneity of protein kinase C and its implications for cellular regulation. *Nature* **1988**, *334*, 661–664.
198. Cha, J. K.; Epstein, O. L. Synthetic approaches to ingenol. *Tetrahedron* **2006**, *62*, 1329–1343.
199. Winkler, J. D.; Rouse, M. B.; Greaney, M. F.; Harrison, S. J.; Jeon, Y. T. The first total synthesis of (±)-ingenol. *J. Am. Chem. Soc.* **2002**, *124*, 9726–9728.
200. Paquette, L. A.; Ross, R. J.; Springer, J. P. Stereocontrolled construction of an ingenol prototype having a complete array of oxygenated and unsaturated centers. *J. Am. Chem. Soc.* **1988**, *110*, 6192–6204.
201. Blanco-Molina, M.; Tron, G. C.; Macho, A.; Lucena, C.; Calzado, M. A.; Munoz, E.; Appendino, G. Ingenol esters induce apoptosis in Jurkat cells through an AP-1 and NF-κB independent pathway. *Chem. Biol.* **2001**, *8*, 767–778 and references therein.
202. Kedei, N.; Lundberg, D. J.; Toth, A.; Welburn, P.; Garfield, S. H.; Blumberg, P. M. Characterization of the interaction of ingenol 3-angelate with protein kinase C. *Cancer Res.* **2004**, *64*, 3243–3255.
203. Ogbourne, S. M.; Hampson, P.; Lord, J. M.; Parsons, P.; De Witte, P. A.; Suhrbier, A. Proceedings of the First International Conference on PEP005. *Anticancer Drugs* **2007**, *18*, 357–362.
204. Mason, S. A.; Cozzi, S. J.; Pierce, C. J.; Pavey, S. J.; Parsons, P. G.; Boyle, G. M. The induction of senescence-like growth arrest by protein kinase C-activating diterpene esters in solid tumor cells. *Invest. New Drugs* **2010**, *28*, 575–586.
205. Appendino, G.; Tron, G. C.; Cravotto, G.; Palmisano, G.; Annunziata, R.; Baj, G.; Surico, N. Synthesis of modified ingenol esters. *Eur. J. Org. Chem.* **1999**, *4*, 345–352.
206. Kupchan, S. M.; Uchida, I.; Branfman, A. Q. R.; Dailey, R. G. Jr.; Fei, B. Y. Antileukemic principles isolated from Euphorbiaceae plants. *Science* **1976**, *191*, 571–572.
207. Winkler, J. D.; Hong, B.; Bahador, A.; Kazanietz, M. G.; Blumberg, P. M. Synthesis of ingenol analogues with affinity for protein kinase C. *Bioorg. Med. Chem. Lett.* **1993**, *3*, 577–580.
208. Cuypers, H. T.; Selten, G.; Quint, W. Zijlstra, M.; Maandag, E. R.; Boelens, W.; van Wezenbeek, P.; Melief, C.; Berns, A. Murine leukemia virus-induced t-cell lymphomagenesis: integration of proviruses in a distinct chromosomal region. *Cell* **1984**, *37*, 141–150.
209. Mikkers, H.; Nawijn, M.; Allen, J.; Brouwers, C.; Verhoeven, E.; Jonkers, J.; Berns, A. Mice deficient for all PIM kinases display reduced body size and impaired responses to hematopoietic growth factors. *Mol. Cell. Biol.* **2004**, *24*, 6104–6115.
210. Qian, K. C.; Wang, L.; Hickey, E. R.; Studts, J.; Barringer, K.; Peng, C.; Kronkaitis, A.; Li, J.; White, A.; Mische, S.; Farmer, B. Structural basis of constitutive activity and a unique nucleotide binding mode of human Pim-1 kinase. *J. Biol. Chem.* **2005**, *280*, 6130–6137.

**

211. Wang, Z.; Bhattacharya, N.; Weaver, M.; Petersen, K.; Meyer, M.; Gapter, L.; Magnuson, N. S. Pim-1: a serine/threonine kinase with a role in cell survival, proliferation, differentiation and tumorigenesis. *J. Vet. Sci.* **2001**, *2*, 167–179.
212. Amson, R.; Sigaux, F.; Przedborski, S.; Flandrin, G.; Givol, D.; Telerman, A. The human protooncogene product p33^{pim} is expressed during fetal hematopoiesis and in diverse leukemias. *Proc. Natl. Acad. Sci. U.S.A.* **1989**, *86*, 8857–8861.
213. Shah, N.; Pang, B.; Yeoh, K. G.; Thorn, S.; Chen, C. S.; Lilly, M. B.; Salto-Tellez, M. Potential roles for the PIM1 kinase in human cancer – a molecular and therapeutic appraisal. *Eur. J. Cancer* **2008**, *44*, 2144–2145
214. Brault, L.; Gasser, C.; Bracher, F.; Huber, K.; Knapp, S.; Schwaller, J. PIM serine/threonine kinases in pathogenesis and therapy of hematological malignancies and solid cancers. *Haematologica* **2010**, *95*, 1004–1015.
215. Magnuson, N. S, Wang, Z.; Ding, G.; Reeves, R. Why target PIM1 for cancer diagnosis and treatment? *Future Oncol.* **2010**, *6*, 1461–1478.
216. Lilly, M.; Sandholm, J.; Cooper, J. J.; Koskinen, P. J.; Kraft, A. The PIM-1 serine kinase prolongs survival and inhibits apoptosis-related mitochondrial dysfunction in part through a *bcl-2*-dependent pathway. *Oncogene* **1999**, *18*, 4022–4031.
217. Zemskova, M.; Sahakian, E.; Bashkirova, S.; Lilly, M. The PIM1 kinase is a critical component of a survival pathway activated by docetaxel and promotes survival of doxorubicin-treated prostate cancer cells. *J. Biol. Chem.* **2008**, *283*, 20635–20644.
218. Peltola, K.; Hollmen, M.; Maula, S. M.; Rainio, E.; Ristamäki, R.; Luukkaa, M.; Sandholm, J.; Sundvall, M.; Elenius, K.; Koskinen, P. J.; Grenman, R.; Jalkanen, S. Pim-1 kinase expression predicts radiation response in squamocellular carcinoma of head and neck and is under the control of epidermal growth factor receptor. *Neoplasia* **2009**, *11*, 629–636.
219. Yan, B.; Zemskova, M.; Holder, S.; Chin, V.; Kraft, A.; Koskinen, P.J.; and Lilly, M. The PIM-2 kinase phosphorylates BAD on serine 112 and reverses BAD-induced cell death. *J. Biol. Chem.* **2003**, *278*, 45358–45367.
220. Aho, T. L. T.; Sandholm, J.; Peltola, K. J.; Mankonen, H. P.; Lilly, M.; Koskinen, P. J. Pim-1 kinase promotes inactivation of the pro-apoptotic Bad protein by phosphorylating it on the Ser112 gatekeeper site. *FEBS Lett.* **2004**, *571*, 43–49.
221. Macdonald, A.; Campbell, D. G.; Toth, R.; McLauchlan, H.; Hastie, C. J.; Arthur, J. S. C. Pim kinases phosphorylate multiple sites on Bad and promote 14-3-3 binding and dissociation from Bcl-XL. *BMC Cell Biology* **2006**, *7*:1.
222. Wang, J.; Kim, J.; Roh, M.; Franco, O. E.; Hayward, S. W.; Wills, M. L.; Abdulkadir, S. A. Pim1 kinase synergizes with c-Myc to induce advanced prostate carcinoma. *Oncogene* **2010**, *29*, 2477–2487.
223. Wang, J.; Anderson, P. D.; Luo, W.; Gius, D.; Roh, M.; Abdulkadir, S. A. Pim1 kinase is required to maintain tumorigenicity in MYC-expressing prostate cancer cells. *Oncogene*, **2011**, doi: 10.1038/onc.2011.371.
224. Santio, N.M.; Vahakoski, R. L.; Rainio, E.M.; Sandholm, J.A.; Virtanen, S.S.; Prudhomme, M.; Anizon, F.; Moreau, P.; Koskinen, P.J. Pim-selective inhibitor DHPCC-9 reveals Pim kinases as potent stimulators of cancer cell migration and invasion. *Mol. Cancer* **2010**, *9*, 279–291.
225. Swords, R.; Kelly, K.; Carew, J.; Nawrocki, S.; Mahalingam, D.; Sarantopoulos, J.; Bearss, D.; Giles, F. The pim kinases: new targets for drug development. *Curr. Drug Targets* **2011**, *12*, 2059–2066.

**

226. Schenone, S.; Tintori, C.; Botta, M. Using insights into Pim1 structure to design new anticancer drugs. *Curr. Pharm. Des.* **2010**, *16*, 3964–3978.
227. Morwick, T. Pim kinase inhibitors: a survey of the patent literature. *Expert Opin. Ther. Pat.* **2010**, *20*, 193–212.
228. Bullock, A. N.; Debreczeni, J. E.; Fedorov, O. Y.; Nelson, A.; Marsden, B. D.; Knapp, S. Structural basis of inhibitor specificity of the human protooncogene proviral insertionsite in Moloney murine leukemia virus (PIM-1) kinase. *J. Med. Chem.* **2005**, *48*, 7604–7614.
229. Kumar, A.; Mandiyan, V.; Suzuki, Y.; Zhang, C.; Rice, J.; Tsai, J.; Artis, D. R.; Ibrahim, P.; Bremer, R. Crystal structures of proto-oncogene kinase Pim1: A target of aberrant somatic hypermutations in diffuse large cell lymphoma. *J. Mol. Biol.* **2005**, *348*, 183–193
230. Jacobs, M. D.; Black, J.; Futer, O.; Swenson, L.; Hare, B.; Fleming, M.; Saxena, K. Pim-1 ligand-bound structures reveal the mechanism of serine/threonine kinase inhibition by LY294002. *J. Biol. Chem.* **2005**, *14*, 13728–13734.
231. Fedorov, O.; Marsden, B.; Pogacic, V.; Rellos, P.; Muller, S.; Bullock, A. N.; Schwaller, J.; Sundstrom, M.; Knap, S. A systematic interaction map of validated kinase inhibitors with Ser/Thr kinases. *Proc. Natl. Acad. Sci. U.S.A.* **2007**, *104*, 20523–20528.
232. Debreczeni, J. E.; Bullock, A. N.; Atilla, G. E.; Williams, D. S.; Bregman, H.; Knapp, S.; Meggers, E. Ruthenium half-sandwich complexes bound to protein kinase pim1. *Angew. Chem. Int. Ed.* **2006**, *45*, 1580–1585.
233. Bregman, H.; Meggers, E. Ruthenium half-sandwich complexes as protein kinase inhibitors: an *N*-succinimidyl ester for rapid derivatizations of the cyclopentadienyl moiety. *Org. Lett.* **2006**, *8*, 5465–5468.
234. Meggers, E.; Atilla-Gokcumen, G. E.; Bregman, H.; Maksimoska, J.; Mulcahy, S. P.; Pagano, N.; Williams, D. S. Exploring chemical space with organometallics: ruthenium complexes as protein kinase inhibitors. *Synlett.* **2007**, *8*, 1177–1189.
235. Williams, D. S.; Atilla, G. E.; Bregman, H.; Arzoumanian, A.; Klein, P. S.; Meggers, E. Switching on a signaling pathway with an organoruthenium complex. *Angew. Chem. Int. Ed.* **2005**, *44*, 1984–1987.
236. Feng, L.; Geisselbrecht, Y.; Blanck, S.; Wilbuer, A.; Atilla-Gokcumen, G. E.; Filippakopoulos, P.; Kräling, K.; Celik, M. A.; Harms, K.; Maksimoska, J.; Marmorstein, R.; Frenking, G.; Knapp, S.; Essen, L-O.; Meggers, E. Structurally sophisticated octahedral metal complexes as highly selective protein kinase inhibitors. *J. Am. Chem. Soc.* **2011**, *133*, 5976–5986.
237. Bullock, A. N.; Russo, S.; Amos, A.; Pagano, N.; Bregman, H.; Debreczeni, J. E.; Lee, W. H.; von Delft, F.; Meggers, E.; Knapp, S. Crystal structure of the PIM2 kinase in complex with an organoruthenium inhibitor. *PLoS ONE* **2009**, *4*, e7112. doi:10.1371/journal.pone.0007112
238. Pogacic, V.; Bullock, A. N.; Federov, O.; Filippakopoulos, P.; Gasser, C.; Biondi, A.; Meyer-Monard, S.; Knapp, S.; Schwaller, J. Structural Analysis Identifies Imidazo[1,2-*b*]Pyridazines as PIM kinase inhibitors with *in vitro* antileukemic activity *J. Cancer Res.* **2007**, *67*, 6916–6924.
239. Berk, G. A. Potent small molecule Pim kinase inhibitor with *in vivo* oral bioavailability and activity in cell Lines form hematological malignancies. European Hematology Association Abstract **2008**.

**

240. Pierce, A. C.; Jacobs, M.; Stuver-Moody, C. Docking study yields four novel inhibitors of the protooncogene Pim-1 kinase. *J. Med. Chem.* **2008**, *51*, 1972–1975
241. Grey, R.; Pierce, A. C.; Bemis, G. W.; Jacobs, M. C.; Moody, S. T.; Jajoo, R.; Mohal, N.; Green, J. Structure-based design of 3-aryl-6-amino-triazolo[4,3-*b*]pyridazine inhibitors of Pim-1 kinase. *Bioorg. Med. Chem. Lett.* **2009**, *19*, 3019–3022
242. Nishiguchi, G. A.; Atallah, G.; Bellamacina, C.; Burger, M. T.; Ding, Y.; Feucht, P. H.; Garcia, P. D.; Han, W.; Klivansky, L.; Lindvall, M. Discovery of novel 3,5-disubstituted indole derivatives as potent inhibitors of Pim-1, Pim-2, and Pim-3 protein kinases. *Bioorg. Med. Chem. Lett.* **2011**, *21*, 6366–6369.
243. Akué-Gédu, R.; Rossignol, E.; Azzaro, S.; Knapp, S.; Filippakopoulos, P.; Bullock, A. N.; Bain, J.; Cohen, P.; Prudhomme, M.; Anizon, F.; Moreau, P. Synthesis, kinase inhibitory potencies, and in vitro antiproliferative evaluation of new pim kinase inhibitors. *J. Med. Chem.* **2009**, *52*, 6369–6381.
244. Akué-Gédu, R.; Nauton, L.; Théry, V.; Bain, J.; Cohen, P.; Anizon, F.; Moreau, P. Synthesis, Pim kinase inhibitory potencies and in vitro antiproliferative activities of diversely substituted pyrrolo[2,3-*a*]carbazoles. *Bioorg. Med. Chem.* **2010**, *18*, 6865–6873.
245. Santio, N. M.; Vahakoski, R. L.; Rainio, E. M.; Sandholm, J. A.; Virtanen, S. S.; Prudhomme, M.; Anizon, F.; Moreau, P.; Koskinen, P. J. Pim-selective inhibitor DHPCC-9 reveals Pim kinases as potent stimulators of cancer cell migration and invasion. *Mol. Cancer* **2010**, *9*, 279–291.
246. Tao, Z.; Hasvold, L. A.; Levenson, J. D.; Han, E. K.; Guan, R.; Johnson, E. F.; Stoll, V. S.; Stewart, K. D.; Stemper, G.; Soni, N.; Buoska, J. J.; Luo, Y.; Sowin, T. J.; Lin, N-H.; Giranda, V. S.; Rosenberg, S. H.; Penning, T. D. Discovery of 3*H*-benzo[4,5]thieno[3,2-*d*]pyrimidin-4-ones as potent, highly selective, and orally bioavailable inhibitors of the human protooncogene proviral insertion site in Moloney murine leukemia virus (PIM) kinases. *J. Med. Chem.* **2009**, *52*, 6621–6636.
247. Qian, K.; Wang, L.; Cywin, C. L.; Farmer, B. T.; Hickey, E.; Homon, C.; Jakes, S.; Kashem, M. A.; Lee, G.; Leonard, S.; Li, J.; Magboo, R.; Mao, W.; Pack, E.; Peng, C.; Prokopowicz, A.; Welzel, M.; Wolak, J.; Morwick, T. Hit to lead account of the discovery of a new class of inhibitors of Pim kinases and crystallographic studies revealing an unusual kinase binding mode. *J. Med. Chem.* **2009**, *52*, 1814–1827
248. Xiang, Y.; Hirth, B.; Asmussen, G.; Biemann, H. P.; Bishop, K. A.; Good, A.; Fitzgerald, M.; Gladysheva, T.; Jain, A.; Jancsics, K.; Liu, J.; Metz, M.; Papoulis, A.; Skerlj, R.; Stepp, J. D.; Wei, R. R. The discovery of novel benzofuran-2-carboxylic acids as potent Pim-1 inhibitors. *Bioorg. Med. Chem. Lett.* **2011**, *21*, 3050–3056.
249. Haddach, M.; Michaux, J.; Schwaebe, M. K.; Pierre, F.; O'Brien, S. E.; Borsan, C.; Tran, J.; Raffaele, N.; Ravula, S.; Drygin, D.; Siddiqui-Jain, A.; Darjania, L.; Stansfield, R.; Proffitt, C.; Macalino, D.; Streiner, N.; Bliesath, J.; Omori, M.; Whitten, J. P.; Anderes, K.; Rice, W. G.; Ryckman, D. M. Discovery of CX-6258. A potent, selective, and orally efficacious pan-Pim kinases inhibitor. *ACS Med. Chem. Lett.* **2012**, *3*, 135–139.
250. Holder, S.; Zemskova, M.; Zhang, C.; Tabrizizad, M.; Bremer, R.; Neidigh, J.; Lilly, M. Characterization of potent and selective small-molecule inhibitor of the PIM1 kinase. *Mol. Cancer Ther.* **2007**, *6*, 163–172.
251. Tong, Y.; Stewart, K. D.; Thomas, S.; Przytulinska, M.; Johnson, E.F.; Klinghofer, V.; Levenson, J.; McCall, O.; Soni, N. B.; Luo, Y.; Lin, N-H.; Sowin, T. J.; Giranda, V. L.; Penning, T. D. Isoxazolo[3,4-*b*]quinoline-3,4(1*H*,9*H*)-diones as unique, potent and

**

- selective inhibitors for Pim-1 and Pim-2 kinases: Chemistry, biological activities, and molecular modelling. *Bioorg. Med. Chem. Lett.* **2008**, *18*, 5206–5208.
252. Xia, Z.; Knaak, C.; Ma, J.; Beharry, Z. M.; McInnes, C.; Wang, W.; Kraft, A. S.; Smith, C. D. Synthesis and evaluation of novel inhibitors of Pim-1 and Pim-2 protein kinases. *J. Med. Chem.* **2009**, *52*, 74–86.
253. Cheney, I. W.; Yan, S.; Appleby, T.; Walker, H.; Vo, T.; Yao, N.; Hamatake, R.; Hong, Z.; Wu, J. Z. Identification and structure activity relationships of substituted pyridones as inhibitors of Pim1 kinase. *Bioorg. Med. Chem. Lett.* **2007**, *17*, 1679–1683.
254. Good, A. C.; Liu, J.; Hirth, B.; Asmussen, G.; Xiang, Y.; Biemann, H.-P.; Bishop, K. A.; Fremgen, T.; Fitzgerald, M.; Gladysheva, T.; Jain, A.; Jancsics, K.; Metz, M.; Papoulis, A.; Skerlj, R.; Stepp, J. D.; Wei, R. R. Implications of promiscuous Pim-1 kinase fragment inhibitor hydrophobic interactions for fragment-based drug design. *J. Med. Chem.* **2012**, *55*, 2641–2648.
255. Lewgowd, W.; Stanczak, A. Cinnoline derivatives with biological activity *Arch. Pharm. Chem. Life Sci.* **2007**, *340*, 65–80.
256. Lei, X.; Zaarur, N.; Sherman, M. Y.; Porco, J. A. Stereocontrolled synthesis of a complex library via elaboration of angular epoxyquinol scaffolds. *J. Org. Chem.* **2005**, *70*, 6474–6483.
257. Su, S.; Acquilano, D. E.; Arumugasamy, J.; Beeler, A. B.; Eastwood, E. L.; Giguere, J. R.; Lan, P.; Lei, X.; Min, G. K.; Yeager, A. R.; Zhou, Y.; Panek, J. S.; Snyder, J. K.; Schaus, S. E.; Porco, J. A. Convergent synthesis of a complex oxime library using chemical domain shuffling. *Org. Lett.* **2005**, *7*, 2751–2754.
258. Moriarty, R. M.; Prakash, I.; Penmasta, R. An improved synthesis of ethyl azodicarboxylate and 1,2,4-triazoline-3,5-diones using hypervalent iodine oxidation *Synth. Commun.* **1987**, *17*, 409–413.
259. Datta, S. C.; Franck, R. W.; Tripathy, R.; Quigley, G. J.; Huang, L.; Chen, S.; Sihaed, A. Effect of allylic substituents on the face selectivity of Diels-Alder reactions of semicyclic dienes *J. Am. Chem. Soc.* **1990**, *112*, 8472–8478.
260. Alder, K.; Mönch, J.; Wirtz, H. Über den sterischen Verlauf der Addition des Butadiens an die Doppelbindung des Bicyclo-[1.2.2]-Hepten-Systems. *Justus Liebigs Ann. Chem.* **1959**, *627*, 47–59.
261. Shioiri, T.; Ninomiya, K.; Yamada, S. Diphenylphosphoryl azide. A new convenient reagent for a modified Curtius reaction and for the peptide synthesis. *J. Am. Chem. Soc.* **1972**, *94*, 6203–6205.
262. Aumüller, I. Azulen-unterstützte Substanzreinigung – eine Strategie für die parallele Ligandsynthese. Ph.D. Thesis, University of Kiel, Germany, **2002**.
263. Bain, J., Plater, L.; Elliott, M.; Shpiro, N., Hastie, C. J.; McLauchlan, H.; Klevernic, I.; Arthur, J. S.; Alessi, D. R., Cohen, P. The selectivity of protein kinase inhibitors: a further update. *Biochem J.* **2007**, *408*, 297–315.
264. Bergmann, E. D. Fulvenes and substituted fulvenes. *Chem. Rev.* **1968**, *68*, 41–84.
265. Pauson, P. L. Tropones and tropolones. *Chem. Rev.* **1955**, *55*, 9–136.
266. Kiriazis, A.; Yli-Kauhaluoma, J. Unpublished results, **2010–2011**.
267. Appukkuttan, P.; Dehaen, W.; Fokin, V. V.; Van der Eycken, E. A. microwave-assisted click chemistry synthesis of 1,4-disubstituted 1,2,3-triazoles via a copper(I)-catalyzed three-component reaction. *Org. Lett.* **2004**, *6*, 4223–4225.
268. Arnaudova, R. Synthesis of novel guaiazulene derivatives as potential inhibitors of Pim-1 kinase. M.Sc. Thesis, University of Helsinki, Finland, **2010**.